



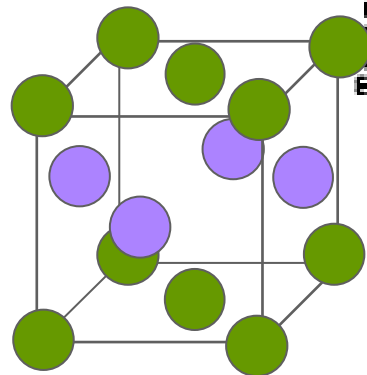
合金材料の結晶粒界と強度特性

北海道大学 大学院工学研究院
材料科学部門 材料数理学研究室
毛利哲雄

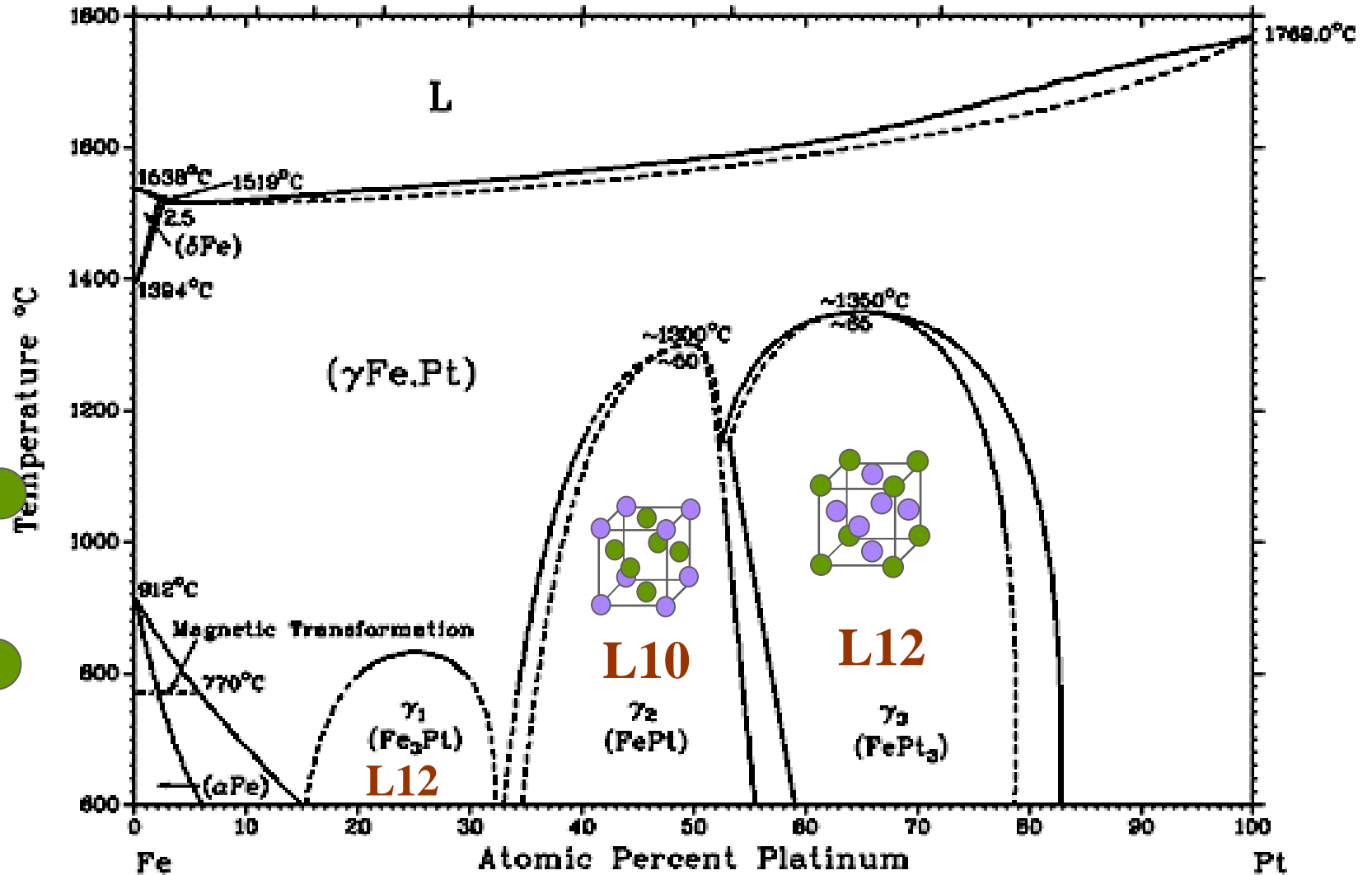
Background Phase Diagram



Fe-Pt



L10



Background



Showing: Atomic weight

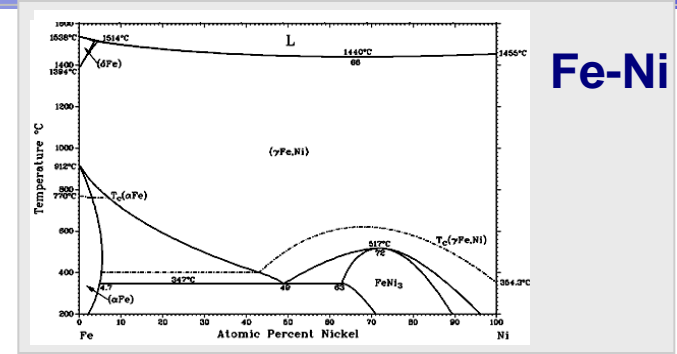
IA																VIII																			
H 1.0079																He 4.0026																			
Li 6.94		Be 9.0121														B 10.81		C 12.011		N 14.006		O 15.999		F 18.998		Ne 20.17									
Na 22.989		Mg 24.305														Al 26.98		Si 28.085		P 30.97		S 32.06		Cl 35.453		Ar 39.948									
K 39.098		Ca 40.08		Sc		Ti 47.88		V 50.94		Cr 51.996		Mn 54.938		Fe 55.845		Co 58.933		Ni 58.71		Cu 63.546		Zn 65.38		Ga 69.723		Ge 72.59		As 74.92		Se 78.96		Br 79.904		Kr 83.80	
Rb 85.467		Sr 87.62		Y 88.905		Zr 91.224		Nb 92.906		Mo 95.94		Tc 98.906		Ru 101.07		Rh 102.905		Pd 106.42		Ag 107.868		Cd 112.411		In 114.818		Sn 118.71		Sb 121.757		Te 127.6		I 126.905		Xe 131.3	
Cs 132.905		Ba 137.327		La		Hf 178.49		Ta 180.948		W 183.84		Re 186.207		Os 190.23		Ir 192.225		Pt 195.084		Au 196.967		Hg 200.59		Tl 204.377		Pb 207.2		Bi 208.98		Po (209)		At (210)		Rn (222)	
Fr (223)		Ra 226.025		Ac		Unq		Unp		Unh		Uns		Uno		Une		Unn																	

Lanthanide Series

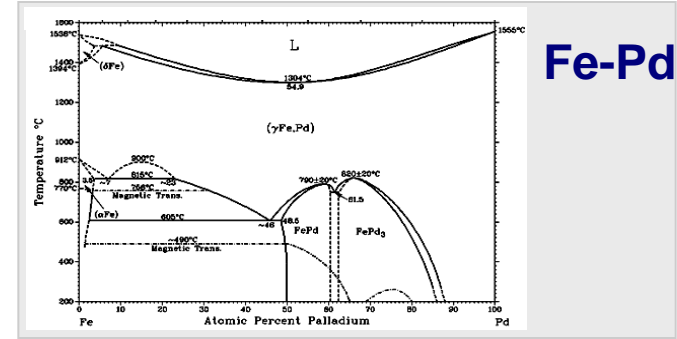
58	59	60	61	62	63	64	65	66	67	68	69	70	71
Ce	Pr	Nd	Pm	Sm	Eu	Gd	Tb	Dy	Ho	Er	Tm	Yb	Lu
140.12	140.908	144.24	(145)	150.4	151.96	157.25	158.925	162.50	164.93	167.26	168.93	173.04	174.96

Actinide Series

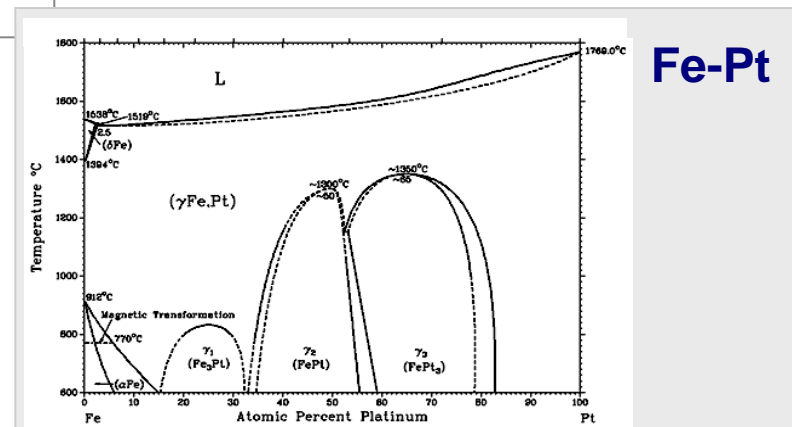
90	91	92	93	94	95	96	97	98	99	100	101	102	103
Th	Pa	U	Np	Pu	Am	Cm	Bk	Cf	Es	Fm	Md	No	Lr
232.0377	231.03688	238.02891	237.0471	(244)	(243)	(247)	(247)	(251)	(254)	(257)	(258)	(259)	(260)



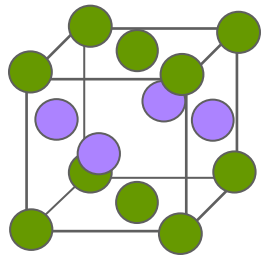
Fe-Ni



Fe-Pd



Fe-Pt

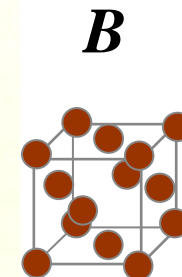
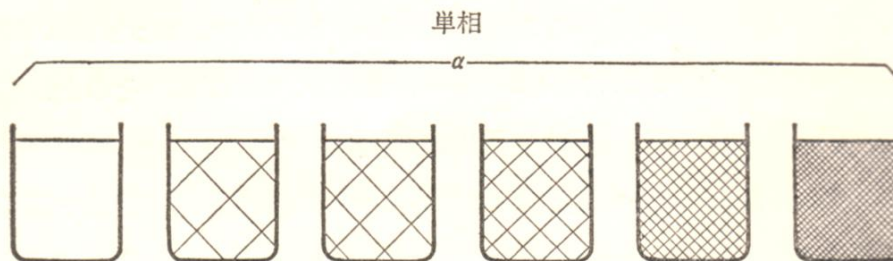
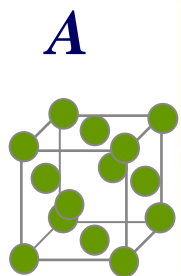


Mechanical property
High density magnetic recording media

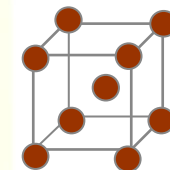
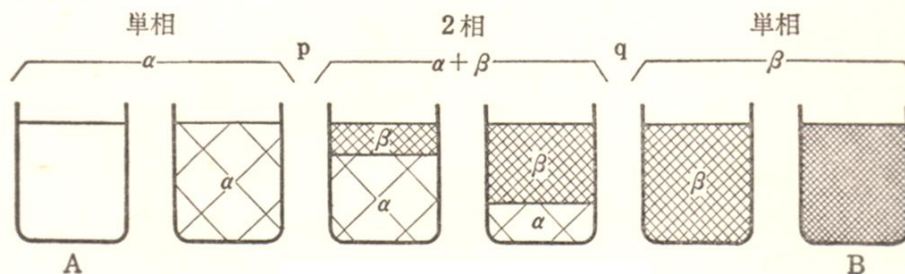
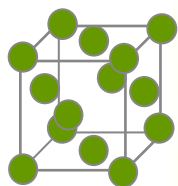
Basic concept



固溶体
Solid Solution

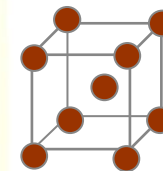
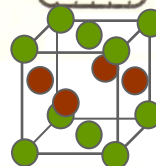
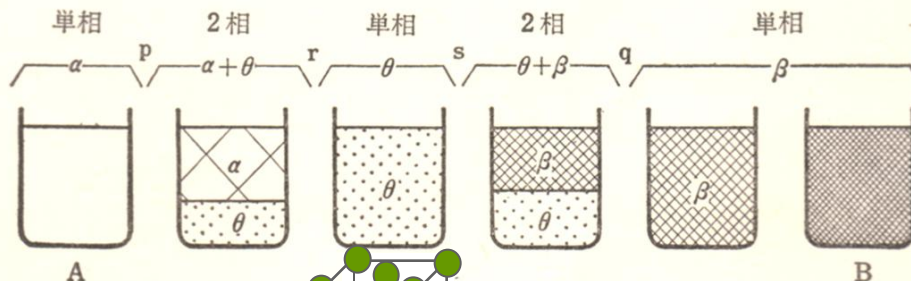
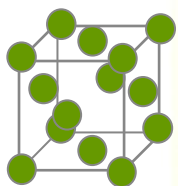


相分離
Phase separation

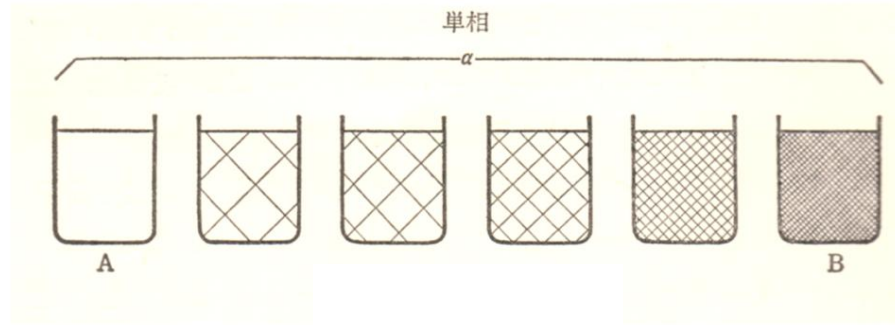
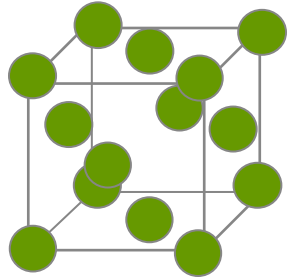


固溶限 Solubility limit

中間相
Intermediate phase



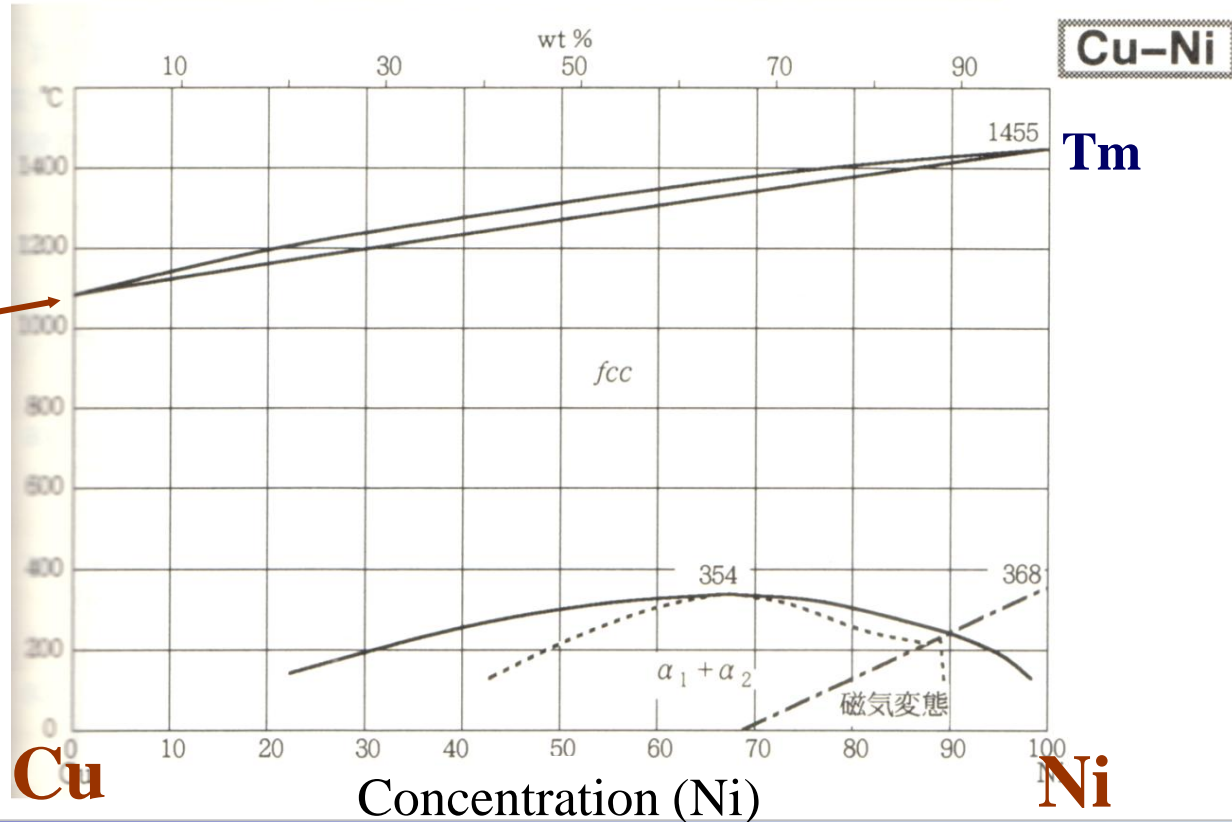
Ordered phase 規則相



Phase Diagram

融点
melting
point

Temperature (C)



Cu

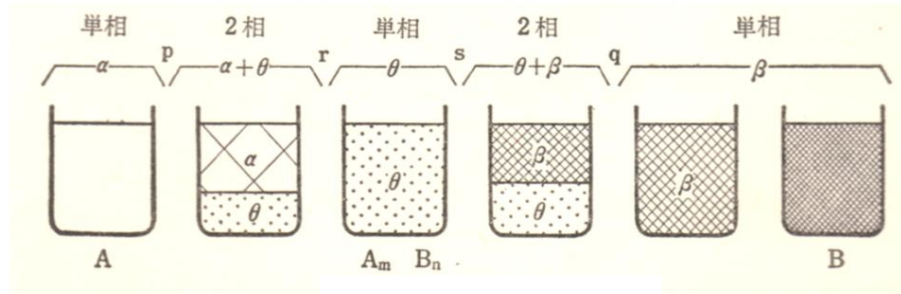
Concentration (Ni)

Ni

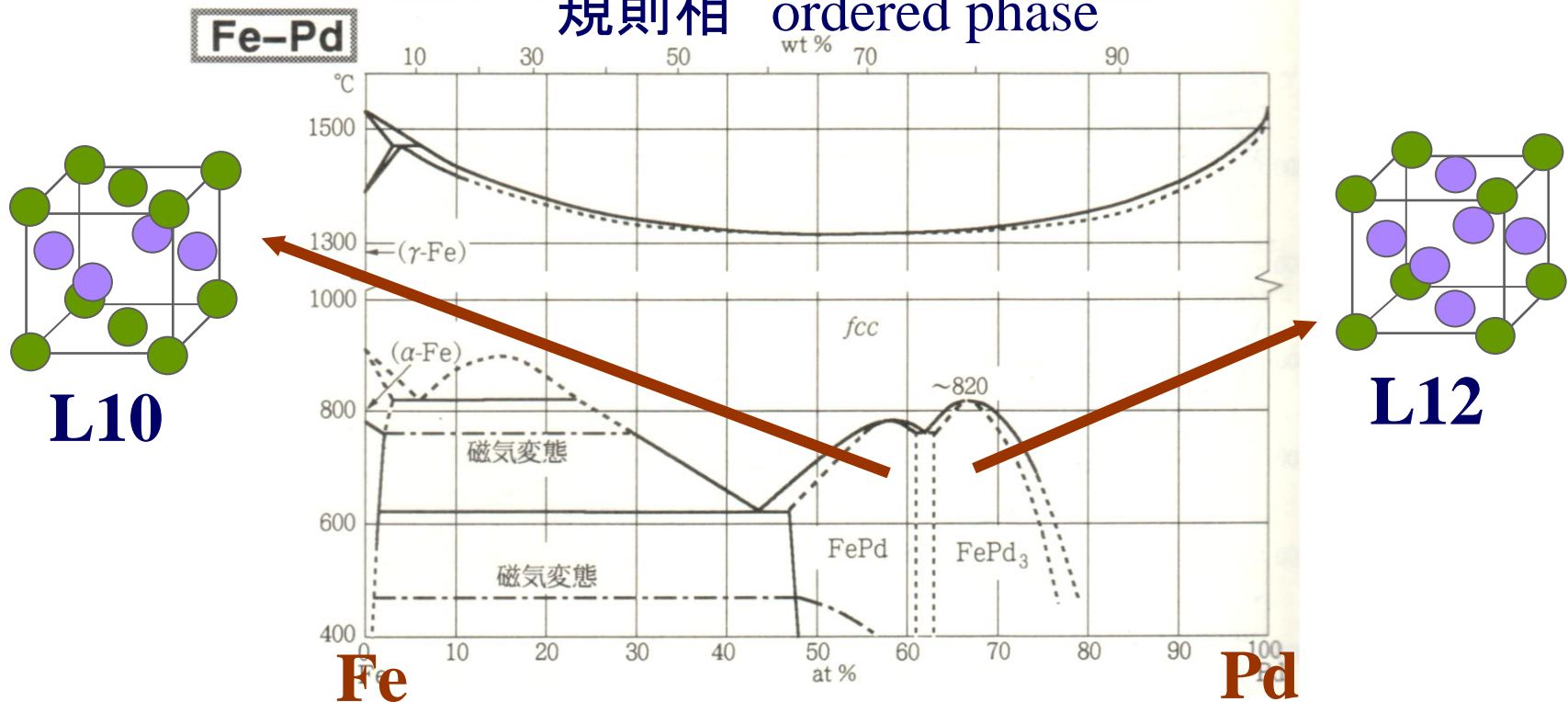


強度・靱性の付与

機能の付与



規則相 ordered phase





- Total energy calculation at the ground state: FLAPW
- Cluster Expansion Method (CEM)

$$\Delta E(V(r), \{\xi_i\}) = \sum_j v_j(V(r)) \cdot \xi_j^m$$

$$(i; \circ \quad \circ \circ \quad \triangle \quad \triangle \dots; \xi_i^m = \langle \sigma_1 \cdot \sigma_2 \cdots \sigma_i \rangle$$

$$v_i = \sum_m \left\{ \xi_j^m \right\}^{-1} \cdot \Delta E^{(m)}$$

- Cluster Variation Method (CVM)

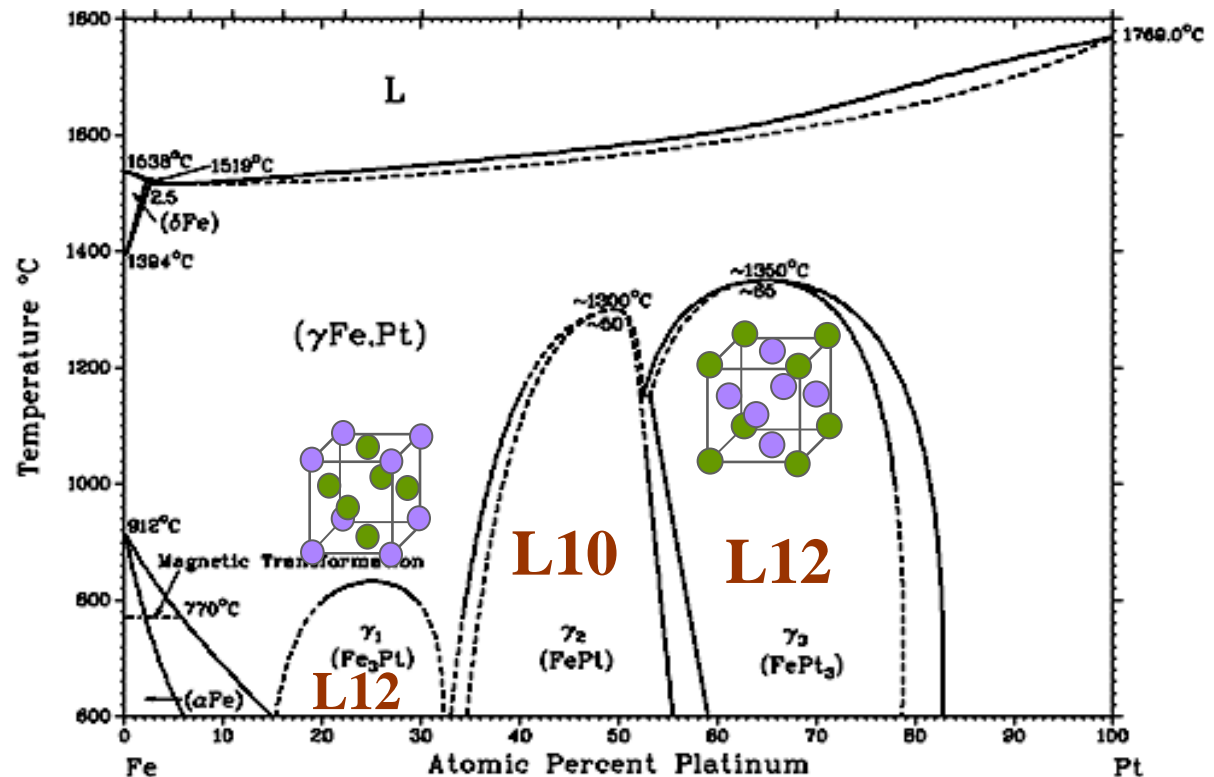
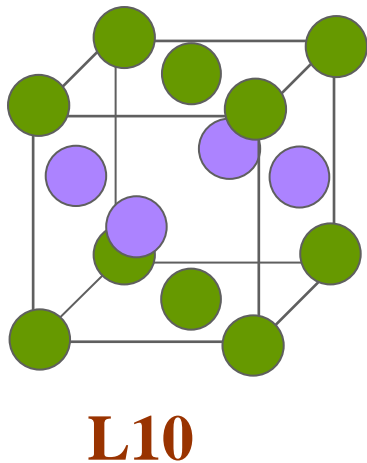
$$S = k_B \cdot \ln \frac{\prod_{i,j} \{N y_{ij}!\}^6 \cdot \{N!\}}{\prod_i \{N x_i!\}^5 \cdot \prod_{i,j,k,l} \{N w_{ijkl}!\}^2} \quad x_i, y_{ij}, (z_{ijk}), w_{ijkl} \rightarrow \{\xi_i\}$$

$$g(T, V(r), \{\xi_i\}) = E(V(r), \{\xi_i\}) - T \cdot S(\{\xi_i\})$$

Background Fe-Pt L10



First-principles calculation of phase stability and **L1₀-disorder** phase equilibria for **Fe-Pt** system

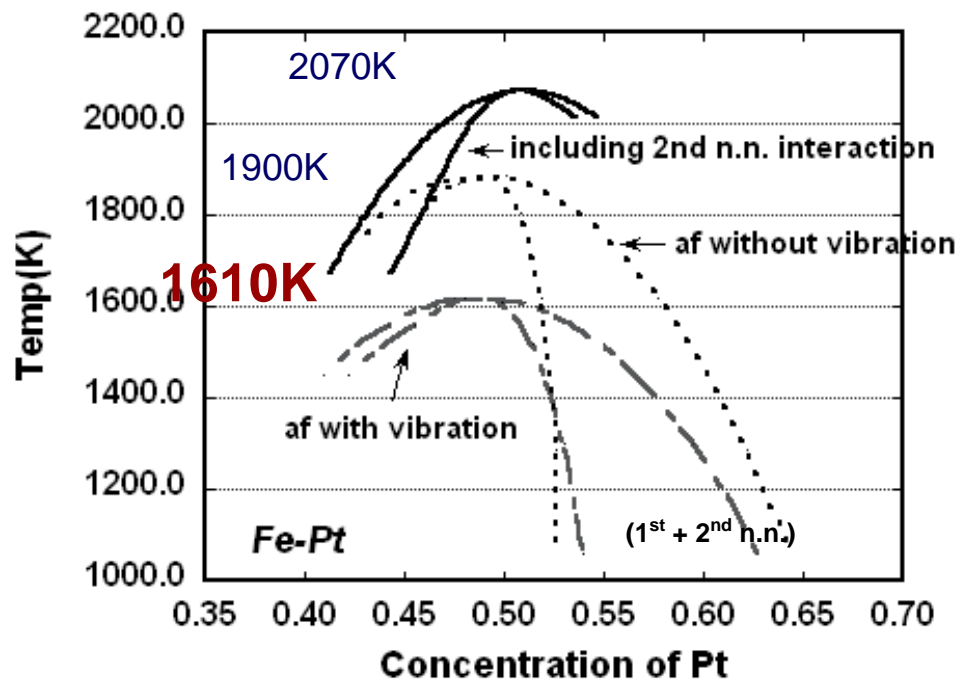


Phase Diagram



L10-disorder

Fe-Pt



Exp. 1600K

26, 78

Fe, Pt

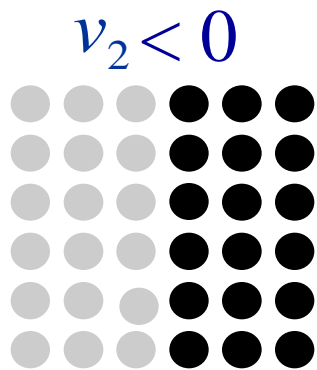


Entropy and Cluster Variation Method (CVM)

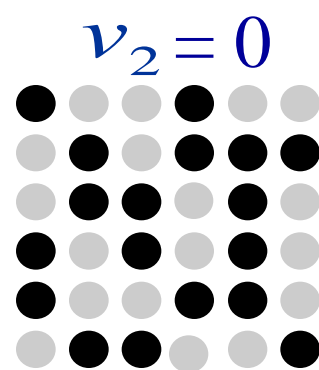
Bragg-Williams approx.

$$S = k_B \cdot \ln \frac{N!}{\prod_i \{N x_i!\}} = -k_B (x \ln x + (1-x) \ln(1-x)), F = F(x)$$

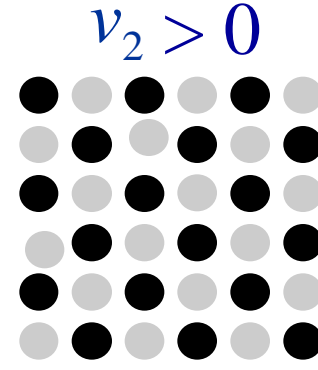
Local atomic configuration ?



$$y_{AA} = y_{BB} = 0.5$$



$$y_{AA} = y_{BB} = y_{AB}$$



$$y_{AB} = 1.0$$

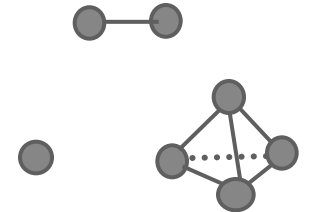
50%

$$F = F(x_i, y_{ij})$$

$$F = F(x_i, y_{ij}, z_{ijk} \dots)$$

CVM

$$S = k_B \cdot \ln \frac{\prod_{i,j} \{N y_{ij}!\}^6 \cdot \{N!\}}{\prod_i \{N x_i!\}^5 \cdot \prod_{i,j,k,l} \{N w_{ijkl}!\}^2}$$

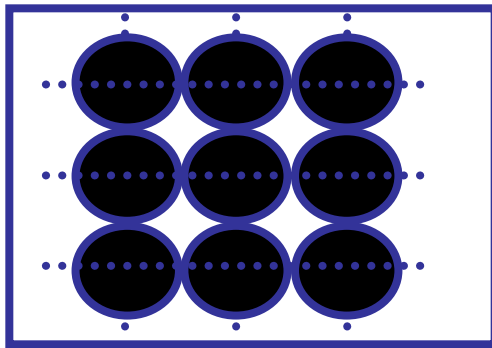


Phase Field Method

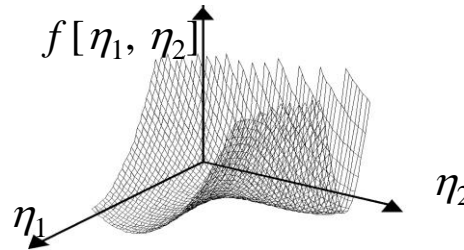


$$F_{chem} = \int (f [\{ \eta_i \}] + \sum_{i=1} \kappa_i (\nabla \eta_i)^2) \cdot dV$$

Microstructure

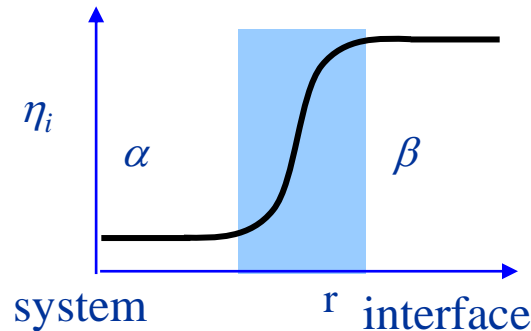


Free energy of microstructure



Free energy of homogeneous system

$\eta_i(\mathbf{r})$: field variable



r interface

Time evolution of $\eta_i(\mathbf{r})$

Conserved

C

Non-Conserved

LRO

$$\frac{\partial \eta_i}{\partial t} = -\nabla \cdot \left(-M \nabla \frac{\delta F_{chem}}{\delta \eta_i} \right)$$

$$\frac{\partial \eta_i}{\partial t} = -\sum_j L_{ij} \frac{\delta F_{chem}}{\delta \eta_j}$$

κ_i : gradient energy coefficient,

M : mobility

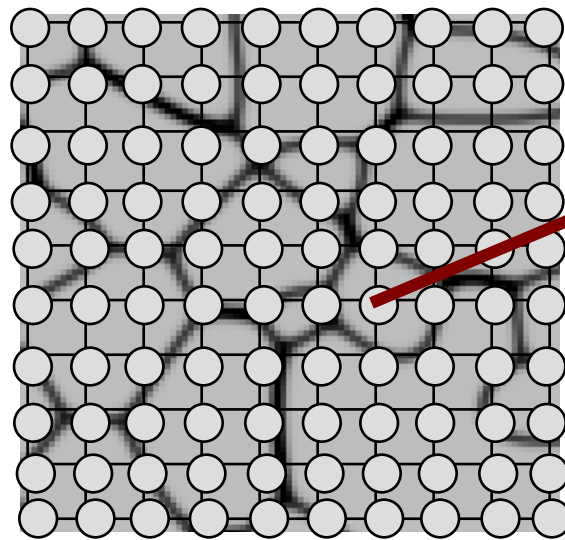
L_{ij} : relaxation constant.

Hybrid Model

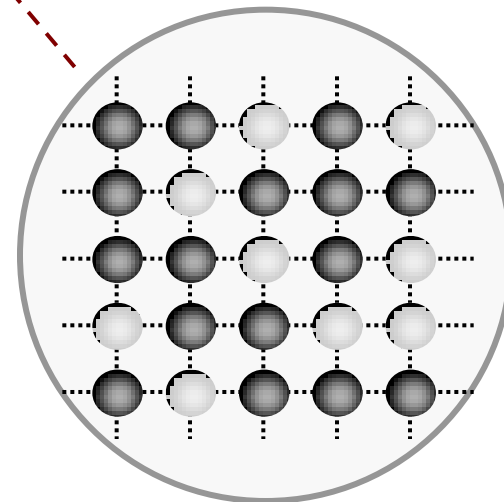


1:1

$$\frac{\partial \xi_i}{\partial t} = -L_i \left\{ \frac{\partial f_{\text{CVM}}}{\partial \xi_i} - \kappa_i \nabla^2 \xi_i \right\}$$

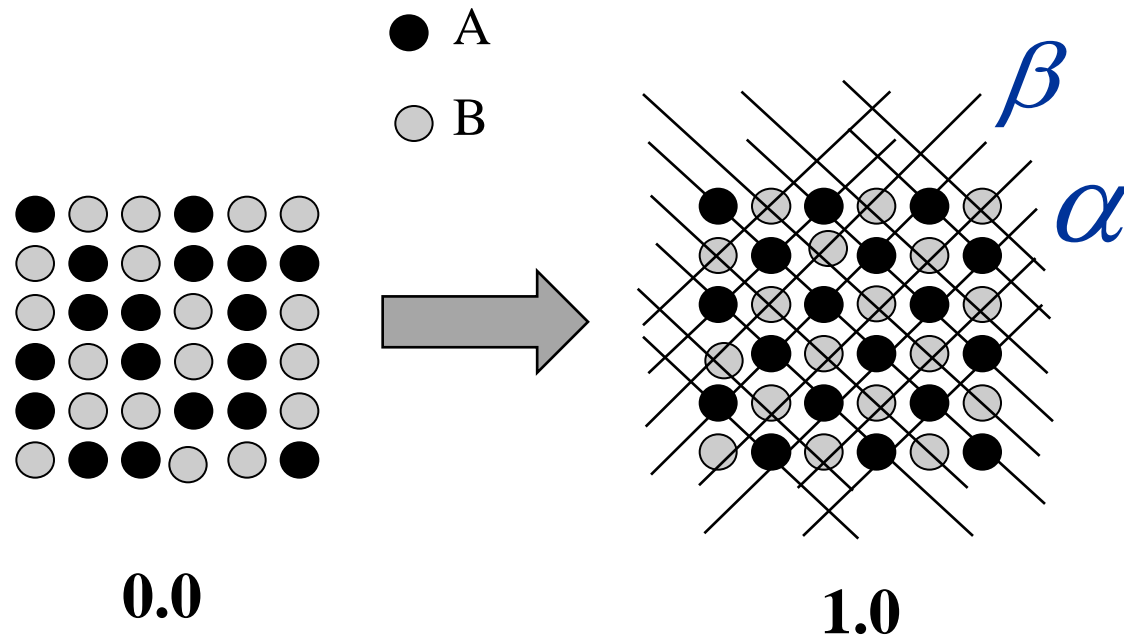


Microstructure
PFM



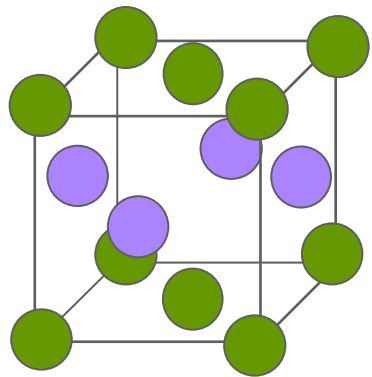
Atomistic
CVM
Multi-scale

Long Range Order parameter

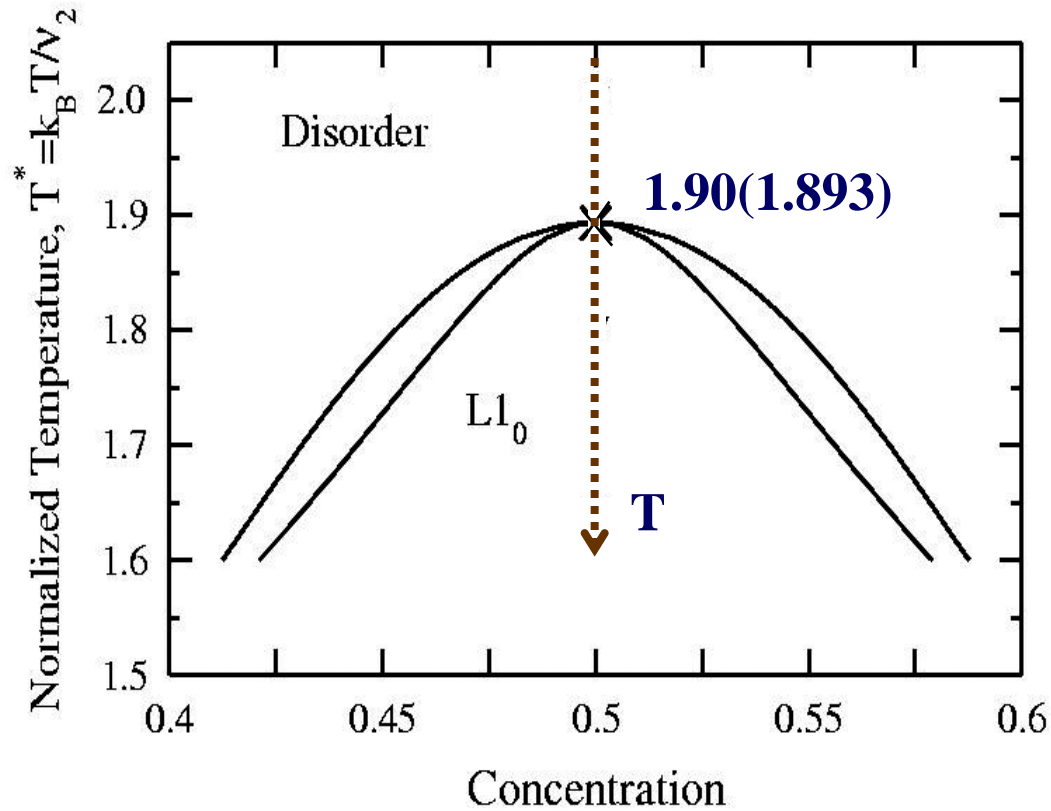


LRO $\eta = x_A^\alpha - x_A^\beta$

Preliminary calculation



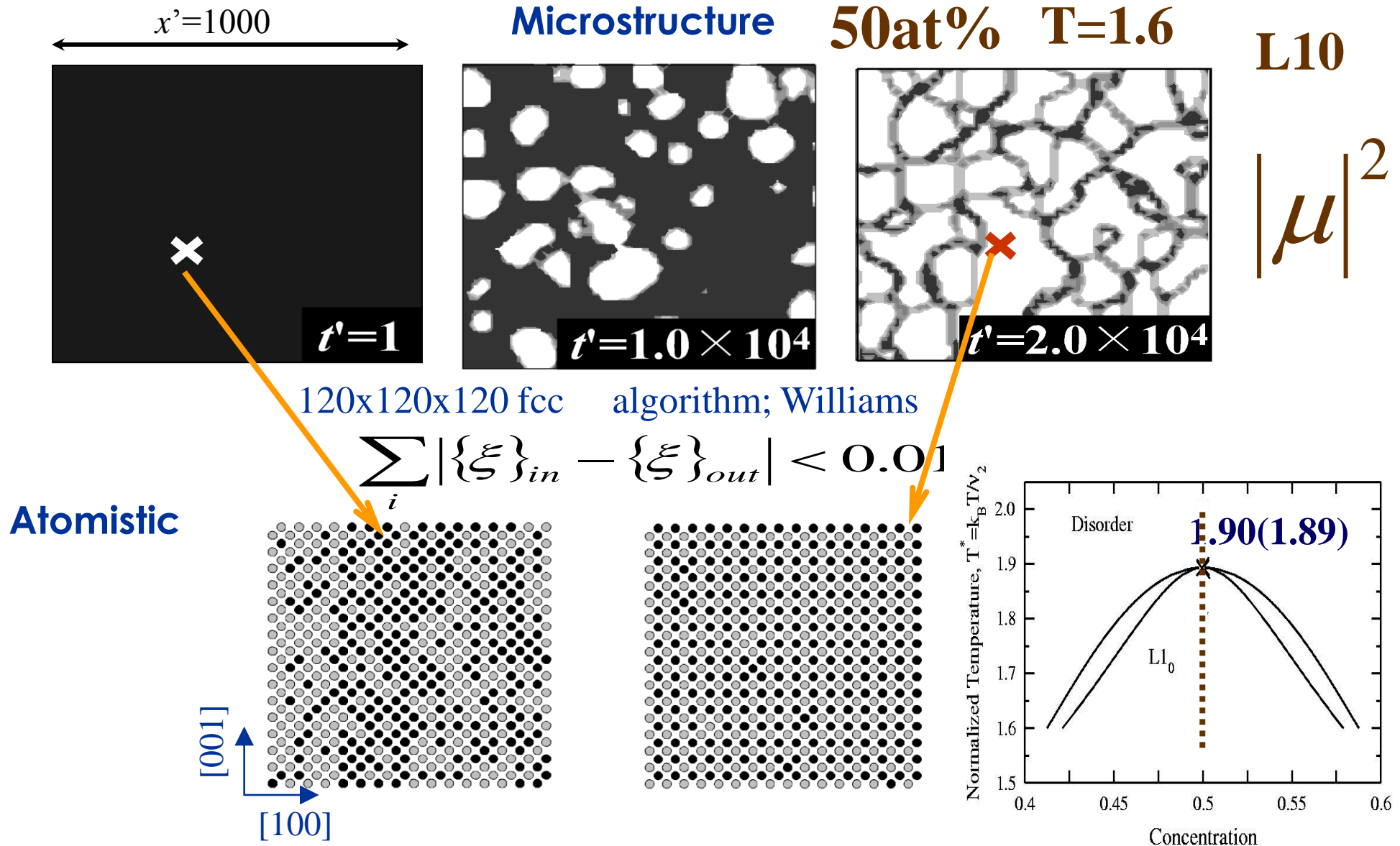
L10



V_2 ; n.n. effective pair interaction energy



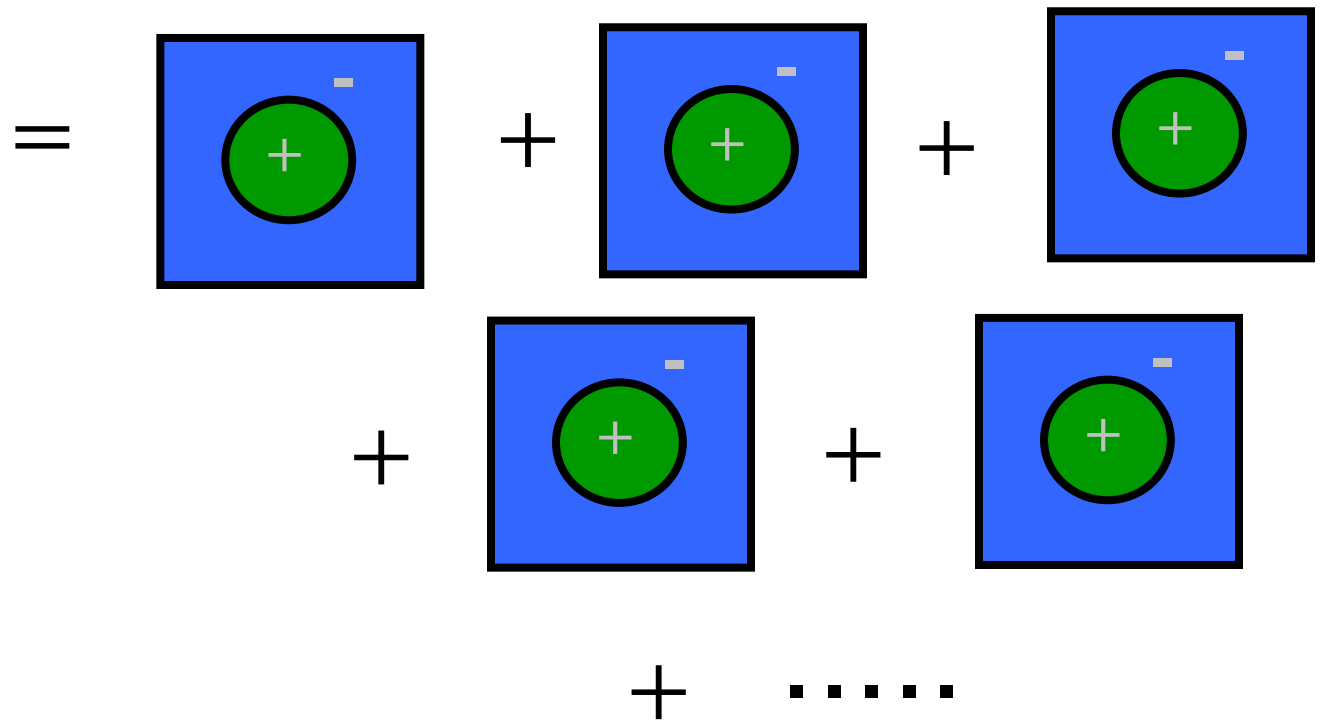
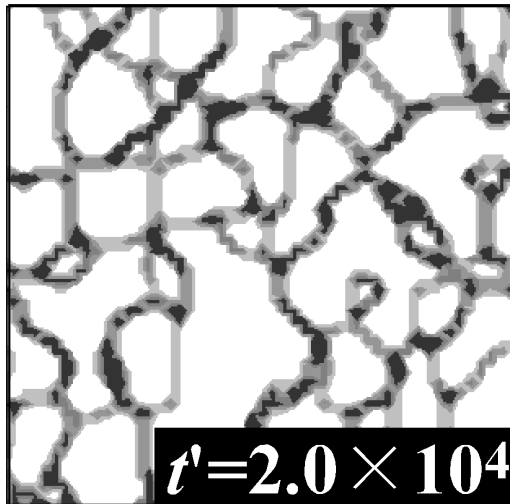
Simultaneous calculations for Multi-scales



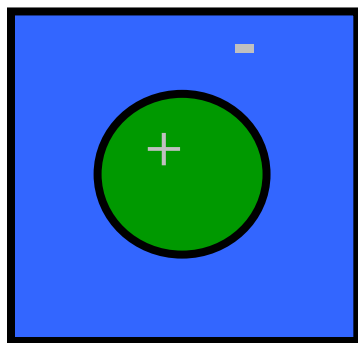


Elementary processes

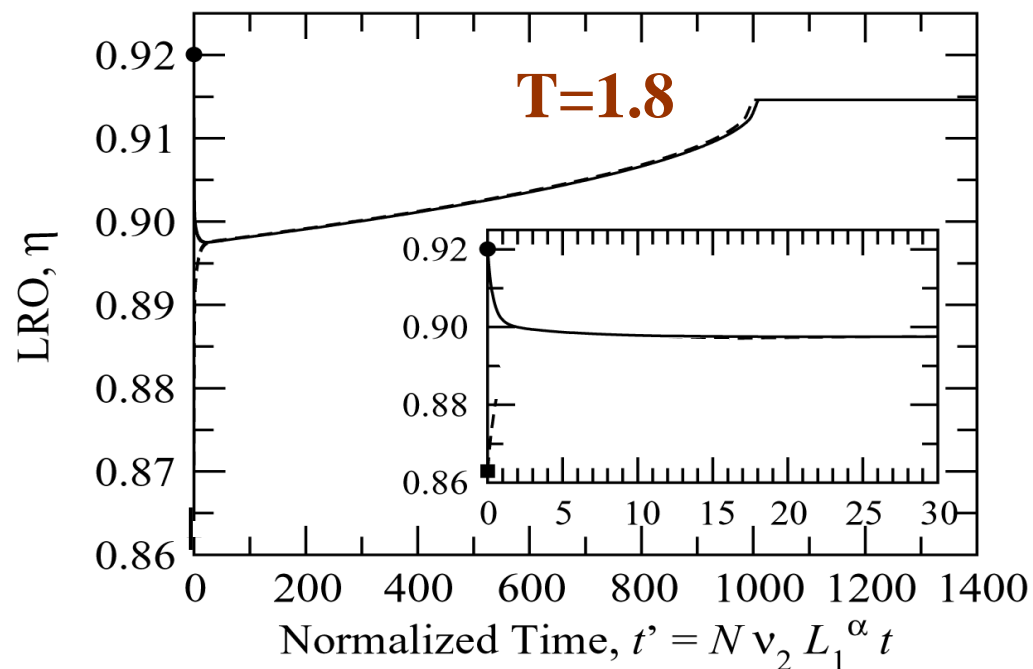
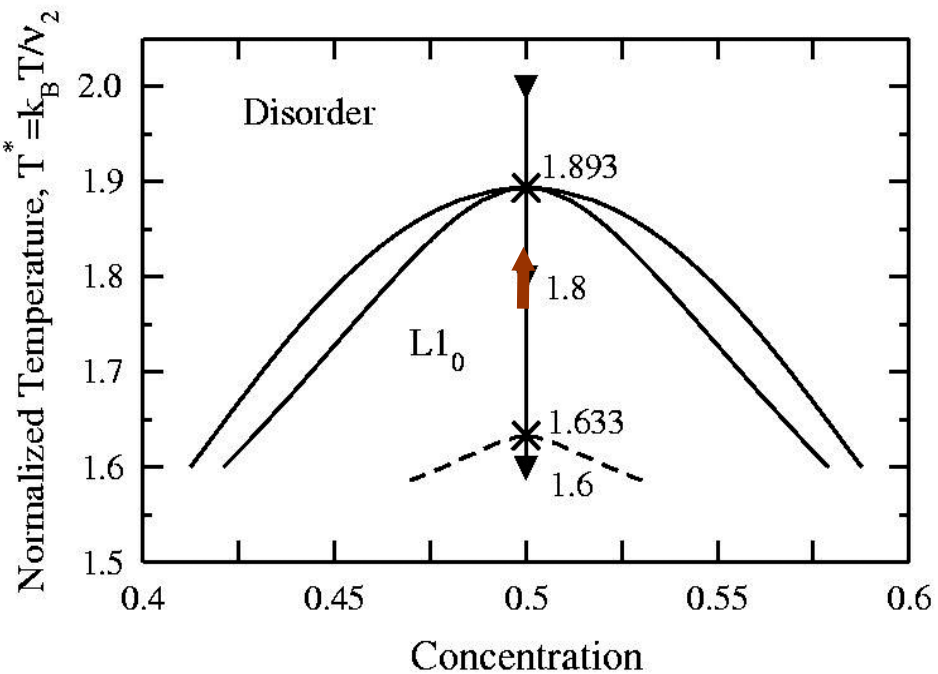
Circle shaped APB



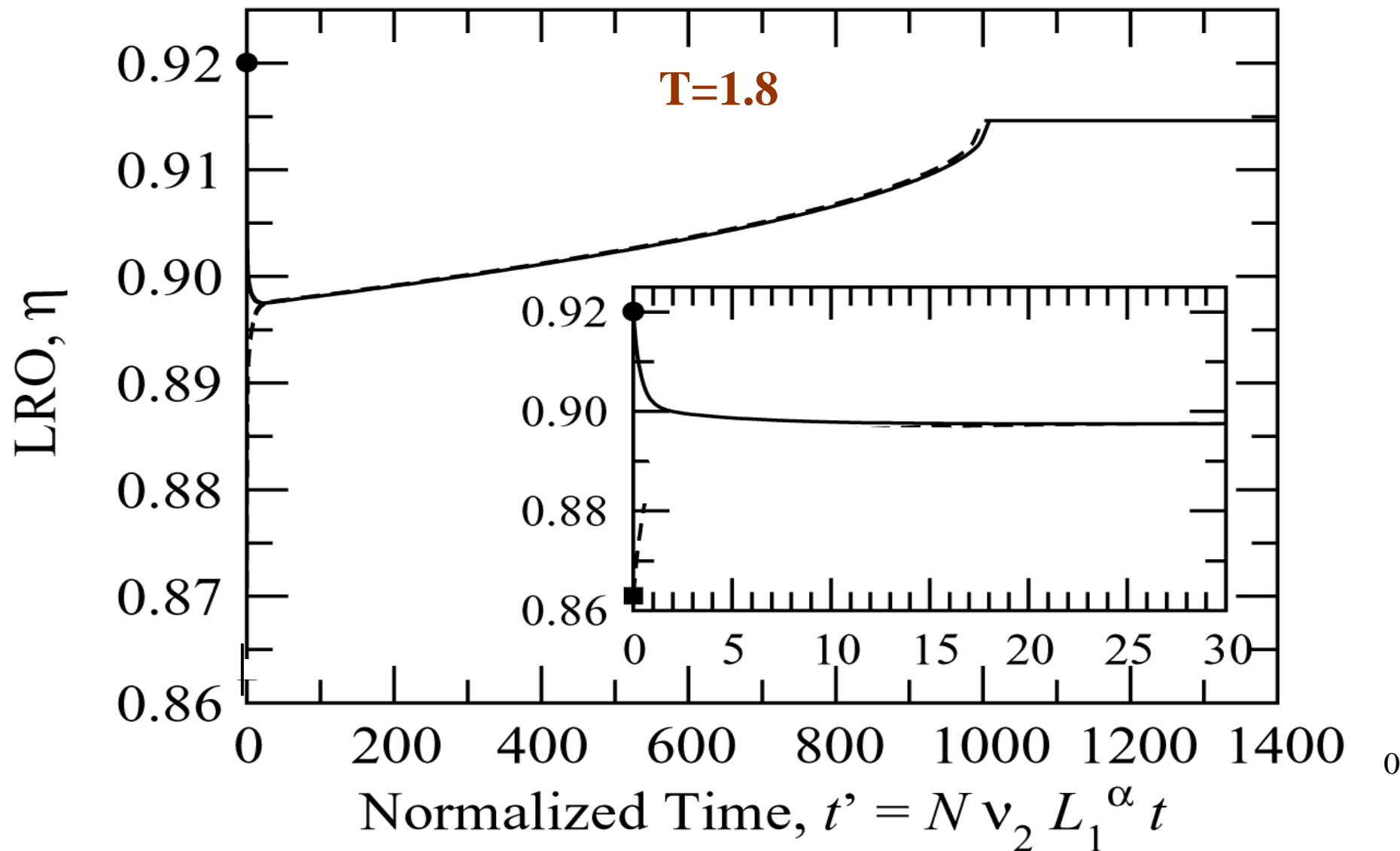
Kinetics of a Circle Shaped APB



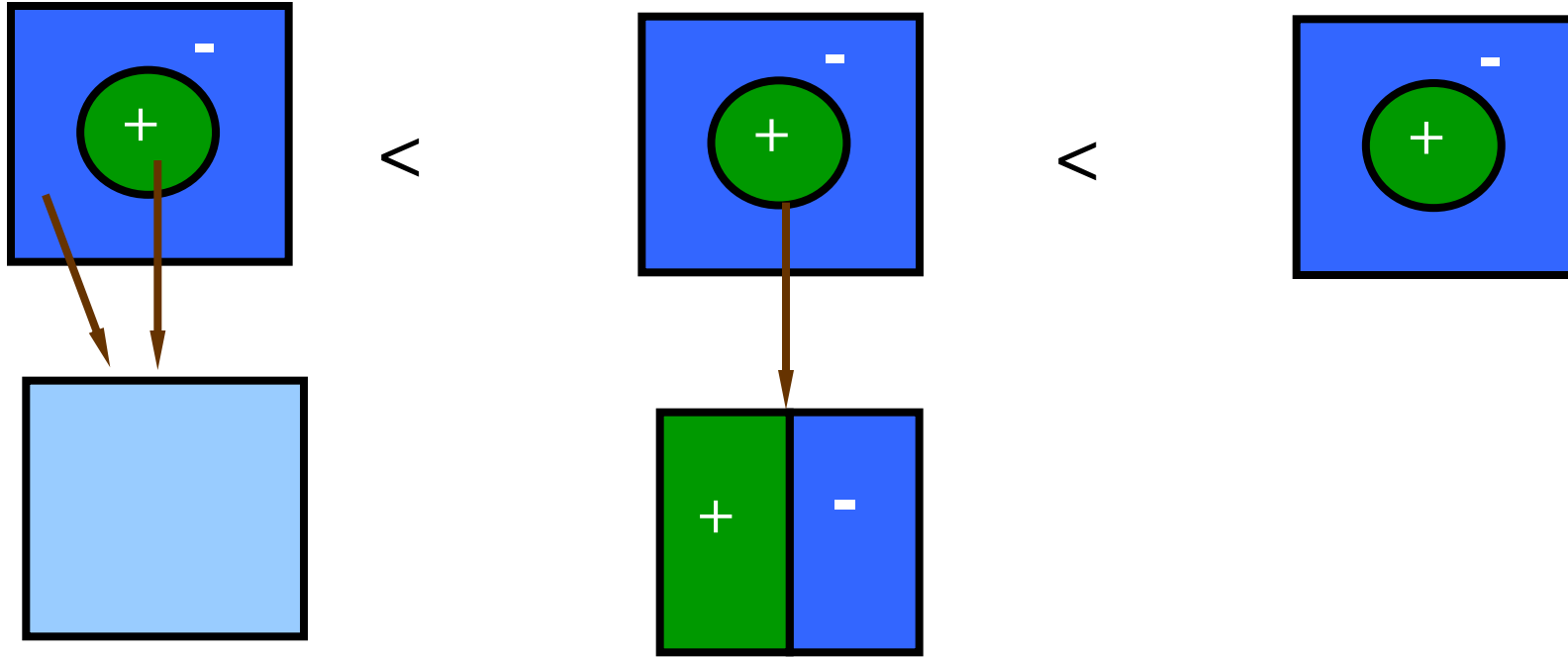
$T=1.75 \rightarrow 1.8$



Kinetics of a circle shaped APB



Elementary process



1. inside/outside APB

homogeneous

$\tau_u = 1 \sim 3$
diffusion

2. at APB

line-shaped APB

3. movement of APB

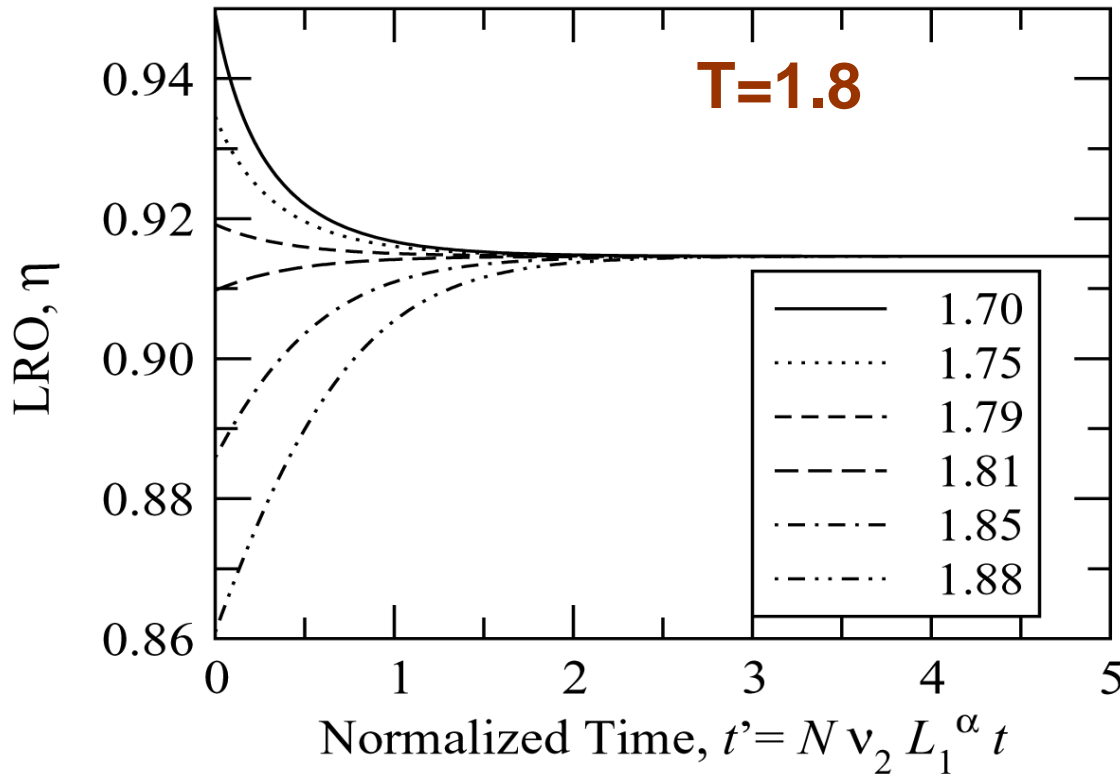
$\tau_u > 100$



kinetics of a Uniform System



$$\frac{\partial \xi_i}{\partial t} = -L_i \left(\frac{\partial f_{CVM} [\{\xi_i\}]}{\partial \xi_i} - \kappa \xi_i^2 \right)$$

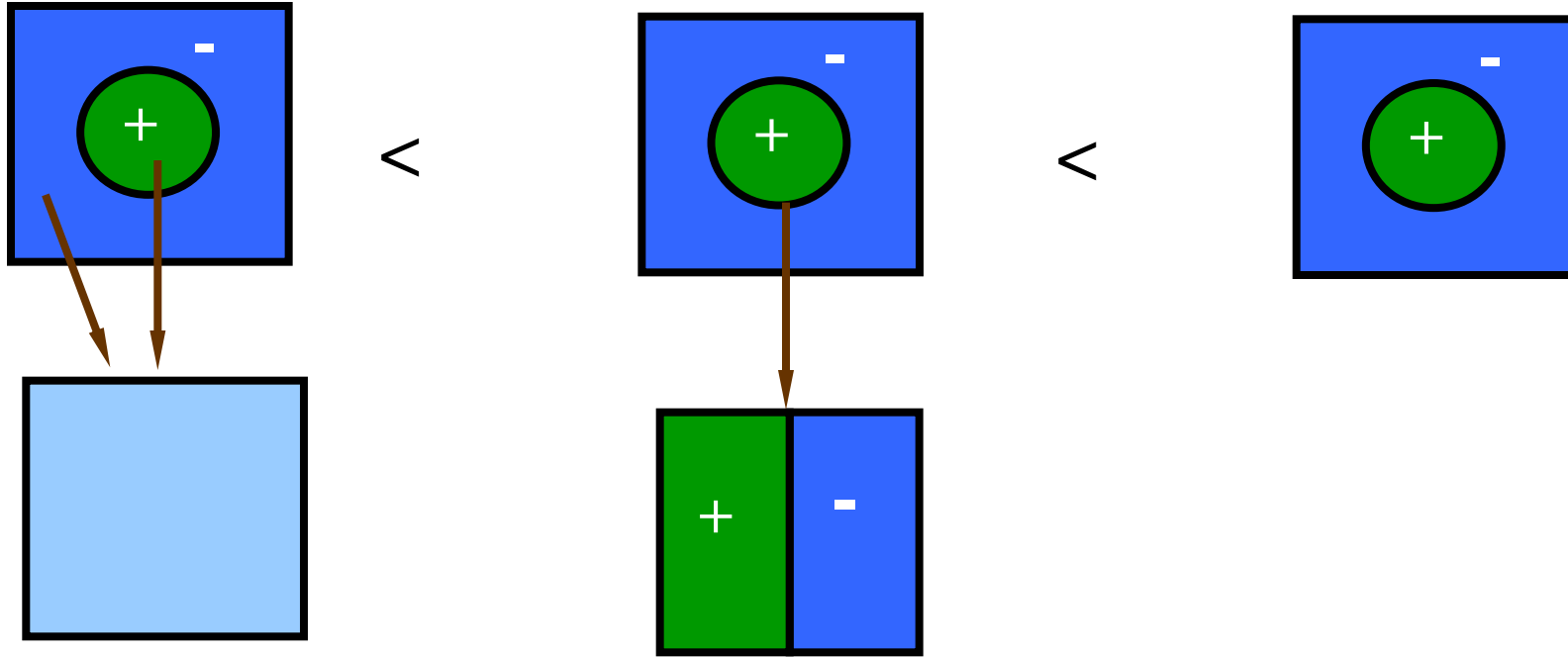


η_e

$$\eta(t) = a \cdot \exp\left(-\frac{t}{\tau_u}\right) + \eta_e$$

$$\tau_u = 1 \sim 3$$

Elementary process



1. inside/outside APB

homogeneous

$$\tau_u = 1 \sim 3$$

diffusion

2. at APB

line-shaped APB

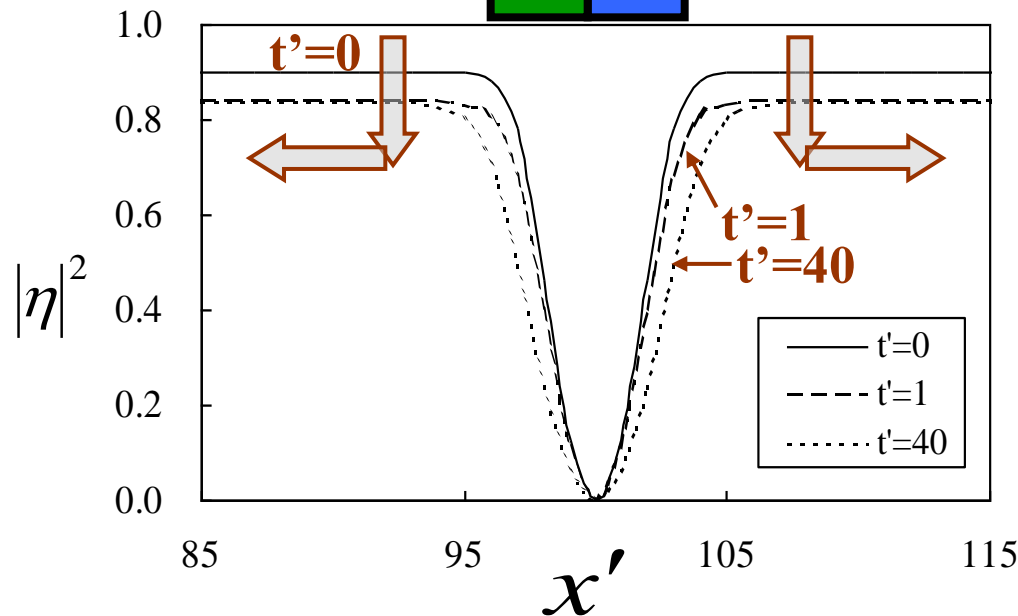
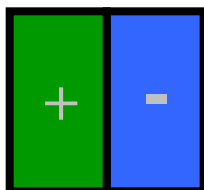
3. movement of APB

$$\tau_u > 100$$

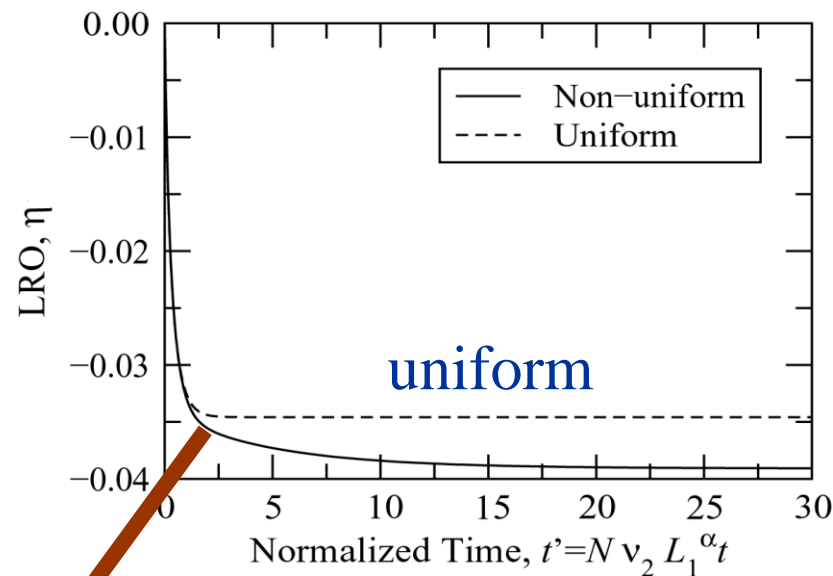
Kinetics of a line-shaped APB



$T=1.7 \longrightarrow 1.8$



Wetting

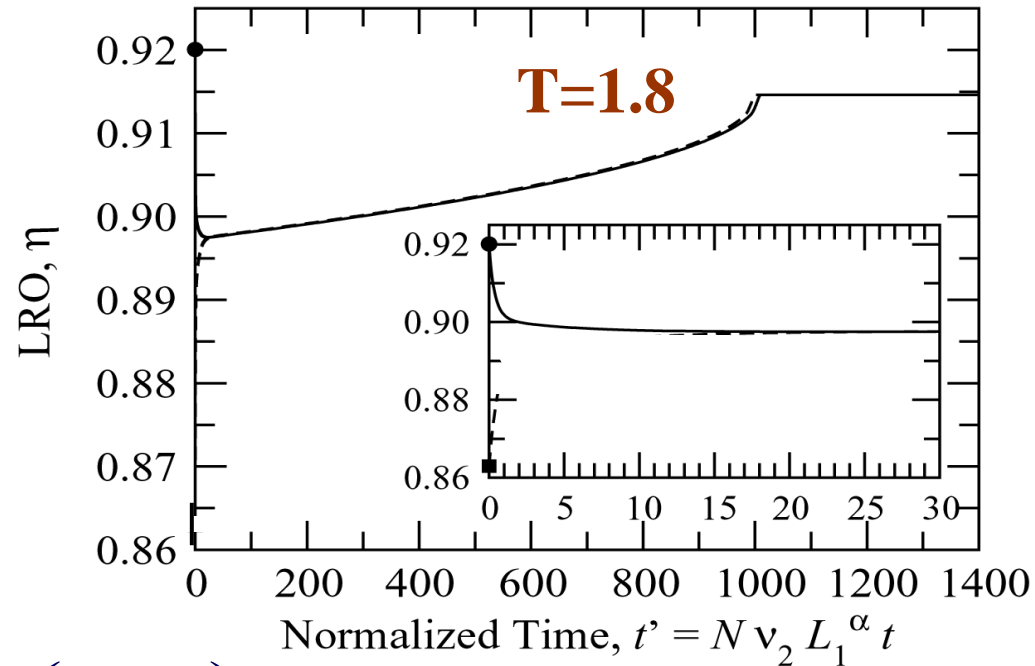
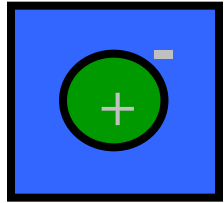


$$\eta(t) = a_f \exp\left(-\frac{t}{\tau_f}\right) + a_s \cdot \exp\left(-\frac{t}{\tau_s}\right) + \eta_e$$

$$\tau_f = 1 \sim 3 \quad \tau_s = 10 \sim 30$$

$$x' = x \cdot \sqrt{(N \cdot v_2) / (2\kappa_1^\alpha)}$$

Hybrid model and multi scale calc.



$$\eta(t) = a_f \exp\left(-\frac{t}{\tau_f}\right) + a_s \cdot \exp\left(-\frac{t}{\tau_s}\right) + \eta_{APB}(t) + \eta_e$$

atomistic

$$\tau_f = 1 \sim 3$$

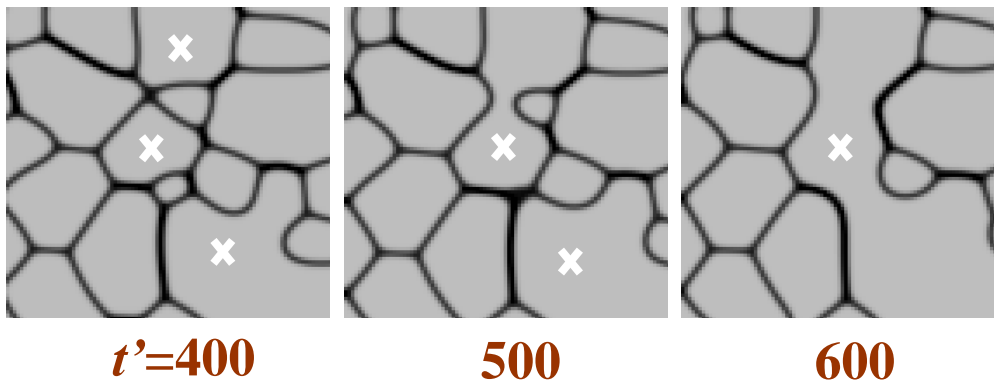
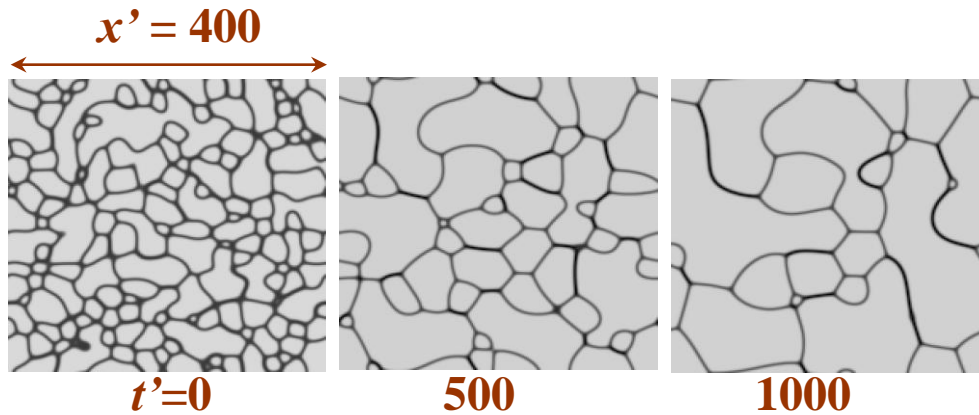
wetting

$$\tau_s = 10 \sim 30$$

motion

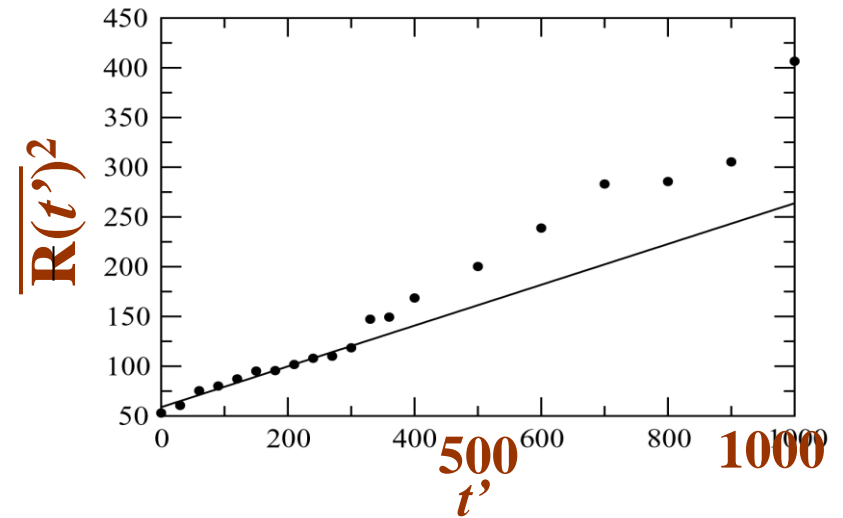
$$\tau > 100$$

Coarsening Process



Coalescence

T=1.8



Curvature driven growth

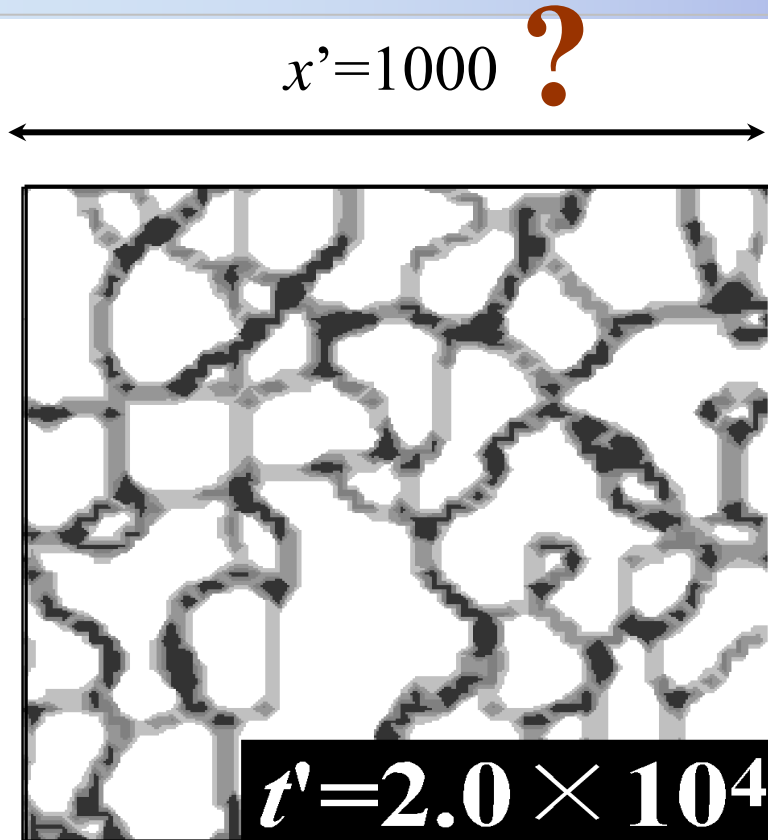
$$V_{APB} = 2\kappa L \cdot H$$

$$\langle R(t) \rangle^2 - \langle R(0) \rangle^2 = b \cdot t$$

H ; local mean curvature

$$\frac{\partial \xi_i}{\partial t} = -L_i \left(\frac{\partial f_{CVM}[\{\xi_i\}]}{\partial \xi_i} - \kappa_i \nabla^2 \xi_i \right)$$

Scale?



$$x' = x \cdot \sqrt{(N \cdot v_2) / (2\kappa_1^\alpha)}$$

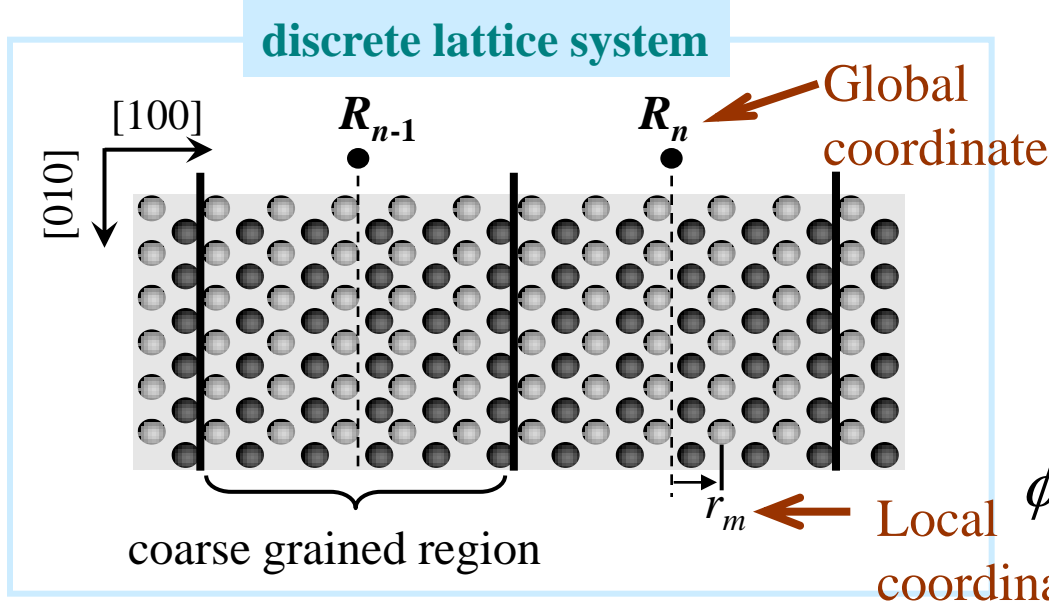
Spatial scale

Crystallographic orientation

v_2 : **Pair interaction energy**

κ_i : **gradient energy coeff.**

Atomistic model of APB



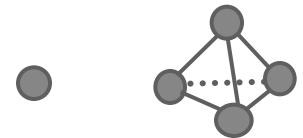
cells

R_n ; Global coordinate

r_m ; Local coordinate

$p_l = R_n + r_m$; atomic plane

$\phi_s(R_n + r_m + h(a))$; cluster probability



$$F = \sum_l f_{CVM}(p_l) = \sum_{n,m} f_{CVM}[\{\phi_s(R_n + r_m + h(a))\}]$$

$$\phi_s(R_n + r_m + h(a)) \cong \phi_s(\underline{R_n}) + (r_m + h(a)) \cdot \nabla \phi_s(R_n) + \frac{1}{2} (r_m + h(a))^2 \cdot \nabla^2 \phi_s(R_n)$$

$$F \cong \sum_{n,m} f_{CVM}(r_m + h(a), \{\phi_s(R_n)\}, \{\nabla \phi_s(R_n)\}, \{\nabla^2 \phi_s(R_n)\})$$



Coarse Graining [2]

$$F \cong \sum_{n,m} f_{CVM} \left(r_m + h(a), \underbrace{\{\phi_s(R_n)\}}_{\downarrow}, \underbrace{\{\nabla \phi_s(R_n)\}}_{\downarrow}, \underbrace{\{\nabla^2 \phi_s(R_n)\}}_{\downarrow} \right)$$

$$f_{CVM} \left(r_m + h(a), \{\phi_s(R_n)\}, 0, 0 \right)$$

$$F \cong \sum_n \left\{ \underbrace{\sum_m f_{CVM}(\{\phi_s(R_n)\})}_{\text{homogeneous state}} + \sum_{m,s} \frac{\partial f_{CVM}}{\partial(\nabla \phi_s)} \Big|_0 (\nabla \phi_s) + \sum_{m,s} \frac{\partial f_{CVM}}{\partial(\nabla^2 \phi_s)} \Big|_0 (\nabla^2 \phi_s) + \frac{1}{2} \sum_{m,s,s'} \frac{\partial^2 f_{CVM}}{\partial(\nabla \phi_s) \partial(\nabla \phi_{s'})} \Big|_0 (\nabla \phi_s)(\nabla \phi_{s'}) \right\}$$

*homogeneous
state*

$$= \sum_n \left\{ \sum_m f_{CVM}(\{\phi_s(R_n)\}) + \sum_{s,m} C_{1,s}(r_m, a, \{J\}) \cdot (\nabla \phi_s) + \sum_{m,s} C_{2,s}(r_m, a, \{J\}) \cdot (\nabla^2 \phi_s) + \sum_{m,s} C_{3,s}(r_m, a, \{J\}) (\nabla \phi_s)^2 \right\}$$

$$F = \frac{1}{L} \int \left\{ \sum_m f_{CVM}(\{\phi_s(R_l)\}) + \sum_{s,m} C_{1,s}(r_m, a, \{J\}) \cdot (\nabla \phi_s) + \sum_{m,s} C_{2,s}(r_m, a, \{J\}) \cdot (\nabla^2 \phi_s) + \sum_{m,s} C_{3,s}(r_m, a, \{J\}) (\nabla \phi_s)^2 \right\} dx$$



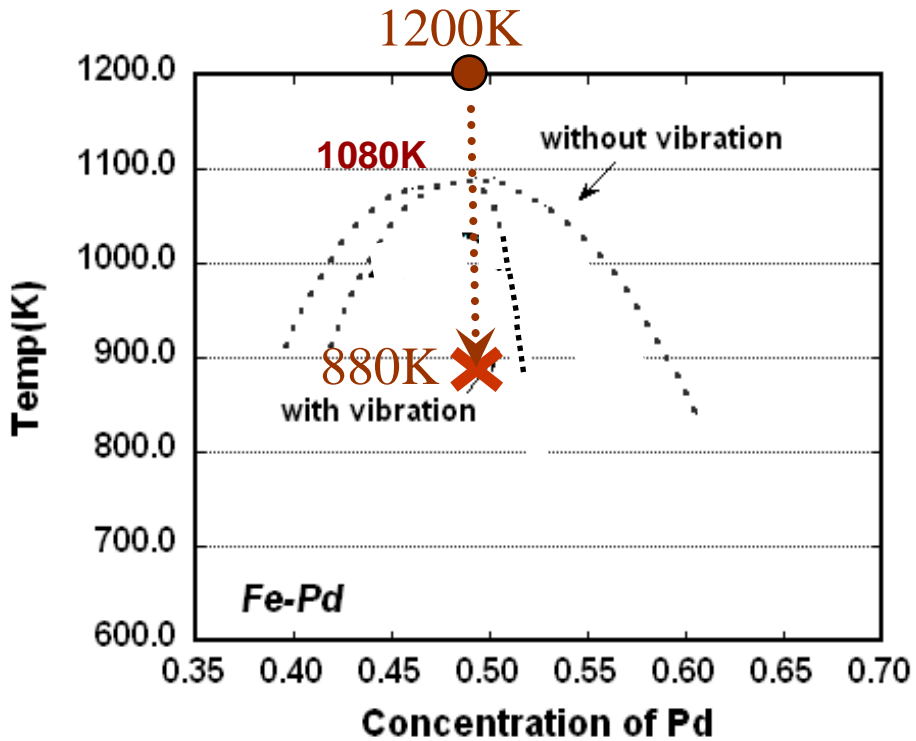
Ginzburg-Landau type

$$F = \frac{1}{L} \int \left[N' \cdot f_{CVM} [\{\phi_s\}] + \sum_{s,s'} \kappa_{s,s'} (\nabla \phi_s) (\nabla \phi_{s'}) \right] \cdot dx$$

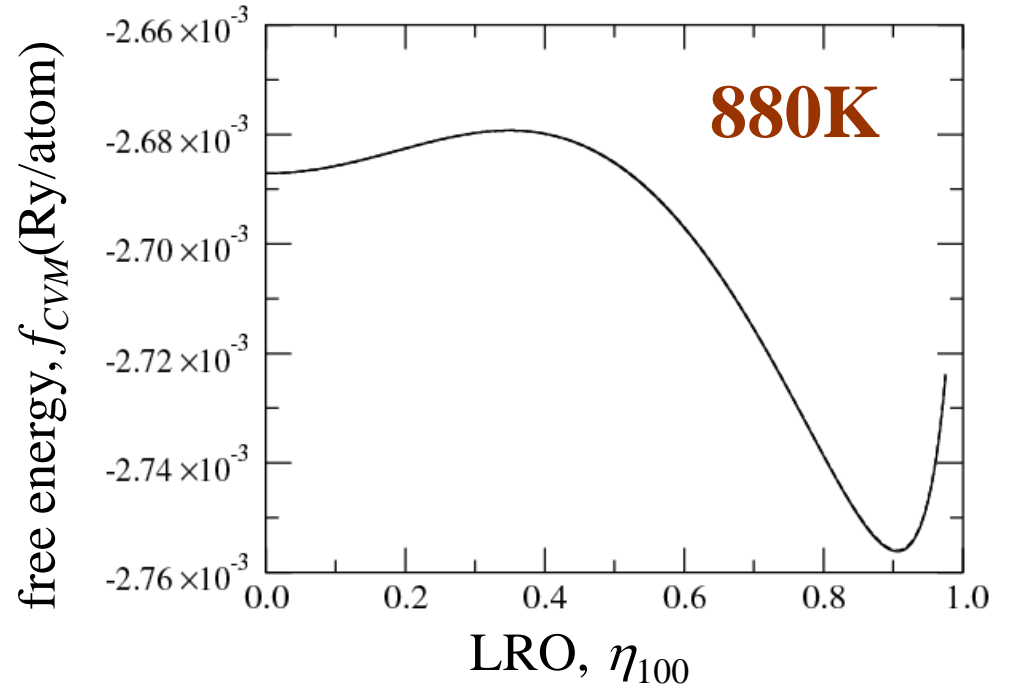
$$\kappa_{s,s'} = N \cdot k_B \cdot T \cdot \sum_J V_{s,s'}(r_m, a, \{J\})$$



Free energy -LRO profile



Fe-Pd



- lattice constant is optimized
- lattice constant is fixed at a_{dis}

$$f_{dis} = -2.687 \text{ (mRy/atom)}$$

$$f_{ord} = -2.756 \text{ (mRy/atom)}$$

$$\Delta f(f_{dis} - f_{ord}) = 0.069 \text{ (mRy/atom)}$$



First principles Microstructural Calculation

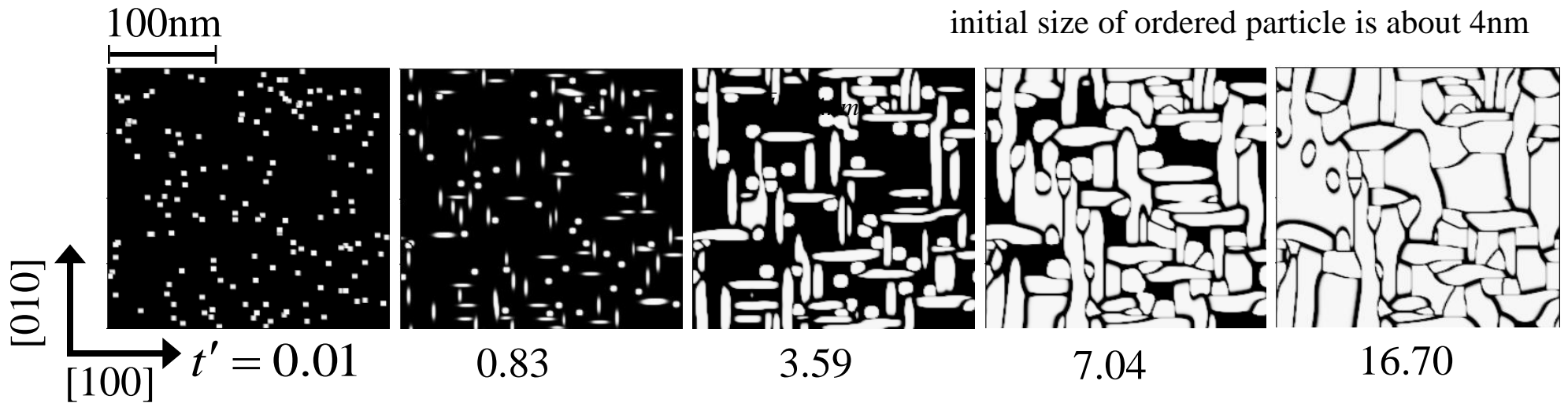
Fe-Pd

disorder – L1₀ at c=0.5

$$\bar{d}_{in} \approx 4nm$$

$$T=1200K \rightarrow 880K$$

initial size of ordered particle is about 4nm



$$\left| \nu_{2,2} / \nu_{2,1} \right| \approx 0.1$$

T-O approximation

$$t' = N \cdot L \cdot \Delta f \cdot t$$

PFM+PPM



科学技術基本計画

ライフサイエンス、情報通信、
環境、ナノテク・材料

構造用材料

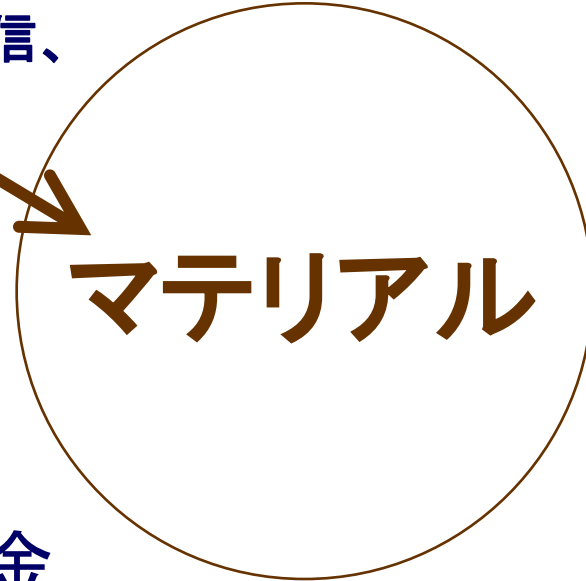
鉄鋼材料

高温耐熱合金

Fe, Ni, Cr, Co, Mo

高比強度軽金属合金

Ti, Al, Mg



マテリアル

ナノ材料

機能性材料

磁性、半導体物性、光物性

強度の高精度設計

エネルギー問題

経済効果

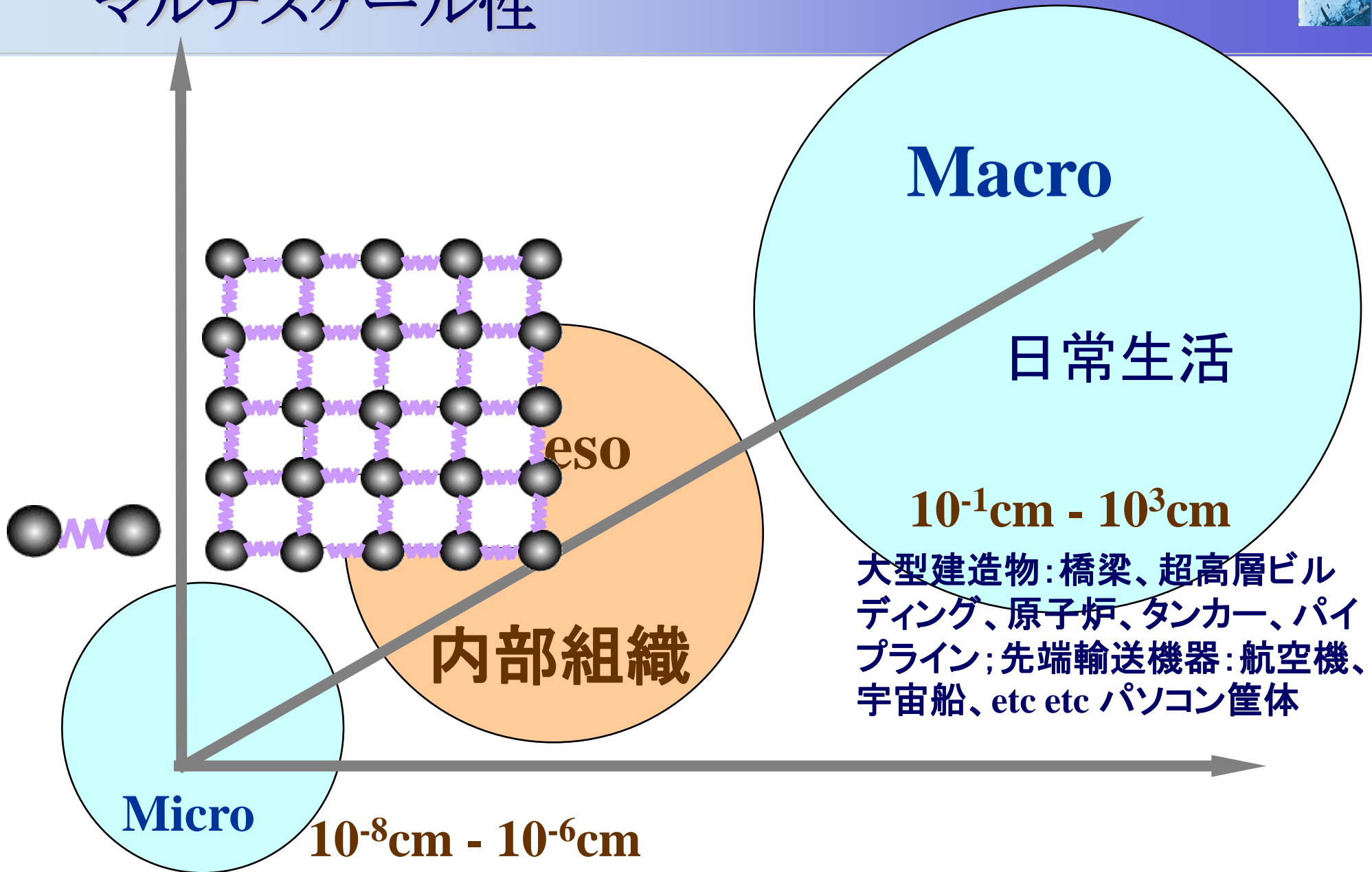
強度

強度の本質

強度の科学

大型建造物：橋梁、超高層ビルディング、原子炉、タンカー、パイプ
ライン；先端輸送機器：航空機、宇宙船、etc etc パソコン筐体

マルチスケール性

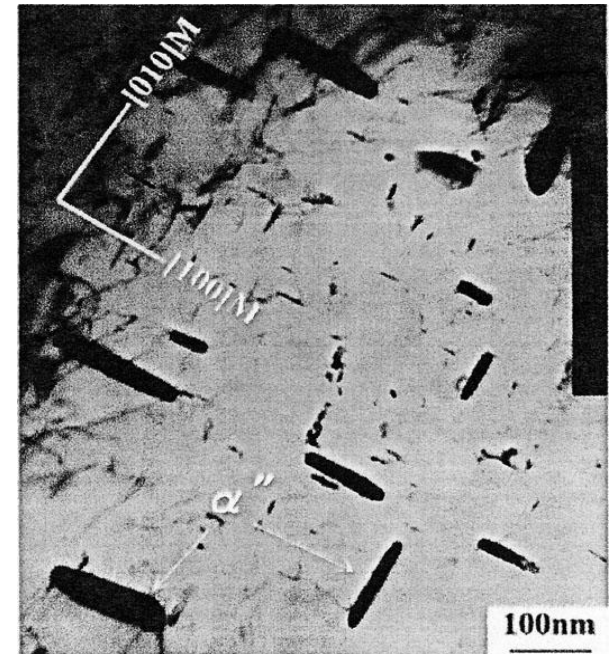
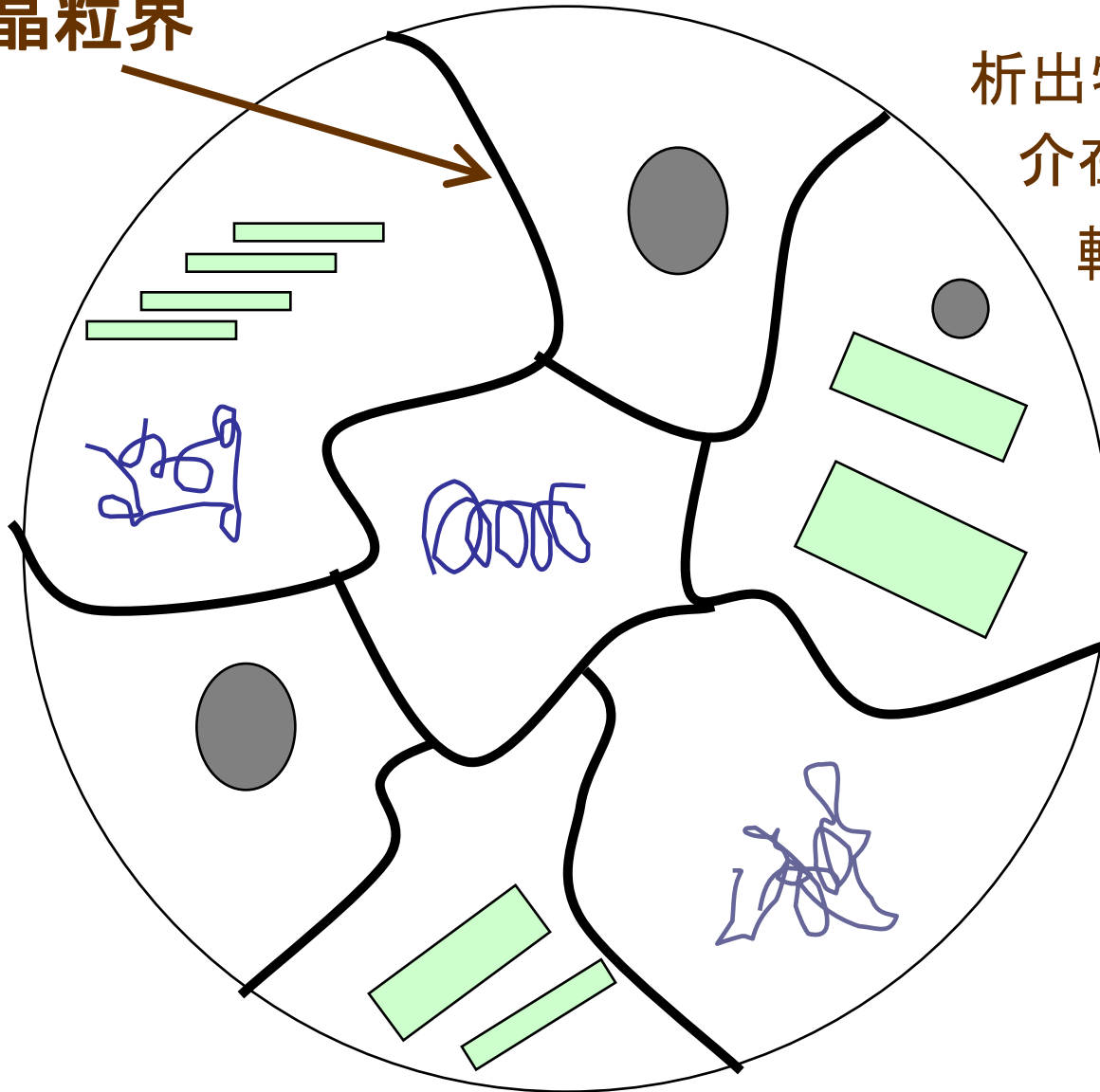


内部組織

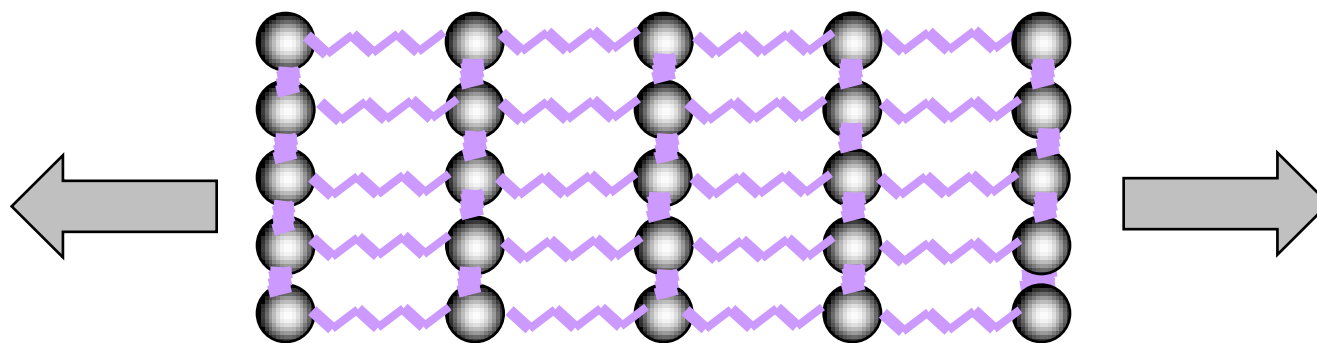
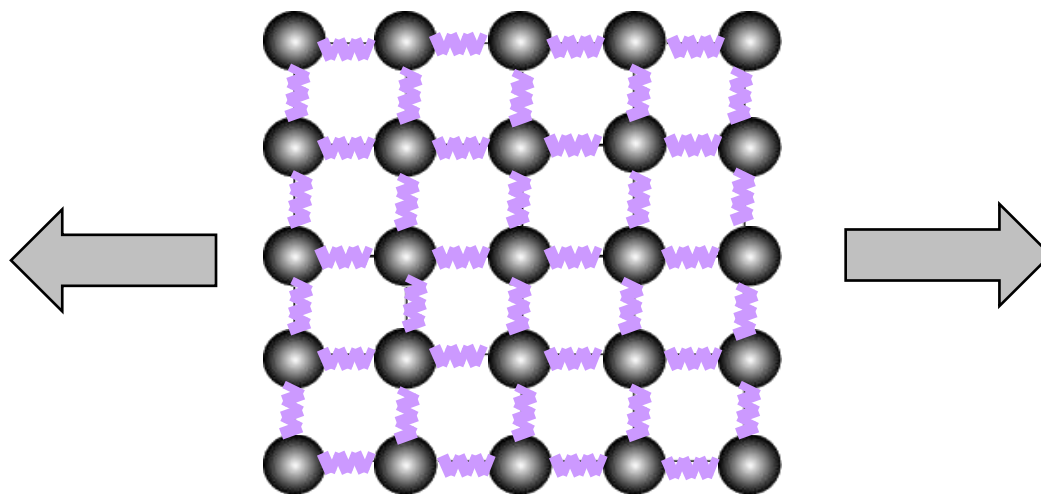


結晶粒界

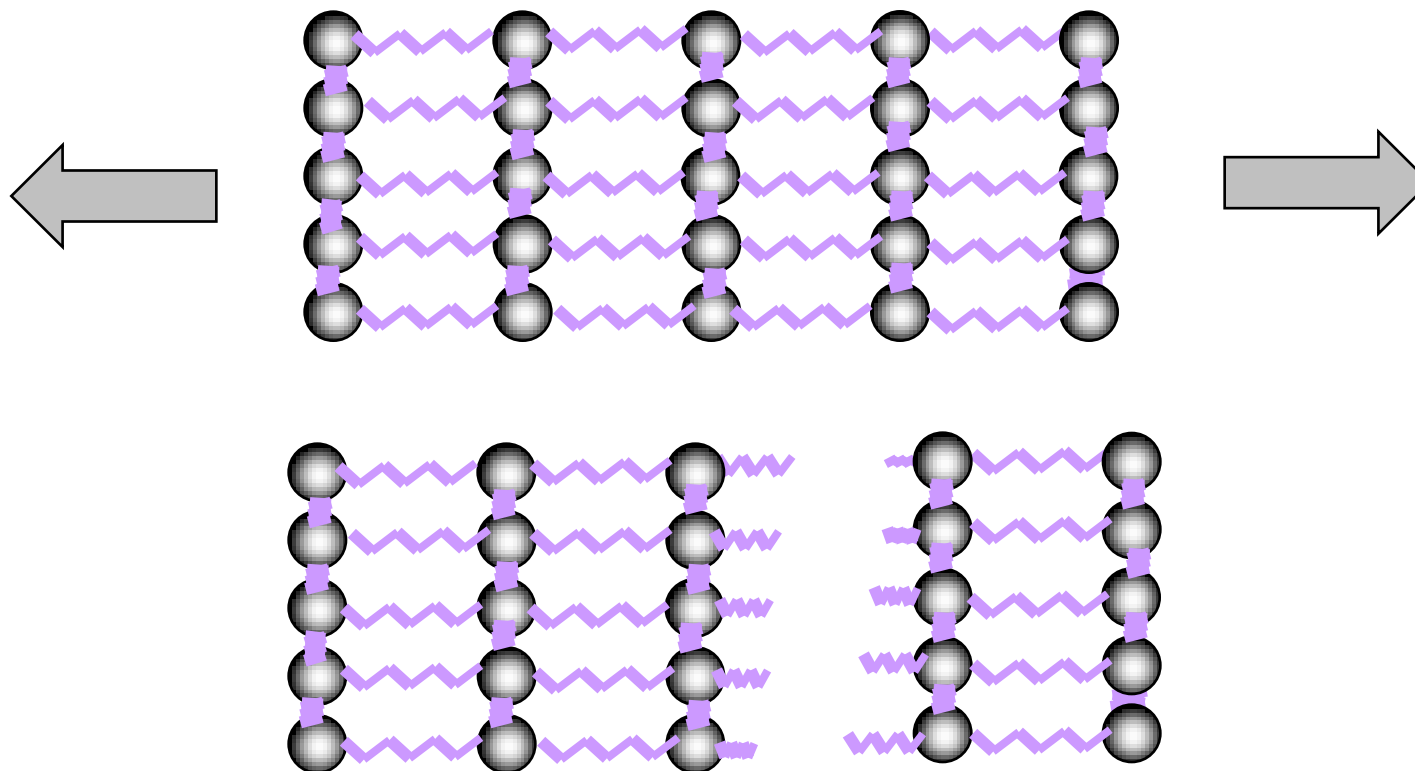
析出物
介在物
転位



変形過程 (弾性変形)

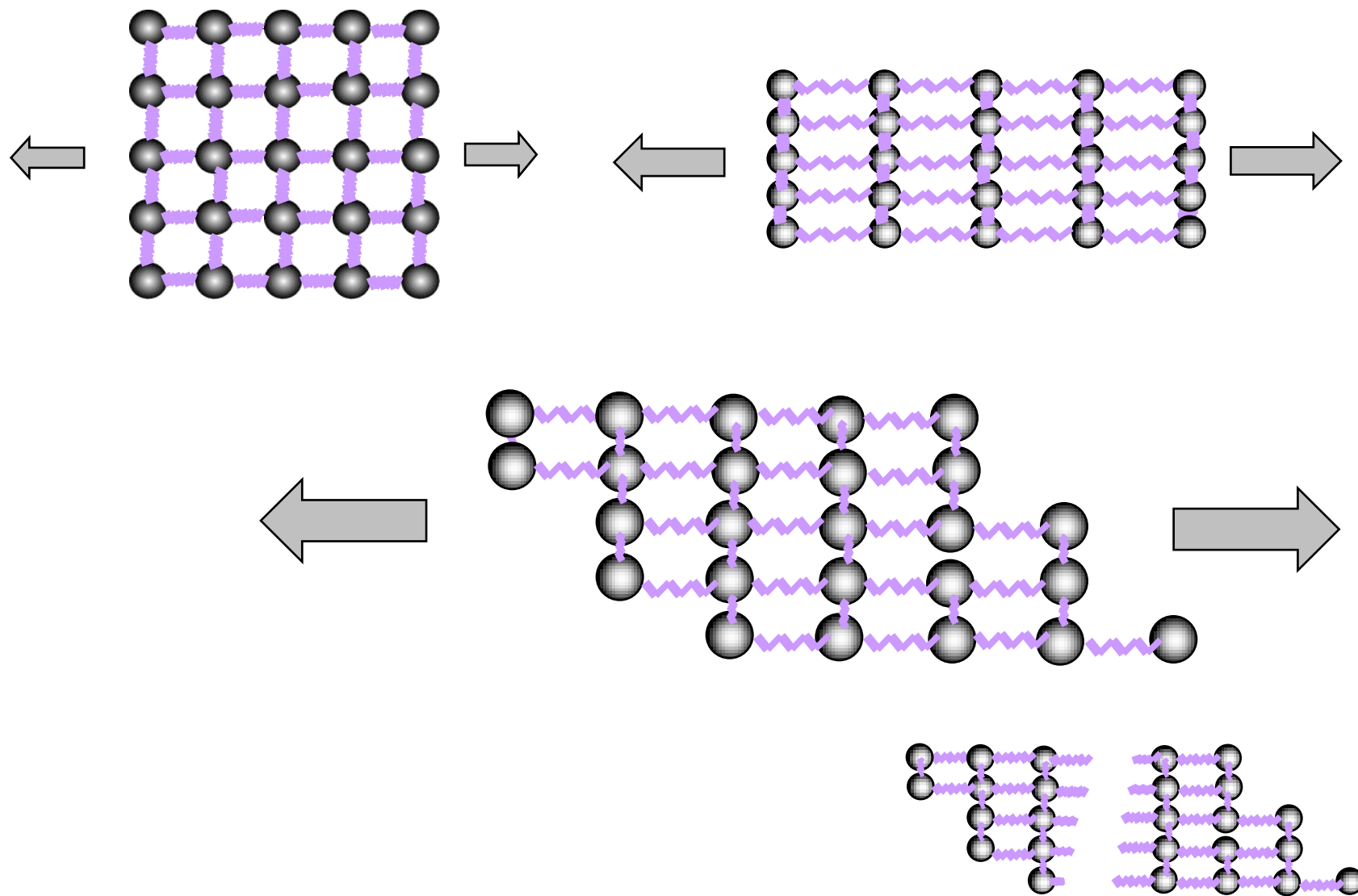


変形過程

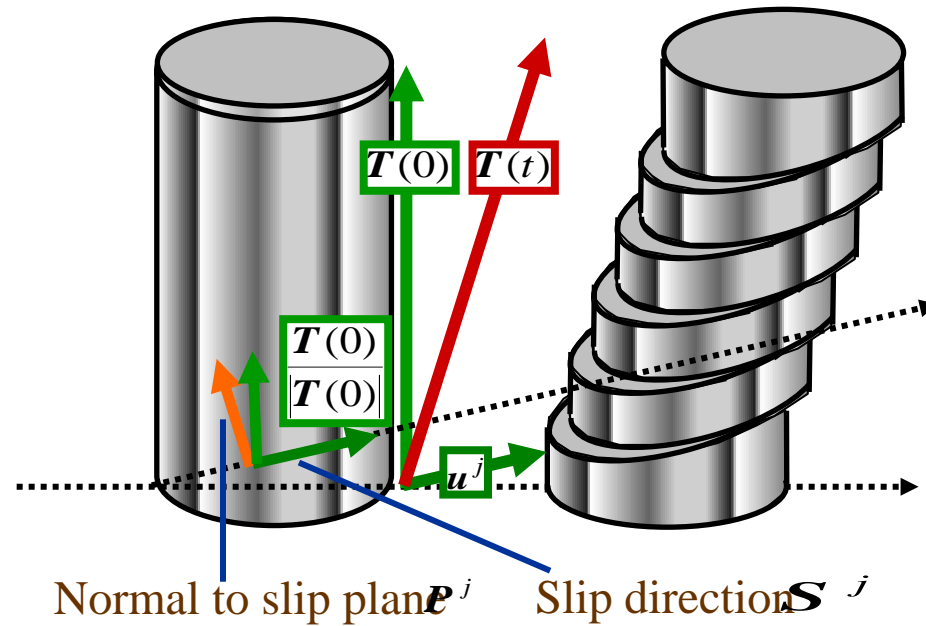
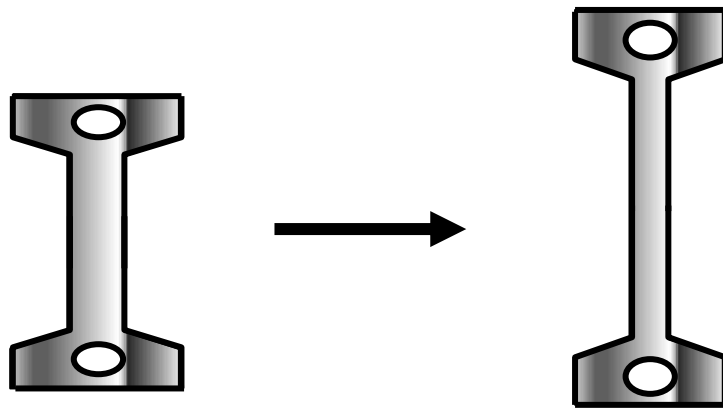


破壊

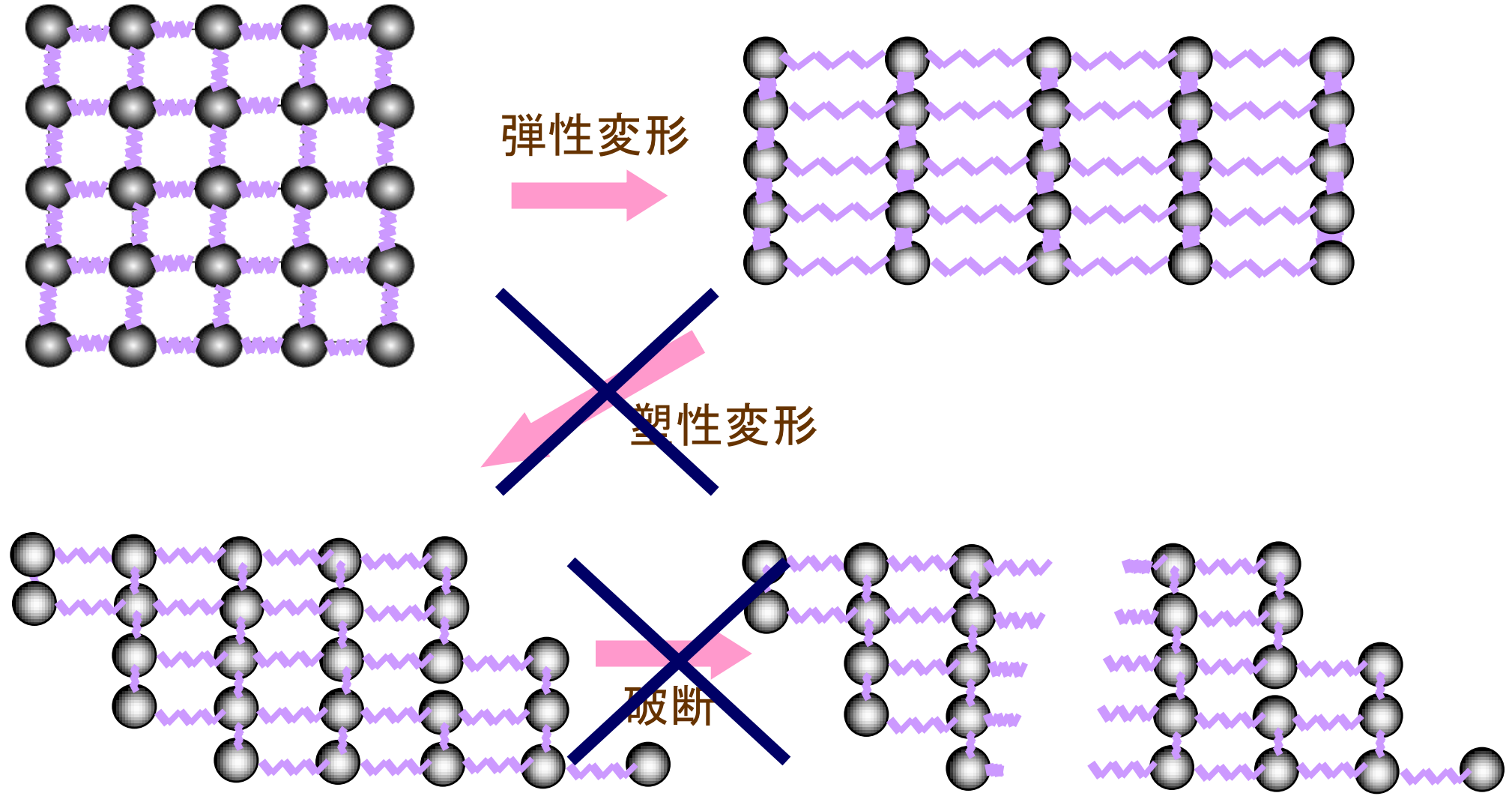
塑性変形



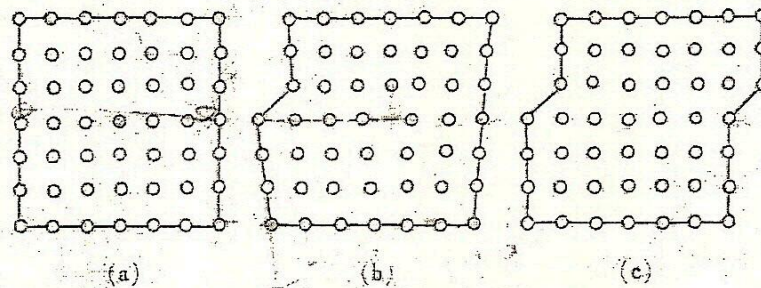
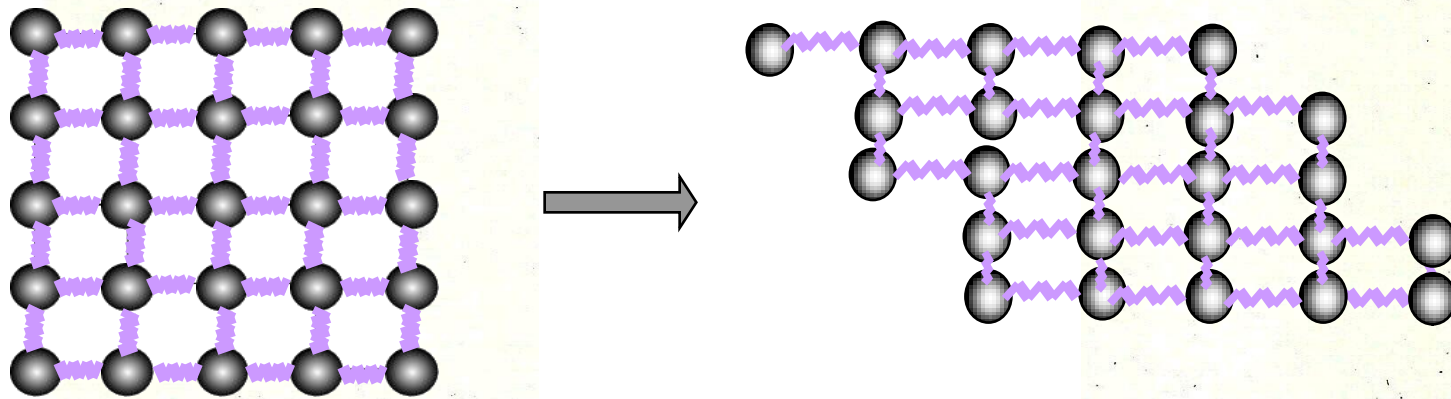
塑性変形



合金材料の変形挙動



塑性変形



“しわ”の伝播

転位運動と変形

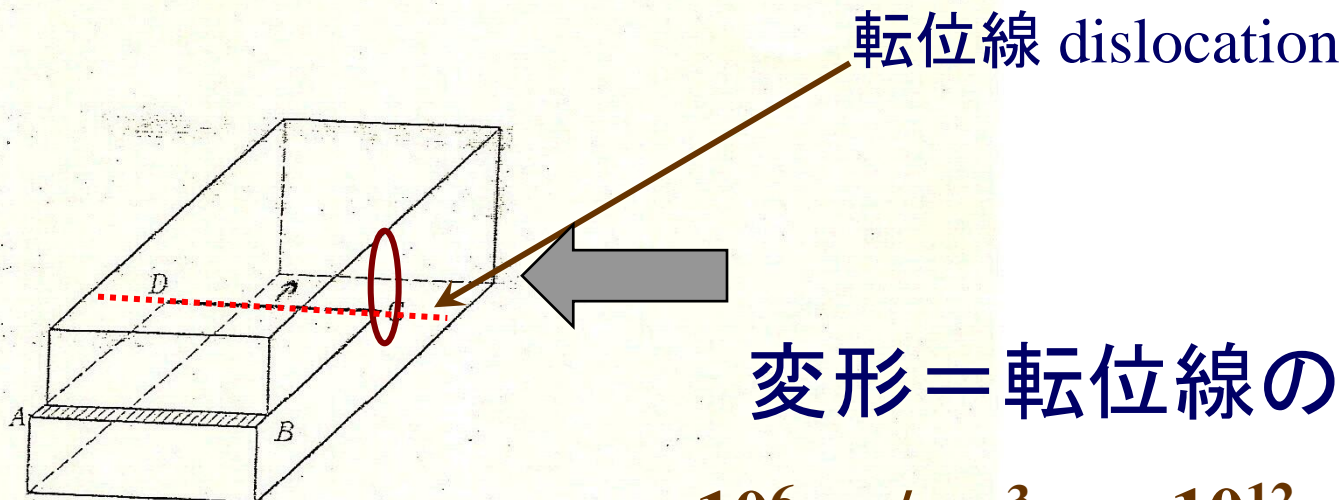


図 8・6 刃状転位によるすべり変形

変形 = 転位線の運動

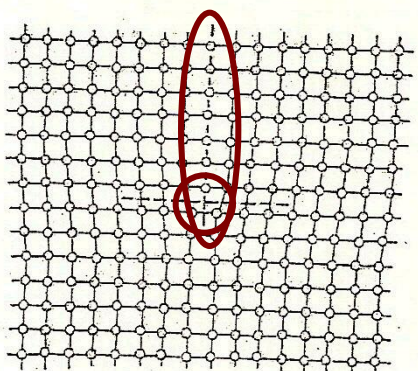
$10^6 \text{cm/cm}^3 \rightarrow 10^{12} \text{cm/cm}^3$

地球の赤道周囲の250倍!

強度設計

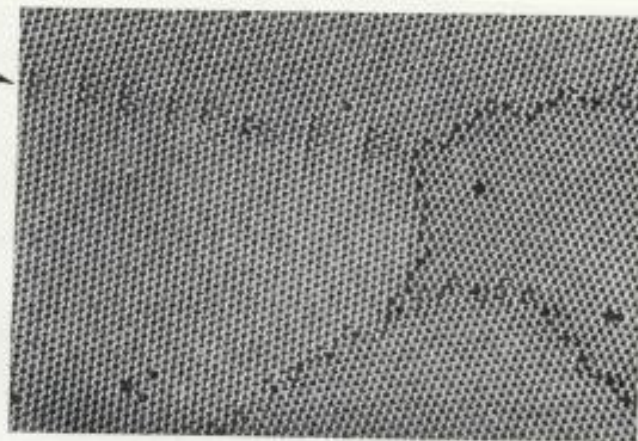
転位運動の制御

内部組織 (障害物_{ex} 析出物)



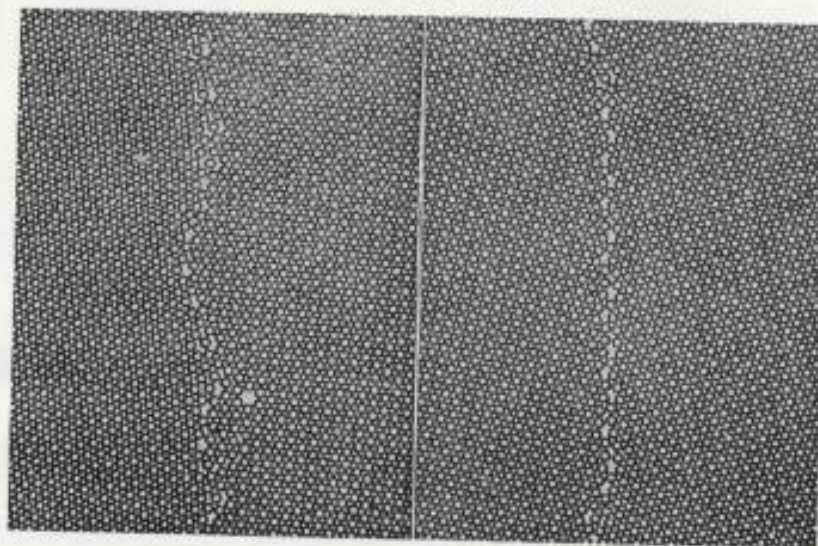
(a)

泡モデルと結晶粒界



小傾角粒界

図 10-1 あわ模型に見られた結晶粒界 (Bragg)

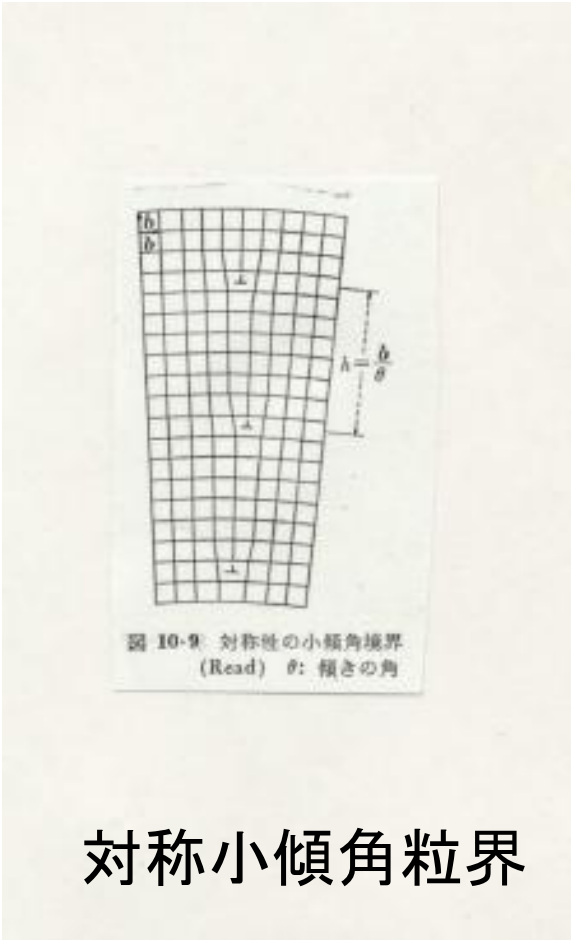


大角粒界

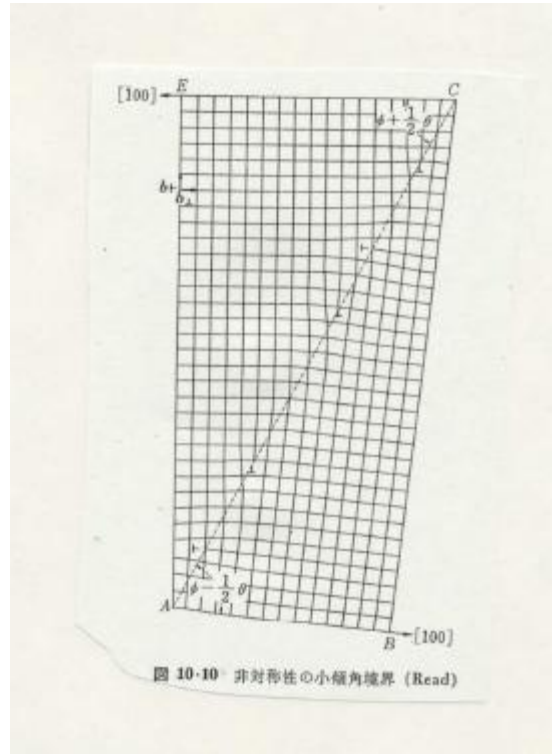
(a) 方位差 25°

(b) 方位差 35°

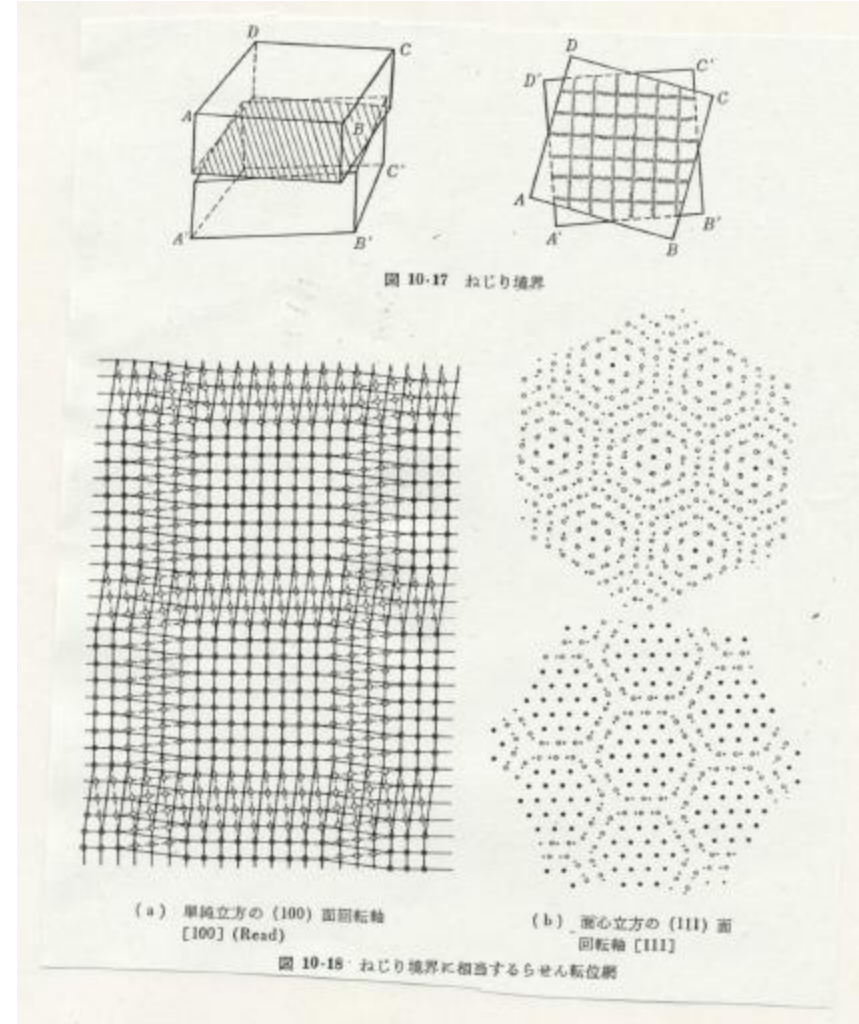
結晶粒界



対称小傾角粒界



非対称小傾角粒界



ねじり境界



Plasticity within dislocation theory

1. 単一転位の挙動

Single dislocation behavior

2. 単一転位の複数障害物場での挙動

Single dislocation behavior in the obstacle field

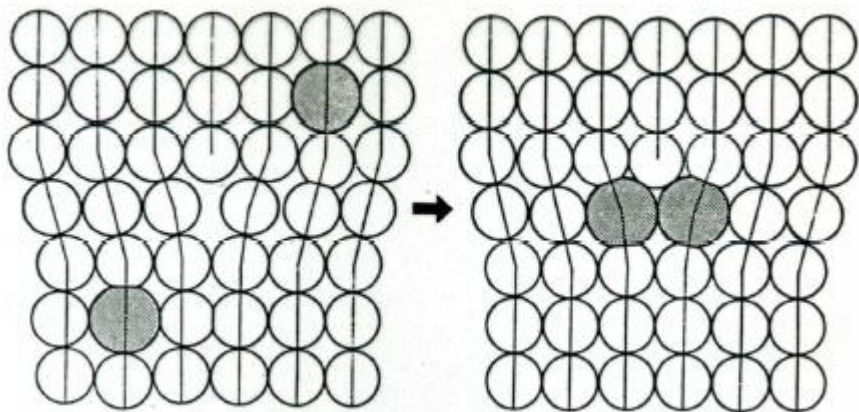
3. 多数転位の(複数障害物場での)挙動

Many-body behavior of dislocations

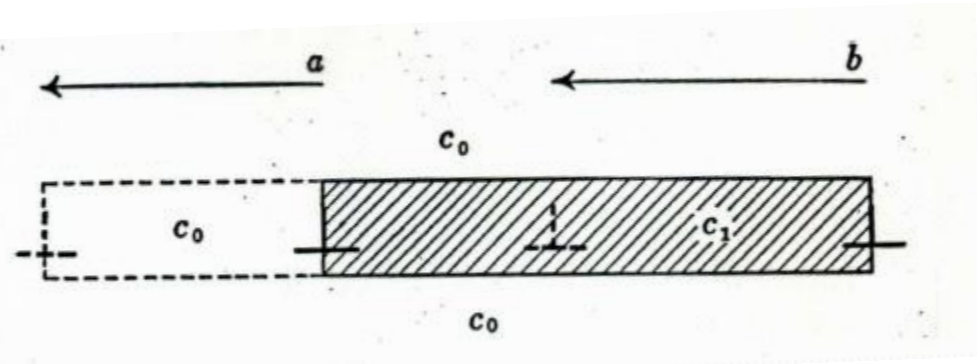
単一転位の挙動 (Elementary Interaction process)[1]



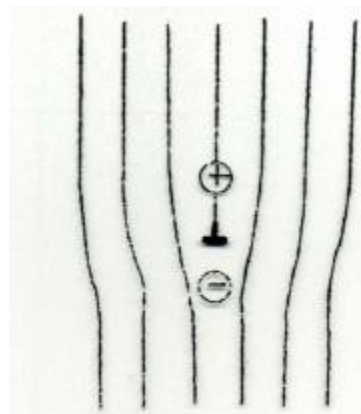
Elastic Interaction



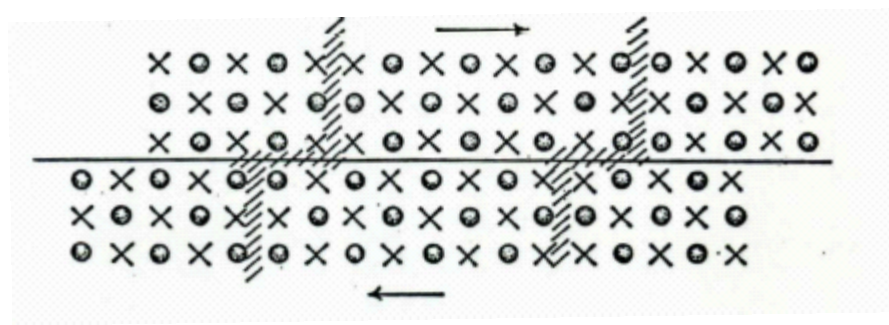
Chemical Interaction



Electric Interaction



Geometrical Interaction





Plasticity within dislocation theory

1. 単一転位の挙動

Single dislocation behavior

2. 単一転位の複数障害物場での挙動

Single dislocation behavior in the obstacle field

3. 多数転位の(複数障害物場での)挙動

Many-body behavior of dislocations

単一転位の複数障害物場での挙動

Single dislocation behavior in the obstacle field



N_i Number of i -th type obstacle

f_i Elementary interaction force with i -th type obstacle

$$\tau = \sum N_i \cdot f_i \quad ?$$

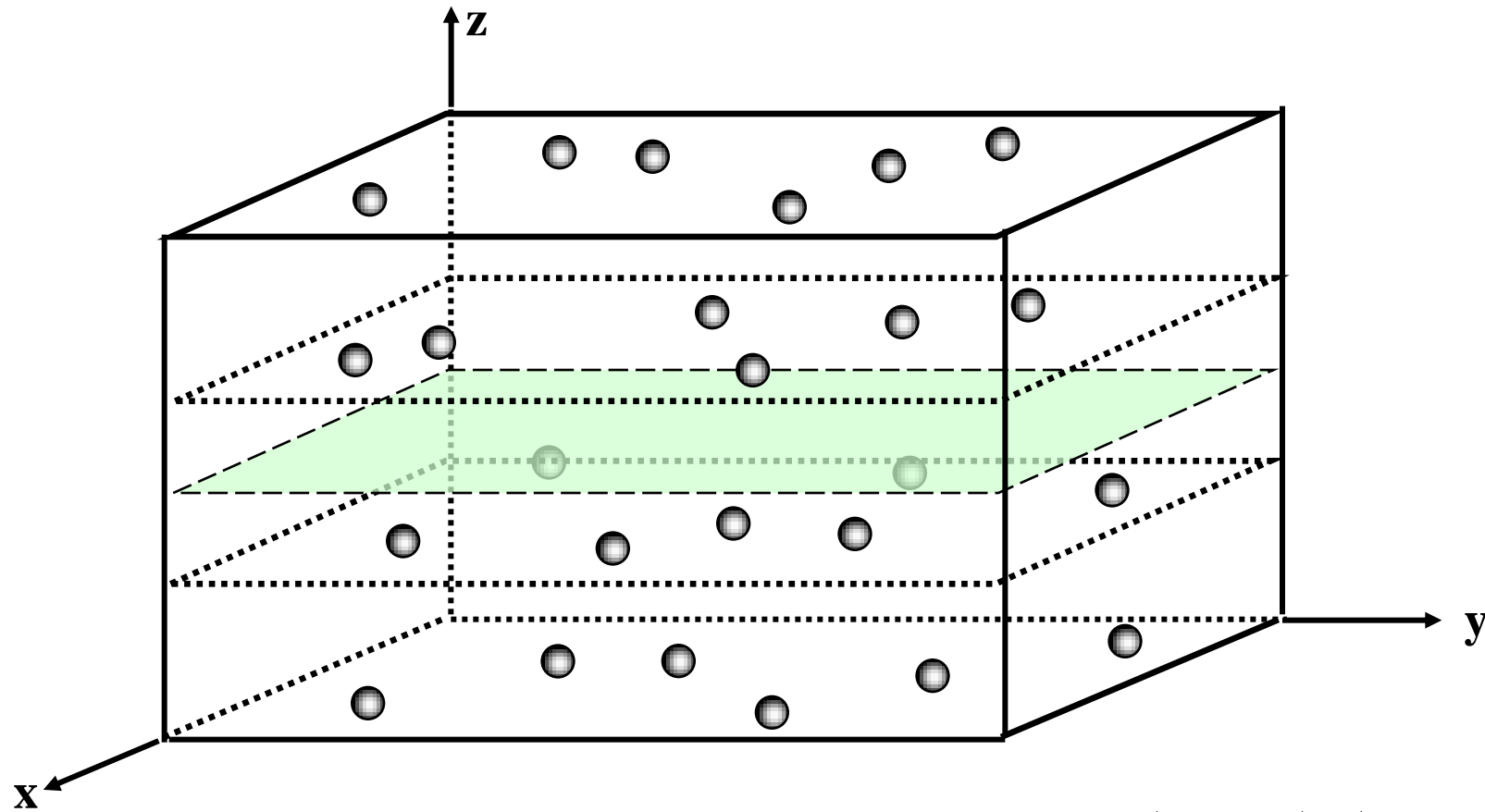
$$\tau = f(\Gamma, w, C, \text{distribution})$$

Γ Line tension

w width of an obstacle

C concentration of an obstacle

Single dislocation behavior



100 x 300 x 4

$$stress(x, y, z) = \frac{(y - y_s) \cdot (z - z_w)}{\left\{ (x - x_s)^2 + (y - y_s)^2 + (z - z_s)^2 + C \right\}^{5/2}}$$

String model of a dislocation



$$m \frac{\partial^2 y}{\partial t^2} + B \frac{\partial y}{\partial t} + \Gamma \frac{\partial^2 y}{\partial x^2} + \tau_{eff} \cdot b = 0$$

m ;mass of a dislocation

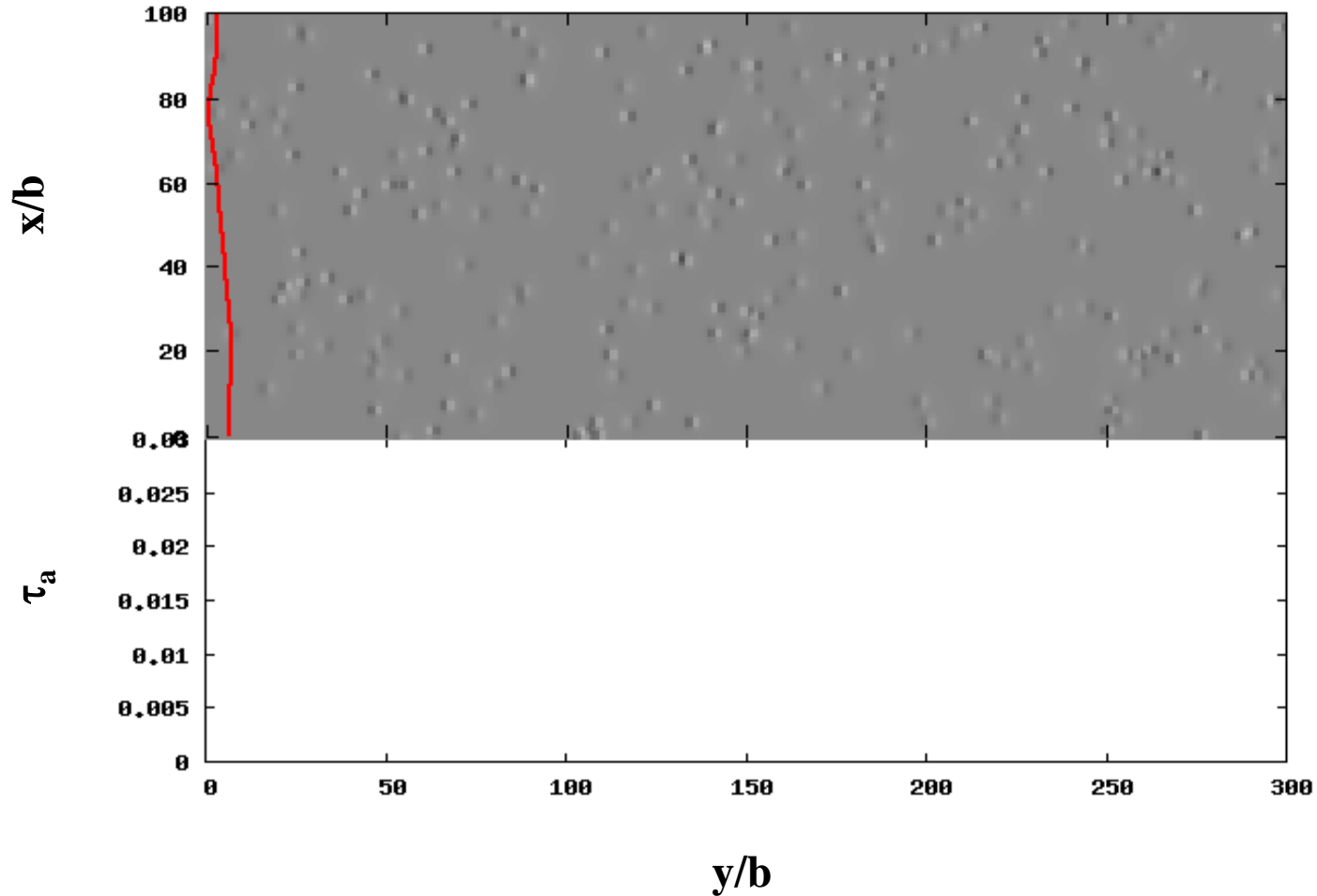
B ;damping

Γ ;line tension

τ_{eff} ;effective stress on a disloc.

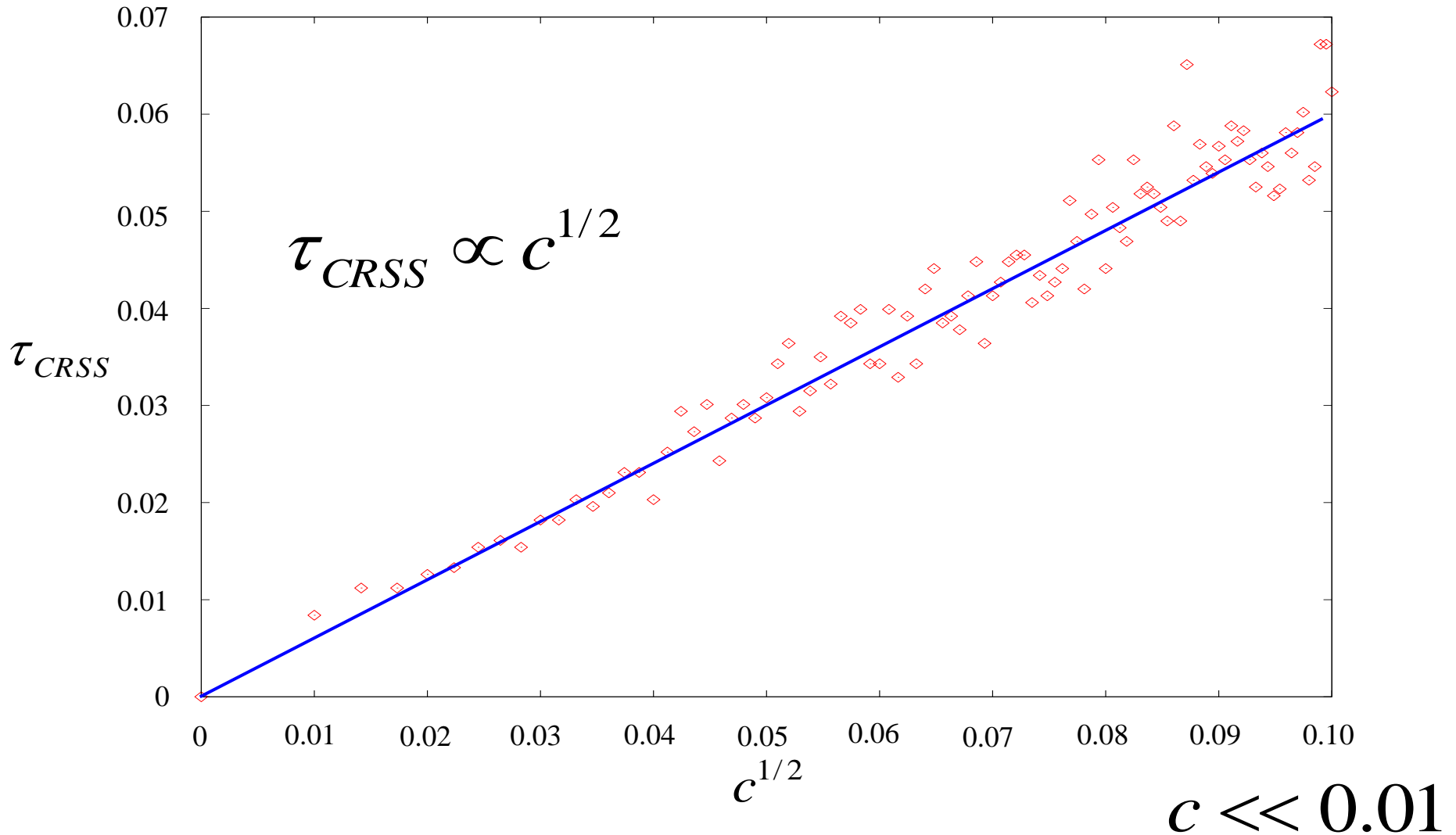
$$\tau_{eff} = \tau_{appl.} - \tau_{int.}$$

外部応力と転位の安定平衡位置

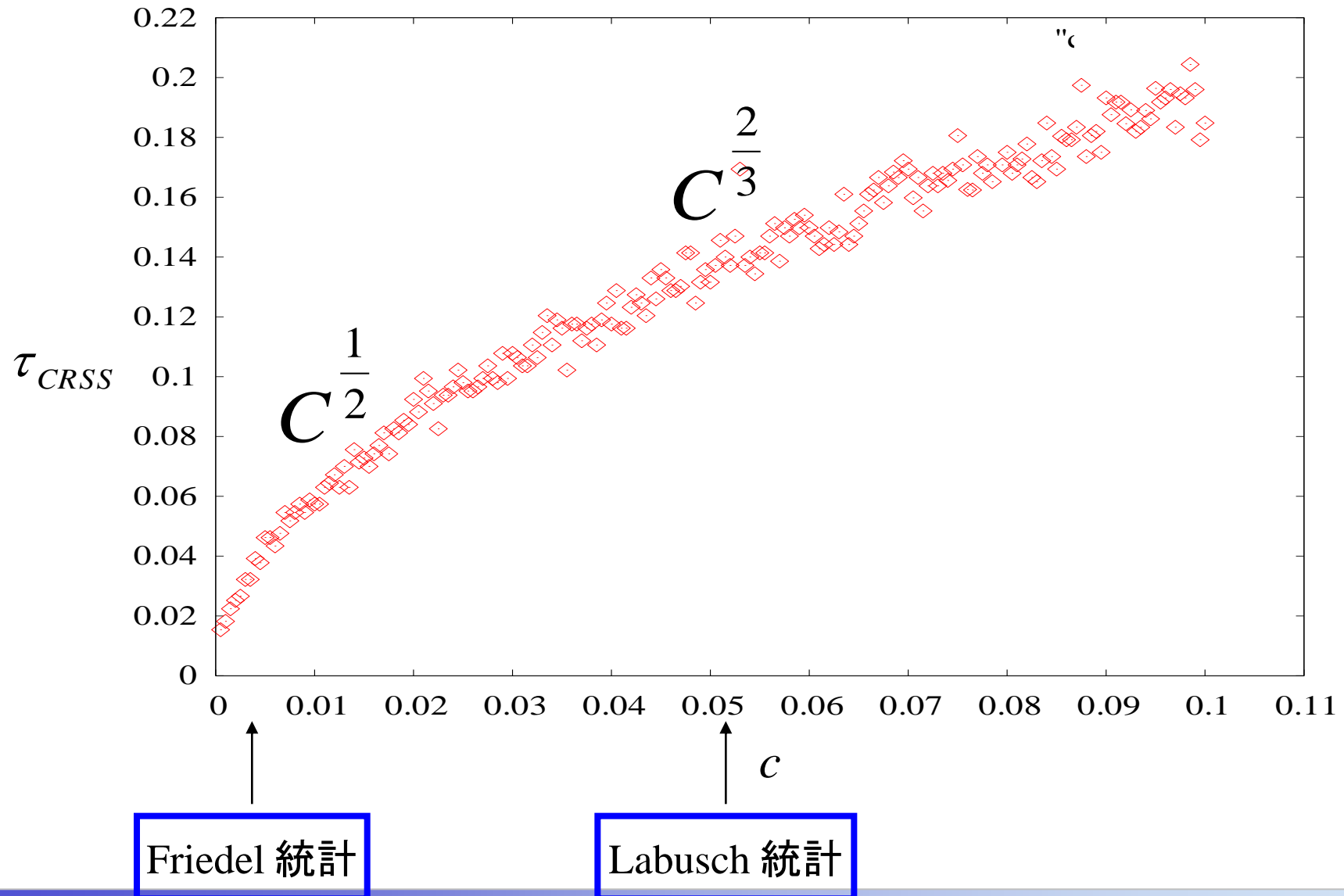


濃度 $c = 0.2\%$

Friedel Regime



Other Regimes





Plasticity within dislocation theory

1. 単一転位の挙動

Single dislocation behavior

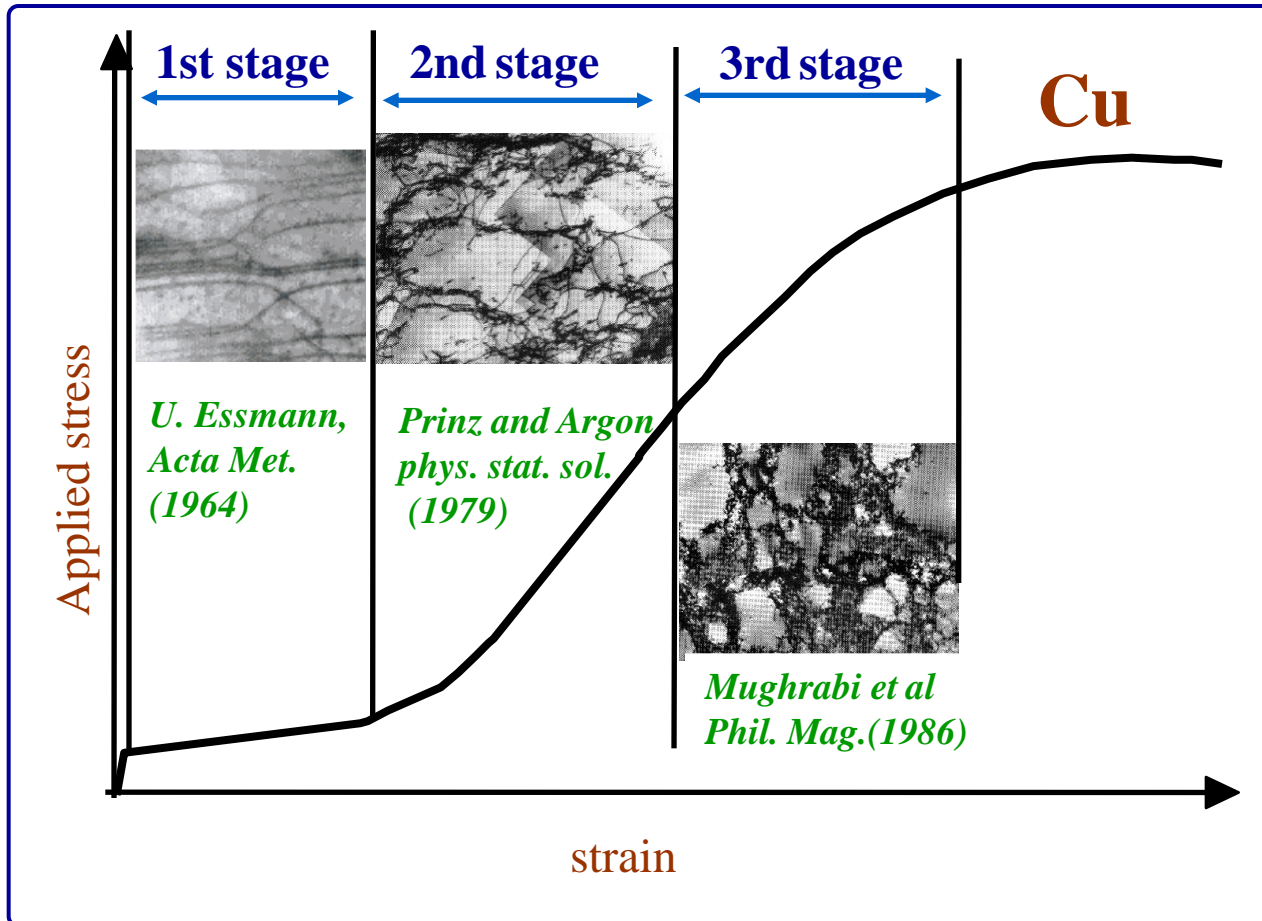
2. 単一転位の複数障害物場での挙動

Single dislocation behavior in the obstacle field

3. 多数転位の(複数障害物場での)挙動

Many-body behavior of dislocations

Actual situations



Dislocation reactions

Multiplication,
Dynamic recovery,
Immobilization/
mobilization of
mobile/immobile
dislocations
tangling

Heterogeneous distribution of dislocations

Reaction-Diffusion equation

*Example : Formation
process of Persistent Slip
Bands(PSBs)*
C. Shiller and D. Walgraef:
Acta Metall. 36, 3 (1988)

Fatigue



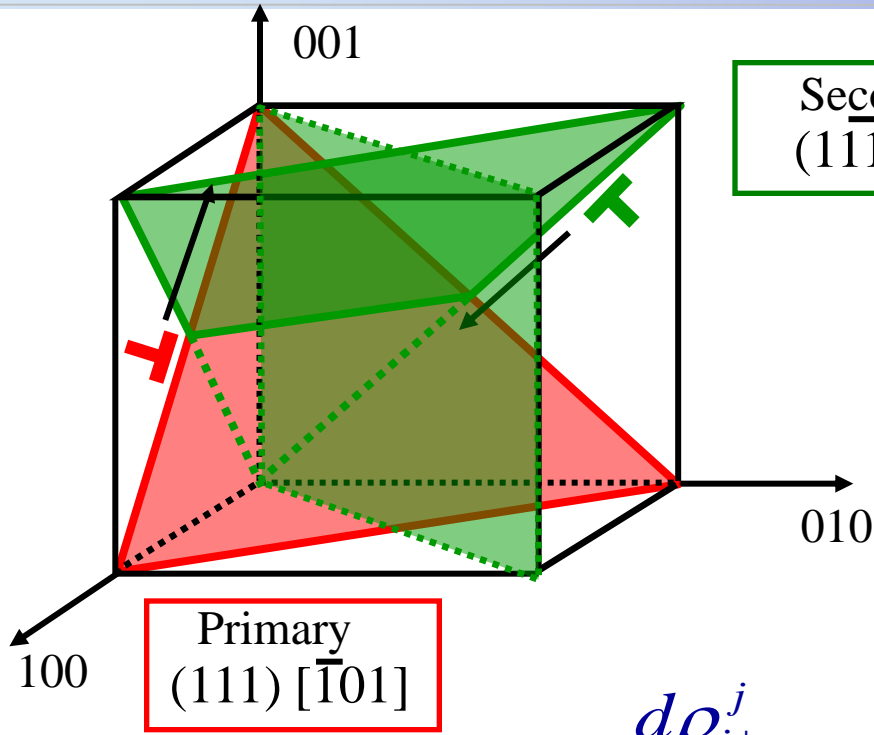
U. Essman : phys. stat.sol. (1963)

Calculation of a *S-S* curve
under
Constant Strain Rate Tensile
Test



- Three stages of *S-S* curve
- dislocation microstructure
- **Energetic origin of dislocation structural formation**

Slip systems and evolution equations (R-D)



Secondary
(111) [011]

Primary
(111) [1-01]

$\rho_{n\pm}^j$ — j — j -th slip system : $j = (p, s)$
 — $n\pm$ — Sign of Burgers vector
 — n — immobile(i), mobile(m) : $n = (i, m)$

$$\frac{d\rho_{i\pm}^j}{dt} = D_i \nabla^2 \rho_{i\pm}^j + \underbrace{f_{i\pm}^j(\rho_{i\pm}^j, \rho_{m\pm}^j, \rho_{i\pm}^k, \rho_{m\pm}^k)}$$

Conservative motion of dislocation

Reaction

$$\frac{d\rho_{m\pm}^j}{dt} = D_m \nabla_x^2 \rho_{m\pm}^j \mp v_{m\pm}^j \nabla_x \rho_{m\pm}^j + \underbrace{f_{m\pm}^j(\rho_{i\pm}^j, \rho_{m\pm}^j, \rho_{i\pm}^k, \rho_{m\pm}^k)}$$

Glide motion

R-D equation and Reaction terms



Mobile and Immobile

$$f_{n\pm}^j(\rho_{n\pm}^j, \rho_{n\pm}^k) = f_{intra}^j(\rho_{n\pm}^j) + \sum_k f_{inter}^{jk}(\rho_{n\pm}^j, \rho_{n\pm}^k)$$

Intra slip system

Inter slip system



$$f_{intra}^j(\rho_{n\pm}^j) = f_{conservative}^j(\rho_{n\pm}^j) + f_{non-conservative}^j(\rho_{n\pm}^j)$$

Conservative reaction

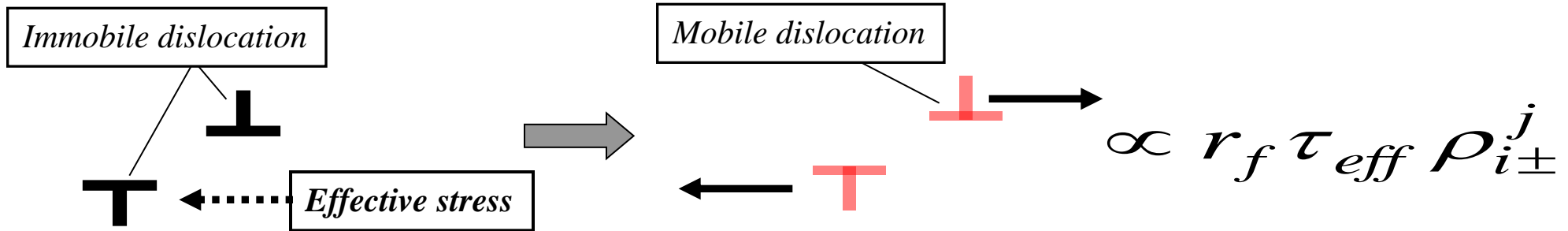
Non-conservative reaction

Reactions: Intra slip system; conservative

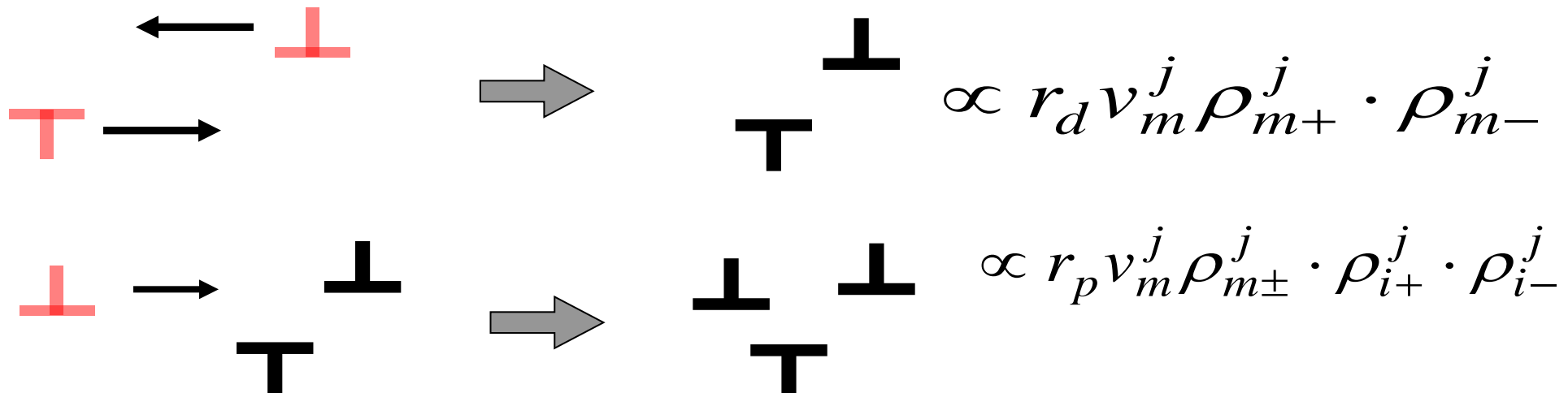


$$f_{intra}^j(\rho_{n\pm}^j) = \underline{f_{conservative}^j(\rho_{n\pm}^j)} + f_{non-conservative}^j(\rho_{n\pm}^j)$$

1. Mobilization



2. Immobilization ; Dipolization · Multi-polization

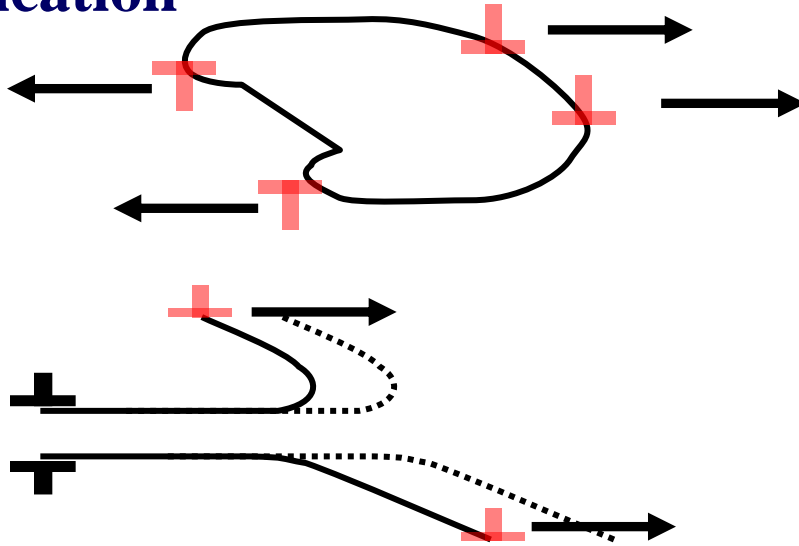


Reactions: Intra slip system; non-conservative



$$f_{intra}^j(\rho_{n\pm}^j) = f_{conservative}^j(\rho_{n\pm}^j) + \underline{f_{non-conservative}^j(\rho_{n\pm}^j)}$$

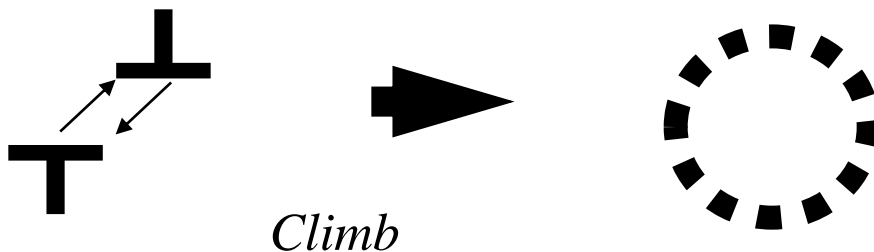
3. Multiplication



$$\propto r_{mm} v_m^j \rho_{m\pm}^j$$

$$\propto r_{im} v_m^j \rho_{m\pm}^j \cdot \rho_{i\pm}^j$$

4. Recovery



$$\propto r_r v_i \rho_{i+}^j \cdot \rho_{i-}^j$$

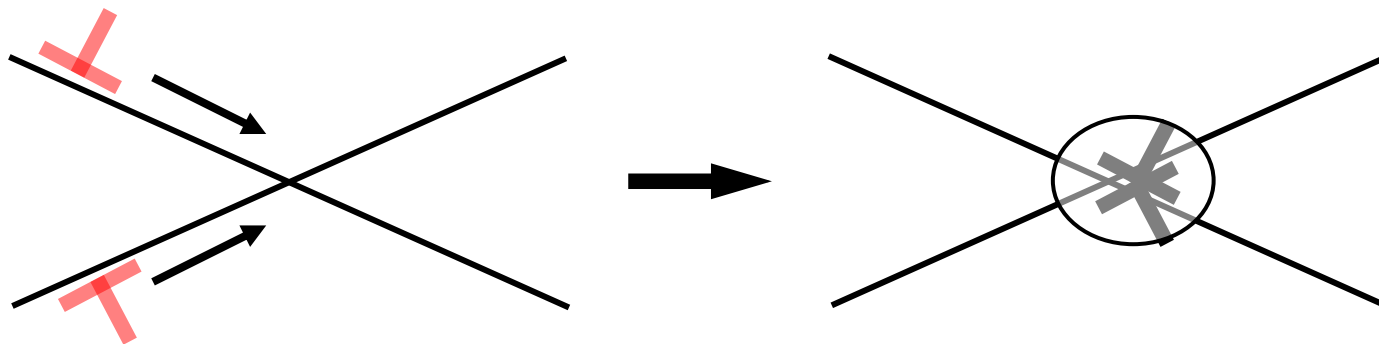


Reactions: Inter slip system



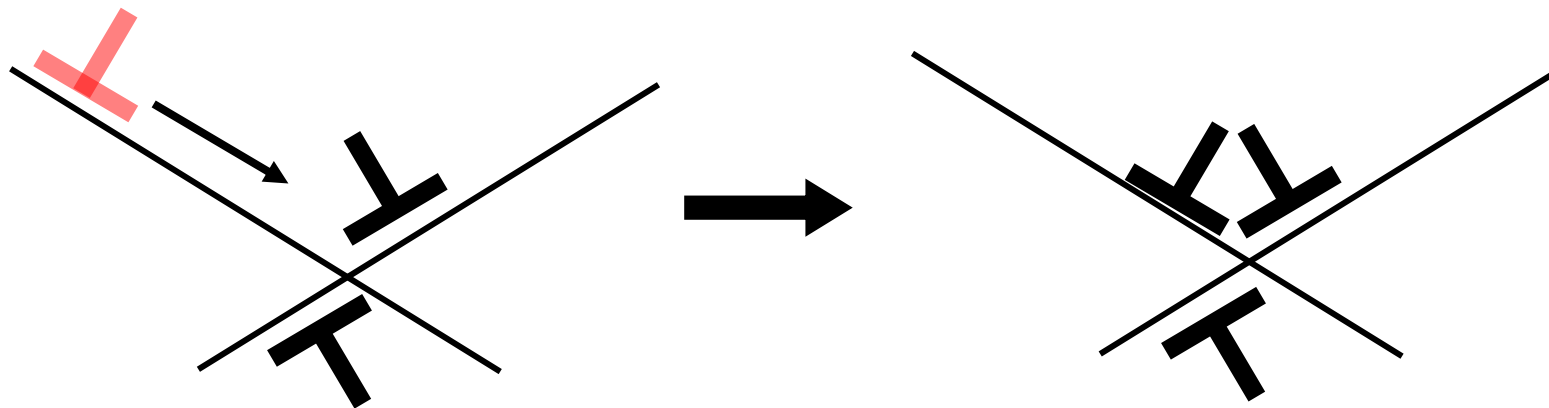
Lomer-Cottrell lock formation

$$\propto r_{LC} v_m^{jk} \rho_{m\pm}^j \cdot \rho_{m\mp}^k \quad (j, k = p, s \quad j \neq k)$$



Tangling of dislocations

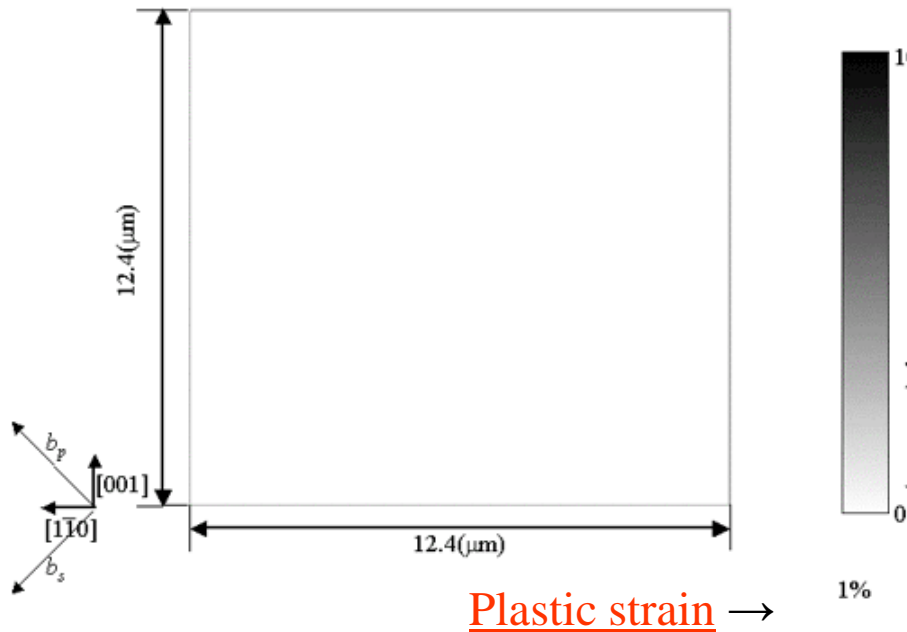
$$\propto r_t v_m^j \rho_m^j \cdot (\rho_i^k)^2 \quad (j, k = p, s \quad j \neq k)$$



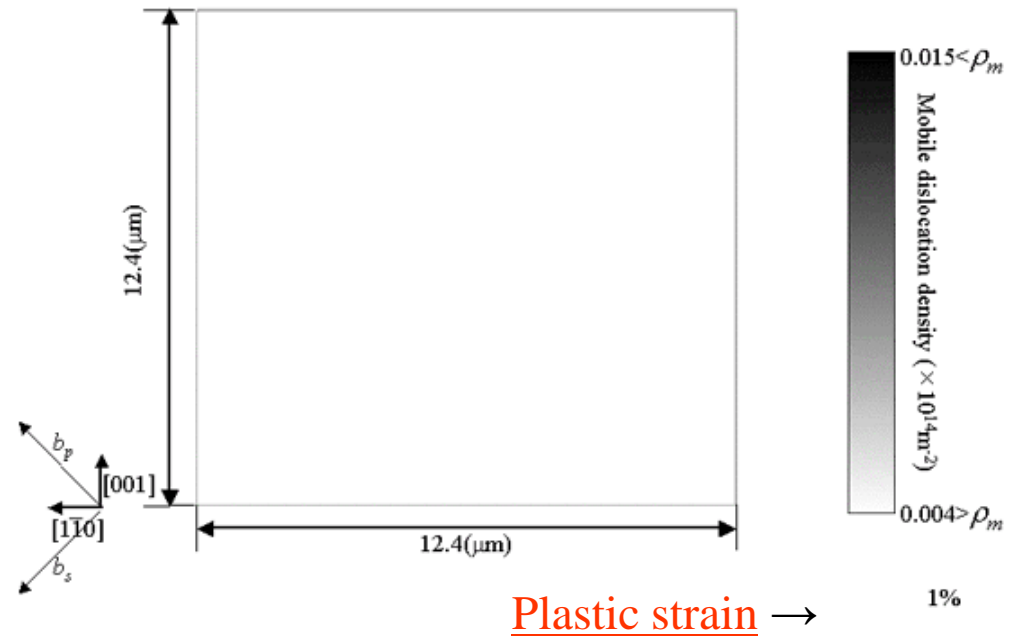
Evolution of dislocation structures

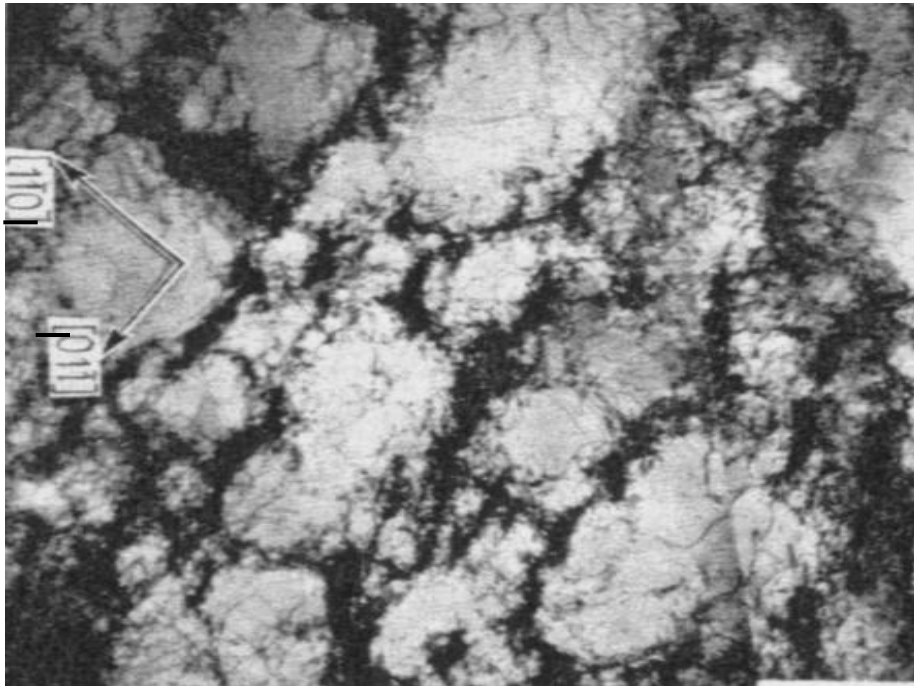


Immobile dislocation



Mobile dislocation





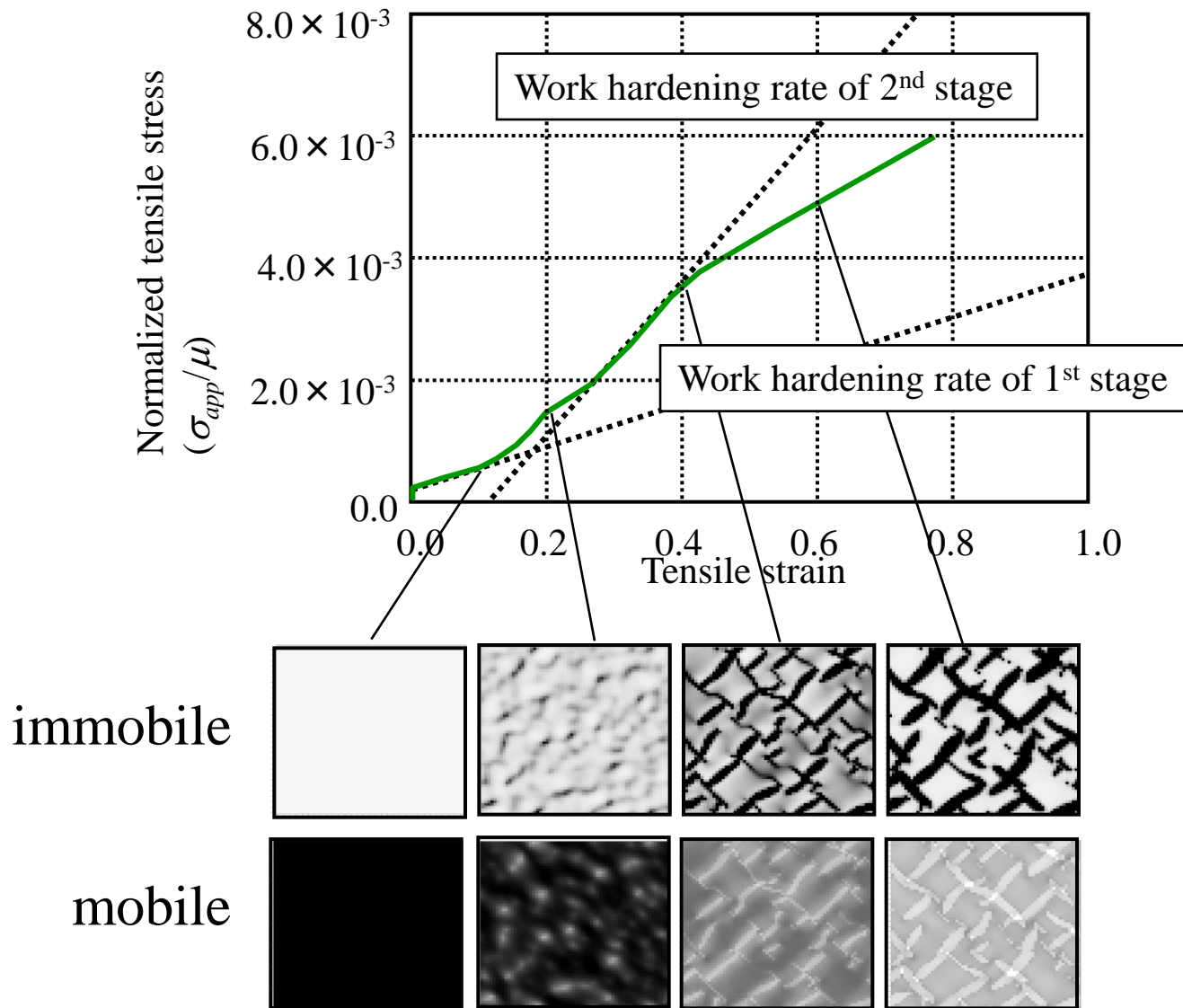
U. Essman : phys. stat.sol. (1963)

Calculation of a *S-S* curve
under
Constant Strain Rate Tensile
Test



- Three stages of *S-S* curve
- dislocation microstructure
- **Energetic origin of dislocation structural formation**

Stress-Strain Curve and Dislocation structure





弾性変形 (Elastic deformation) 外力下での系の静的平衡状態

Static equilibrium of a system under the applied stress

塑性変形 (Plastic deformation)

降伏強度 (yielding), クリープ強度 (creep), 超塑性 (super plasticity)

etc.

転位密度 (dislocation density), 内部組織 (microstructure) etc

外力下での系の状態の時間的変化 非平衡状態

Time evolution process of a microstructure under the applied stress

原理？

静止転位



Internal energy due to stored dislocations

Line energy of dislocation per unit length

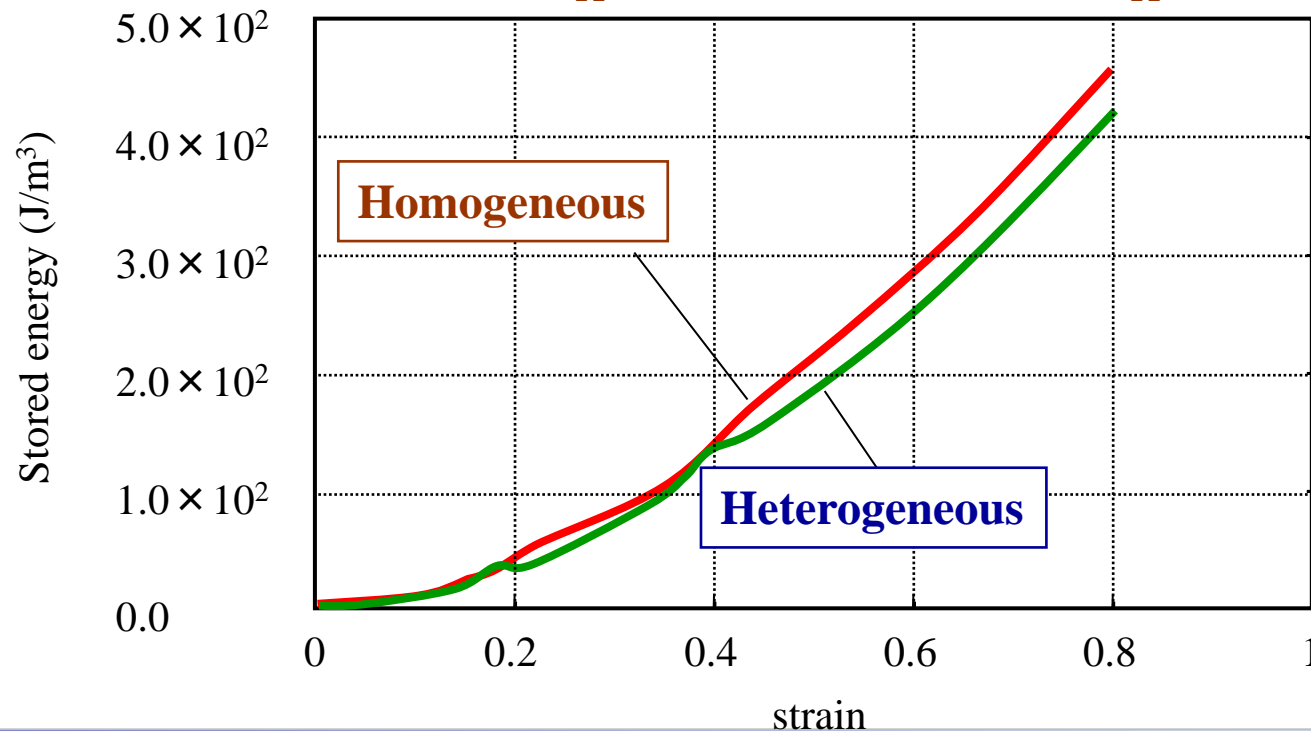
$$e_{line}(\rho(\mathbf{x})) \approx \mu b^2 \frac{1-\nu/2}{4\pi(1-\nu)} \ln \left(\frac{1}{b(\rho(\mathbf{x}))^{1/2}} \right)$$

• Homogeneous distribution

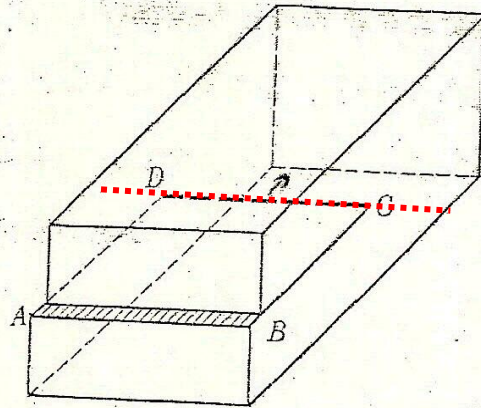
$$E_{store}^{homo} = \langle \rho \rangle e_{line}(\langle \rho \rangle)$$

• Heterogeneous distribution

$$E_{store}^{hetero} = \frac{1}{\Omega} \int_{\Omega} E_{store}^{local}(\rho(\mathbf{x})) d\mathbf{x} = \frac{1}{\Omega} \int_{\Omega} \rho(\mathbf{x}) e_{line}(\rho(\mathbf{x})) d\mathbf{x}$$

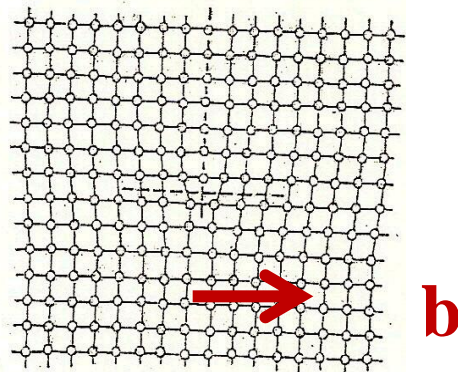


転位運動と変形



Burgers vector

図 8・6 刃状転位によるすべり変形



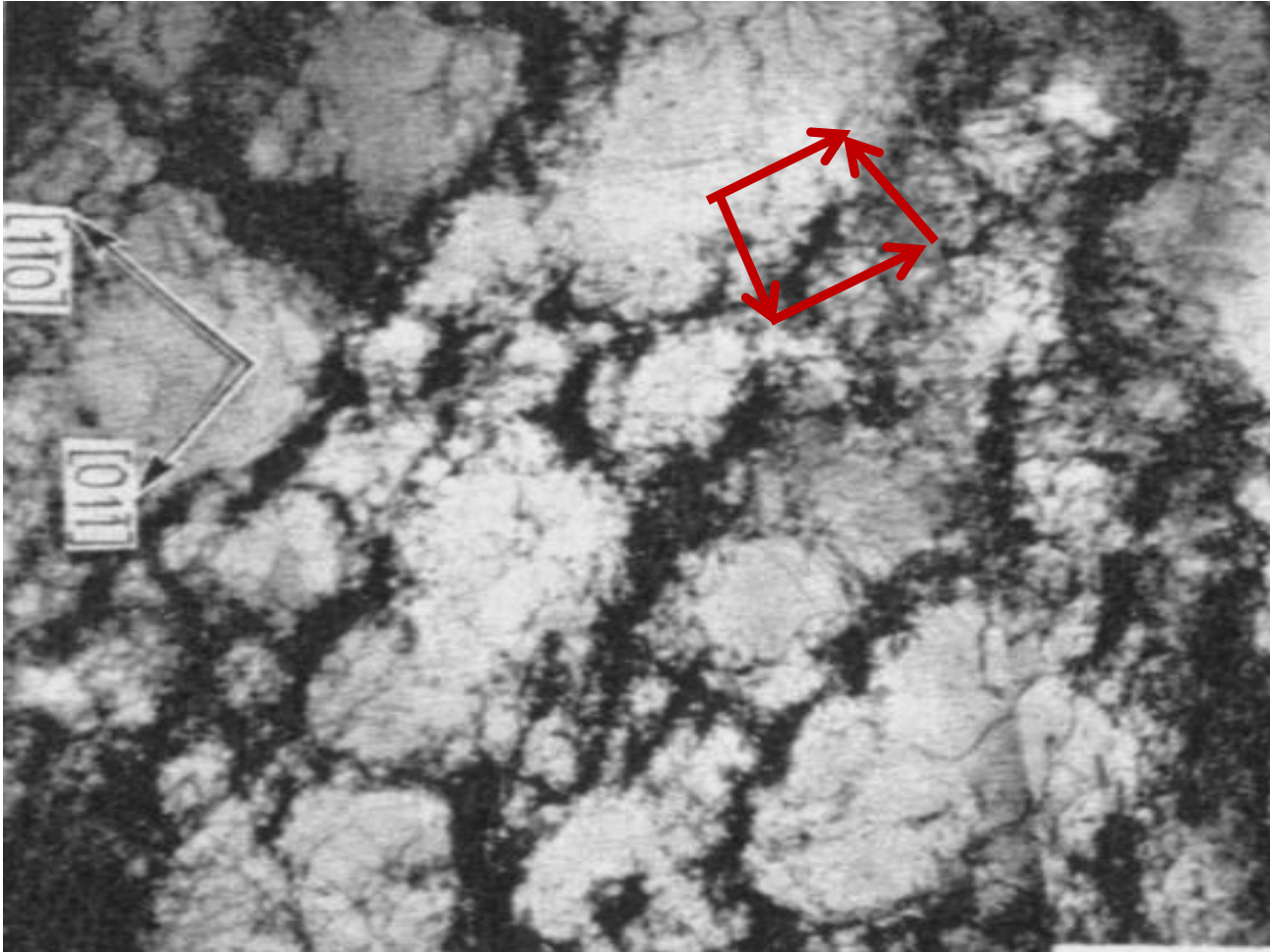
(a)

(b)

多数転位の挙動 Many-body behavior of dislocations



静止転位 (static dislocation) $\sum_i |\mathbf{b}_i|^2 = \textit{minimum}$





弾性変形 (Elastic deformation) 外力下での系の静的平衡状態

Static equilibrium of a system under the applied stress

塑性変形 (Plastic deformation)

降伏強度 (yielding), クリープ強度 (creep), 超塑性 (super plasticity)

etc.

転位密度 (dislocation density), 内部組織 (microstructure) etc

外力下での系の状態の時間的变化 非平衡状態

Time evolution process of a microstructure under the applied stress

原理？

静止転位

動転位??

転位密度-応力??

保存則 Conservation law



$$\frac{\partial n}{\partial t} = -\nabla \cdot \mathbf{J}_n + \Gamma \cdot \nu_n$$

$$\frac{\partial u}{\partial t} = -\nabla \cdot \mathbf{J}_u$$

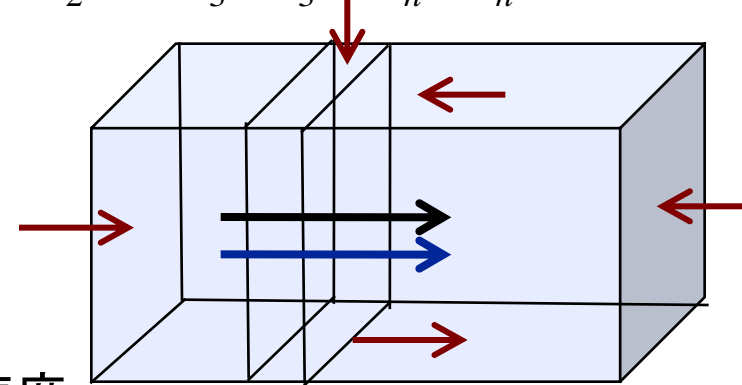
$$\frac{\partial s}{\partial t} \neq -\nabla \cdot \mathbf{J}_s \quad \dot{s} = \frac{\partial s}{\partial t} + \nabla \cdot \mathbf{J}_s$$

$$\rho \frac{du}{dt} = -\nabla \cdot \mathbf{J}_u + \sigma_{ij} \cdot \frac{\partial w_i}{\partial x_j}$$

熱エネルギー (thermal energy)

力学的エネルギー (mechanical energy)

$$\nu_1 \cdot B_1 + \nu_2 \cdot B_2 \leftrightarrow \nu_3 \cdot B_3 + \nu_n \cdot B_n$$



エントロピー生成速度
(entropy production rate)

n 粒子数 (number of species)

u 内部エネルギー (internal energy)

Γ 反応速度 (reaction rate)

ρ 密度 (density)

σ_{ij} 応力 (stress)

w_i 速度 (component of the velocity)

Energy conservation



$$\rho \frac{du}{dt} = -\nabla \mathbf{J}_u + \sigma_{ij} \cdot \frac{\partial w_i}{\partial x_j}$$

w_i 速度(component of the velocity)

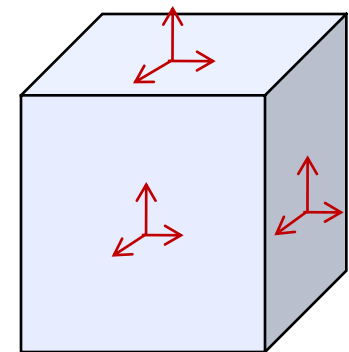
$$\frac{du}{dt} = -p \cdot \frac{\partial v}{\partial t} + \frac{1}{\rho} \sigma'_{ij} \cdot \frac{\partial w_i}{\partial x_j} - \frac{1}{\rho} \nabla \mathbf{J}_u$$

$$\sigma_{ij} = \begin{pmatrix} \sigma_{xx} & \sigma_{xy} & \sigma_{xz} \\ \sigma_{yx} & \sigma_{yy} & \sigma_{yz} \\ \sigma_{zx} & \sigma_{zy} & \sigma_{zz} \end{pmatrix}$$

$$\frac{\partial w_i}{\partial x_j} = \dot{\varepsilon}_{ij} + \omega_{ij} \quad \dot{\varepsilon}_{ij} = \frac{1}{2} \left\{ \left(\frac{\partial w_i}{\partial x_j} \right) + \left(\frac{\partial w_j}{\partial x_i} \right) \right\} \quad \omega_{ij} = \frac{1}{2} \left\{ \left(\frac{\partial w_i}{\partial x_j} \right) - \left(\frac{\partial w_j}{\partial x_i} \right) \right\}$$

$$\frac{du}{dt} = -p \cdot \frac{\partial v}{\partial t} + \frac{1}{\rho} \sigma'_{ij} \cdot \dot{\varepsilon}_{ij} - \frac{1}{\rho} \nabla \mathbf{J}_u$$

ρ 密度(density)



\mathbf{J}_u 熱流束(component of the heat flux)

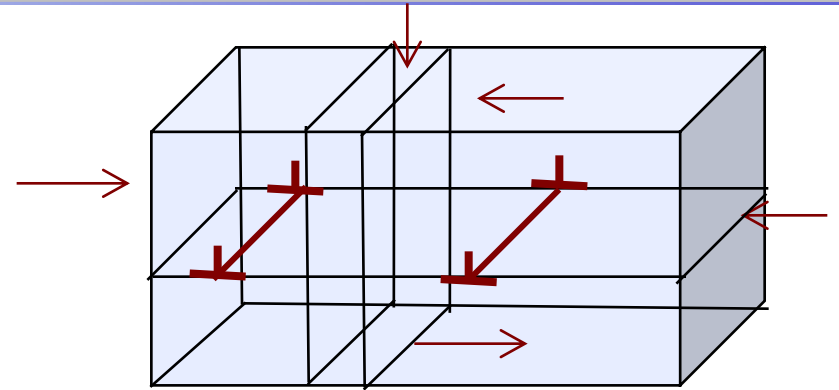


Local equilibrium and energy conservation

$$du = T \cdot ds - p \cdot dv + \lambda \cdot dN_d$$

N_d 転位密度 (dislocation density)

$$\lambda = \frac{\partial u}{\partial N_d}$$



$$\frac{du}{dt} = T \cdot \frac{\partial s}{\partial t} - p \cdot \frac{\partial v}{\partial t} + \lambda \cdot \frac{\partial N}{\partial t}$$

$$\sigma_{ij} = \begin{pmatrix} \sigma_{xx} & \sigma_{xy} & \sigma_{xz} \\ \sigma_{yx} & \sigma_{yy} & \sigma_{yz} \\ \sigma_{zx} & \sigma_{zy} & \sigma_{zz} \end{pmatrix}$$

$$\frac{du}{dt} = -p \cdot \frac{\partial v}{\partial t} + \frac{1}{\rho} \sigma'_{ij} \cdot \dot{\epsilon}_{ij} - \frac{1}{\rho} \nabla \mathbf{J}_u$$

$$\mathbf{J}_s = \frac{1}{T} \mathbf{J}_u$$

$$\dot{s} = \frac{\partial s}{\partial t} + \nabla \cdot \mathbf{J}_s = \mathbf{J}_u \cdot \nabla \left(\frac{1}{T} \right) + \frac{1}{T} \left(\sigma_{ij} \cdot \dot{\epsilon}_{ij} - \rho \cdot \lambda \cdot \frac{\partial N}{\partial t} \right)$$

Entropy Production Rate



$$\dot{s} = \frac{\partial s}{\partial t} + \nabla \cdot \mathbf{J}_s = \mathbf{J}_u \cdot \nabla \left(\frac{1}{T} \right) + \frac{1}{T} \left(\sigma_{ij} \cdot \dot{\varepsilon}_{ij} - \rho \cdot \lambda \cdot \frac{\partial N}{\partial t} \right) = \frac{1}{T} \left(\tau \cdot \dot{\varepsilon} - \rho \cdot \lambda \cdot \frac{\partial N}{\partial t} \right)$$

$$\tau_{app} = \tau_{eff} + \tau_i + \tau_h$$

$$\dot{\varepsilon} = N_m \cdot \bar{v} \cdot b$$

$$\tau_h \cdot N_m \cdot \bar{v} \cdot b = \rho \cdot \lambda \cdot \frac{\partial N_m}{\partial t}$$

$$\bar{v} = k \cdot \tau_{eff}^{2/3}$$

$$\tau_i = C \cdot \sqrt{N_m}$$

τ_{app} 付加応力(applied stress)

τ_{eff} 有効応力(effective stress)。

τ_i 動転位の相互作用応力 (interaction stress)

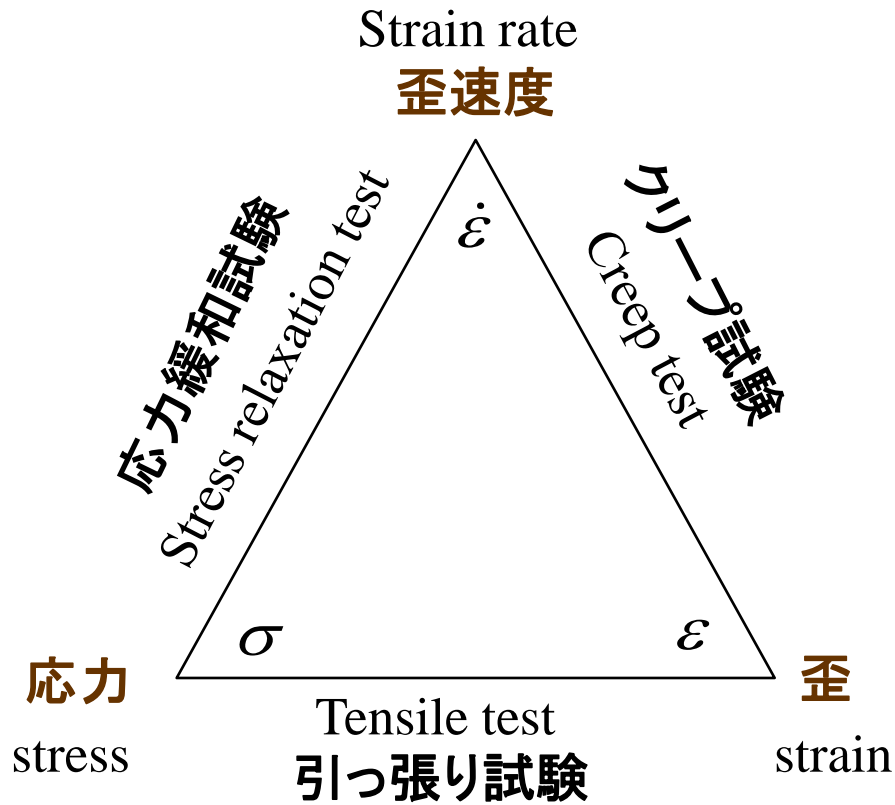
τ_h 加工硬化(work hardening)

$$\dot{s} = \frac{1}{T} \cdot \left\{ \left(\frac{\dot{\varepsilon}}{k \cdot b} \right)^{2/3} \cdot N_m^{-2/3} + C \cdot N_m^{1/2} \right\}$$

$$= f(N_m)$$

$$\begin{aligned} \dot{s} &= (\tau_{eff} + \tau_i) \cdot \dot{\varepsilon} \\ &= \tau(N) \cdot \dot{\varepsilon} \end{aligned} \quad \left. \frac{\partial \dot{s}}{\partial N} \right|_{\dot{\varepsilon}} \propto \left. \frac{\partial \tau}{\partial N} \right|_{\dot{\varepsilon}}$$

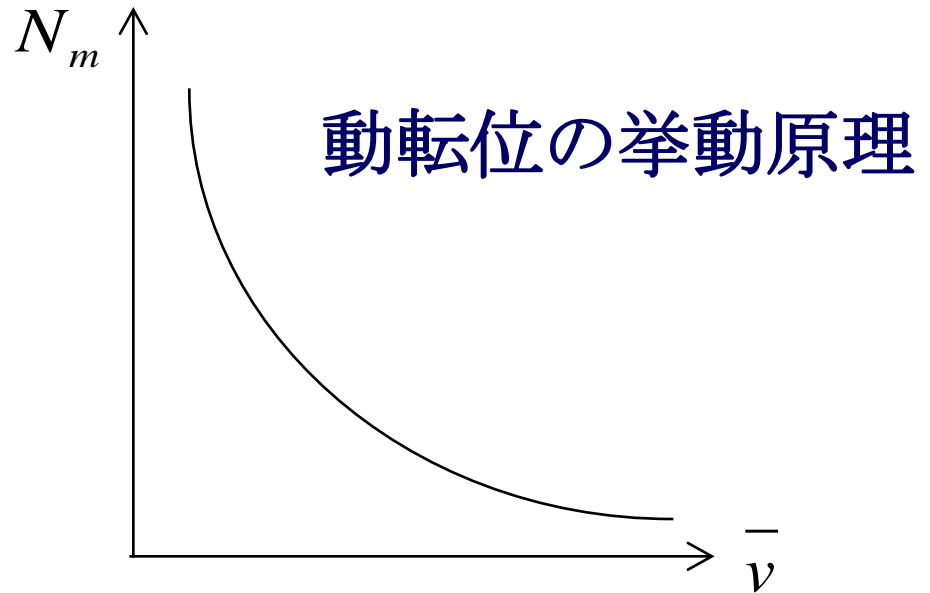
塑性変形の原理 (principle of deformation)



変形応力が一定の条件下では変形速度を最大とするように運動転位の密度が決定される。

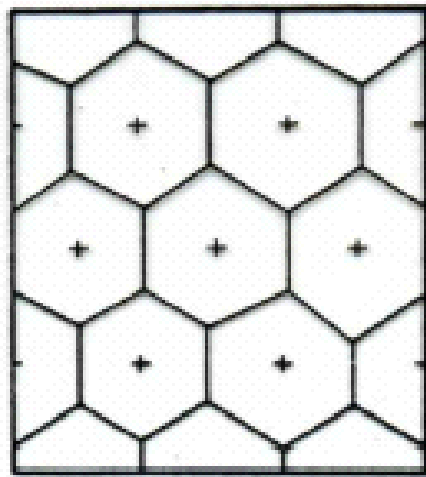
$$\dot{s} = (\tau_{eff} + \tau_i) \cdot \dot{\epsilon} \quad \left. \frac{\partial \dot{s}}{\partial N} \right|_{\dot{\epsilon}} \propto \left. \frac{\partial \tau}{\partial N} \right|_{\dot{\epsilon}}$$

$$= \tau(N) \cdot \dot{\epsilon}$$

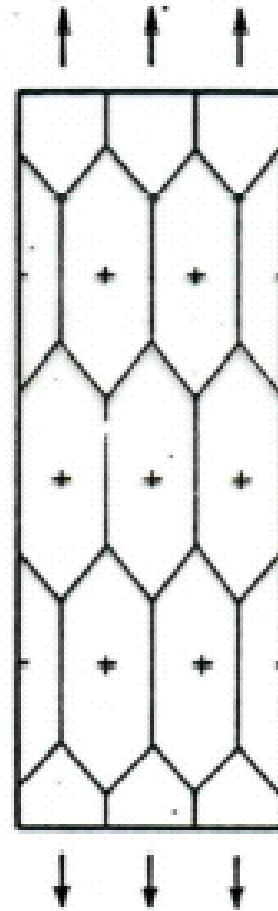


ひずみ速度一定条件下では(ある変形速度が与えられたとき)、運動転位の密度は、そのひずみ速度を保つのに必要な変形応力が最小となるように決まる。

超塑性 (Superplasticity)



数ミクロン程度の微細結晶粒
高温変形
異常に大きな破断伸び
(a)



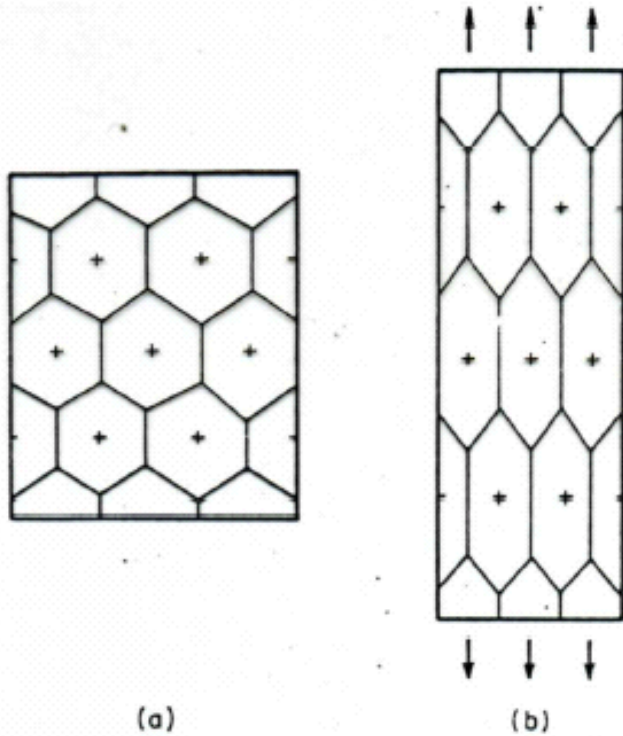
(b)

Non-equilibrium
Statistical Thermodynamics

Refined grain
High temperature
Abnormal deformation

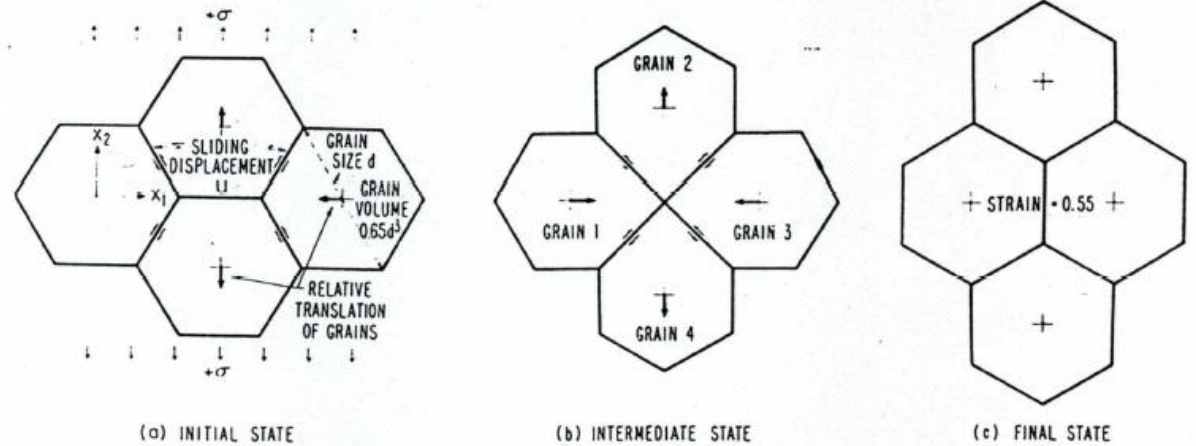
粒界すべり(超塑性)の**非平衡**統計熱力学

超塑性 (Super plasticity)



DIFFUSION-ACCOMMODATED FLOW AND SUPERPLASTICITY*

M. F. ASHBY† and R. A. VERRALL†



超塑性 (Super plasticity)



Slip deformation (すべり変形)

$$\text{Strain rate(歪速度)} \quad \dot{\varepsilon} = N_m \cdot \bar{v} \cdot b$$

N_m Mobile dislocation density (可動転位密度)

\bar{v} Average dislocation velocity (可動転位の平均速度)

b Burgers vector (バーガースベクトル)

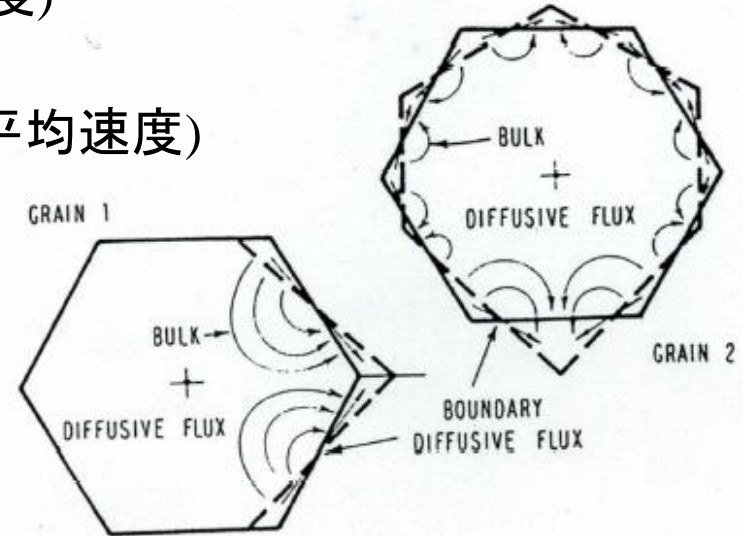
Super plasticity (超塑性)

$$\text{Strain rate(歪速度)} \quad \dot{\varepsilon} = N_g \cdot \bar{\omega} \cdot \varepsilon_0$$

N_g Rotational grain density (可動結晶粒密度)

$\bar{\omega}$ Average rotational velocity (可動粒の平均回転速度)

ε_0 回転の素過程の歪への寄与



Hall-Petch relation 1

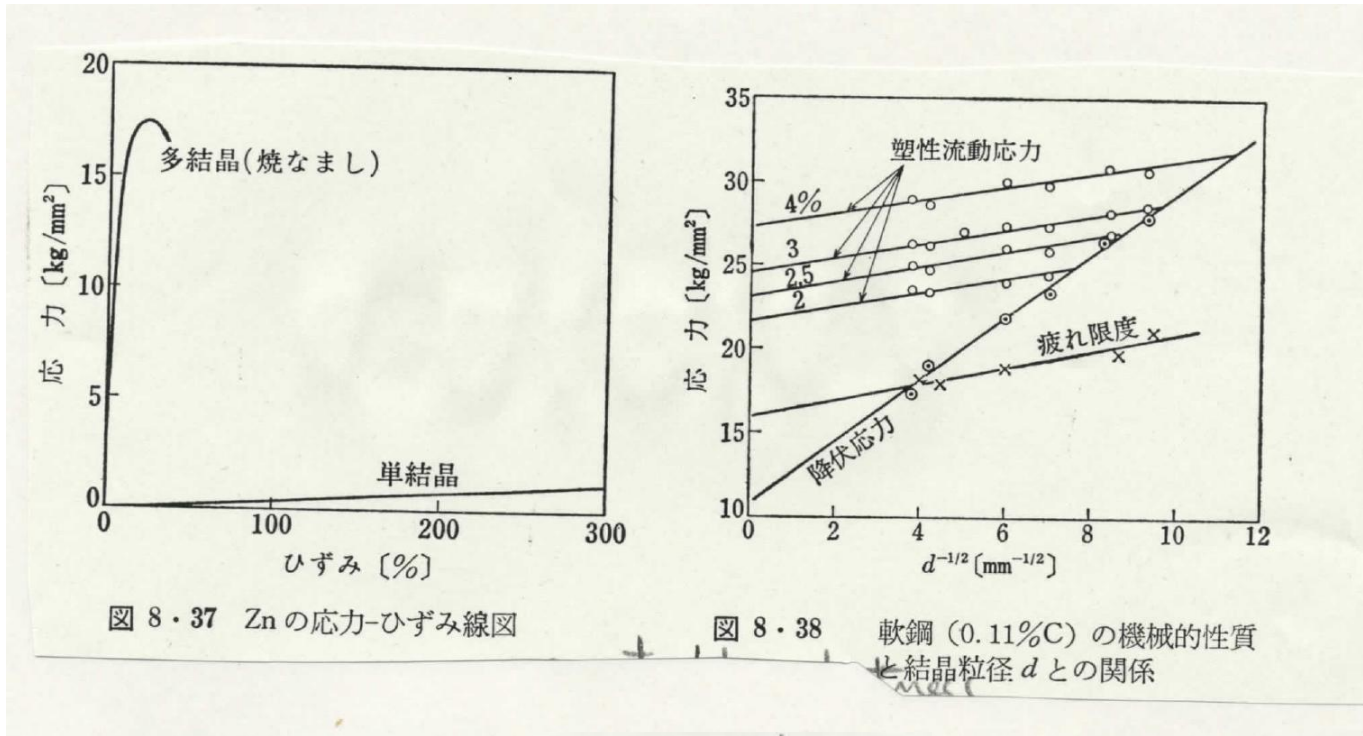


図 8・37 Zn の応力-ひずみ線図

図 8・38 軟鋼 (0.11% C) の機械的性質と結晶粒径 d との関係

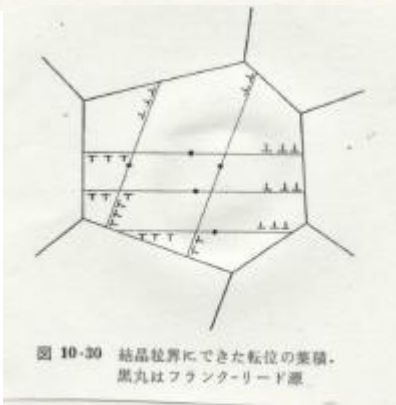


図 10-30 結晶粒界にできた転位の集積。黒丸はフランクリン源

Hall-Petch relation 2

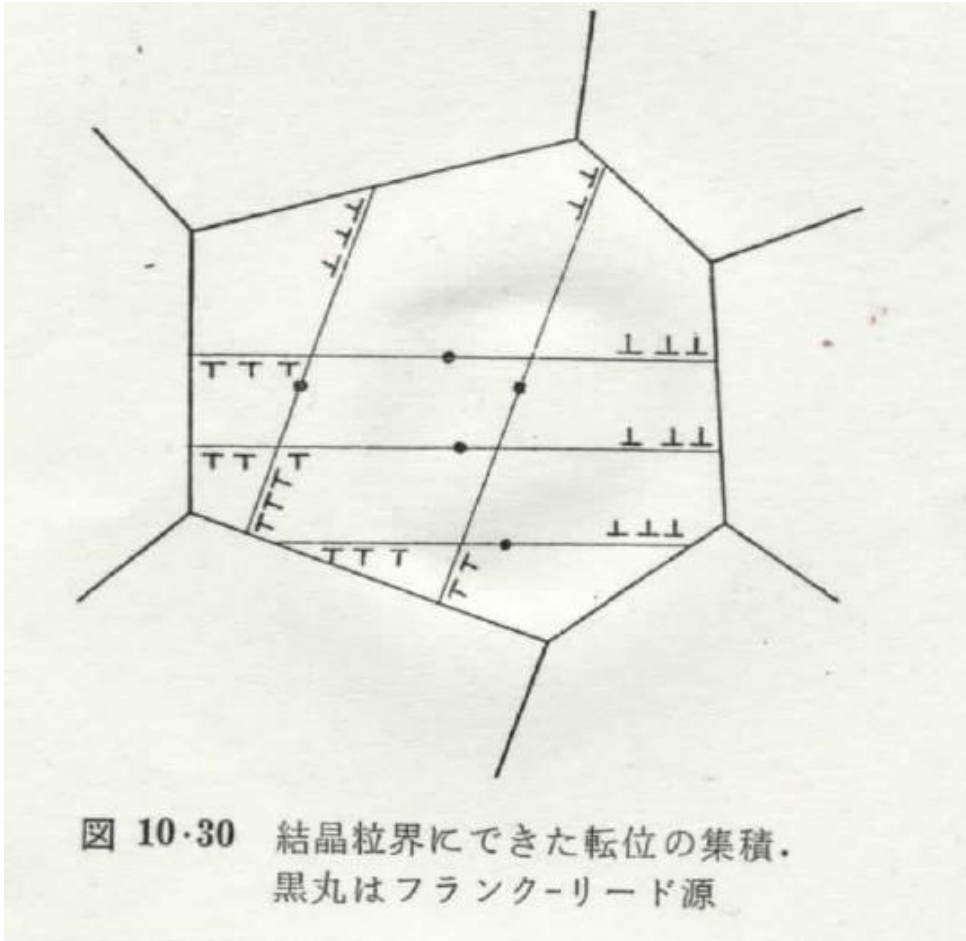


図 10-30 結晶粒界にできた転位の集積.
黒丸はフランク-リード源

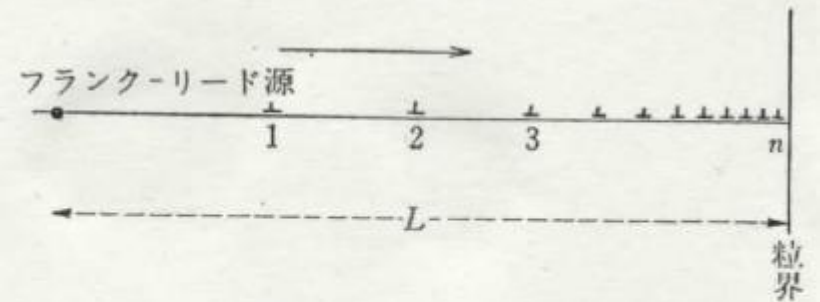


図 10-29 粒界のような障害物でとめられ集積した転位群

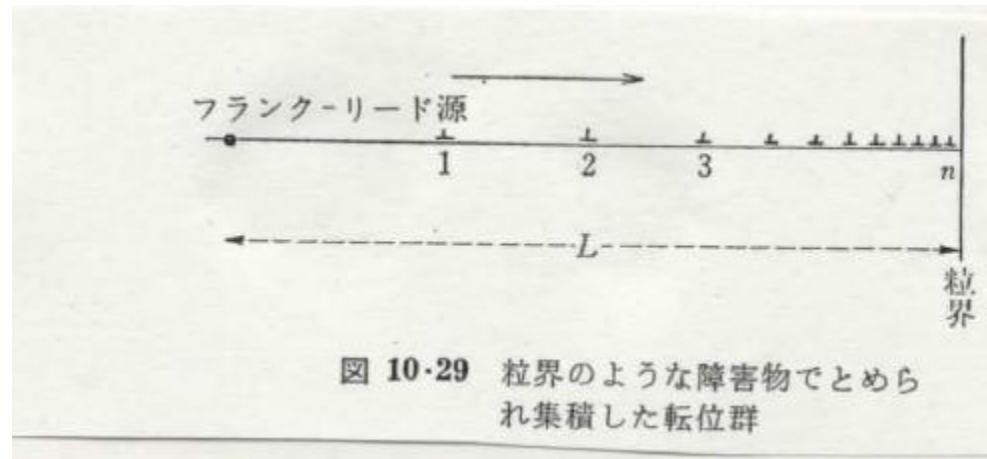
Hall-Petch relation 3



$$\tau(\xi) = \frac{A}{\xi - \eta}$$



$$\tau(\xi) = A \int \frac{D(x)}{\xi - x} dx$$



$$\tau(\xi) + \tau_a(\xi) = 0$$

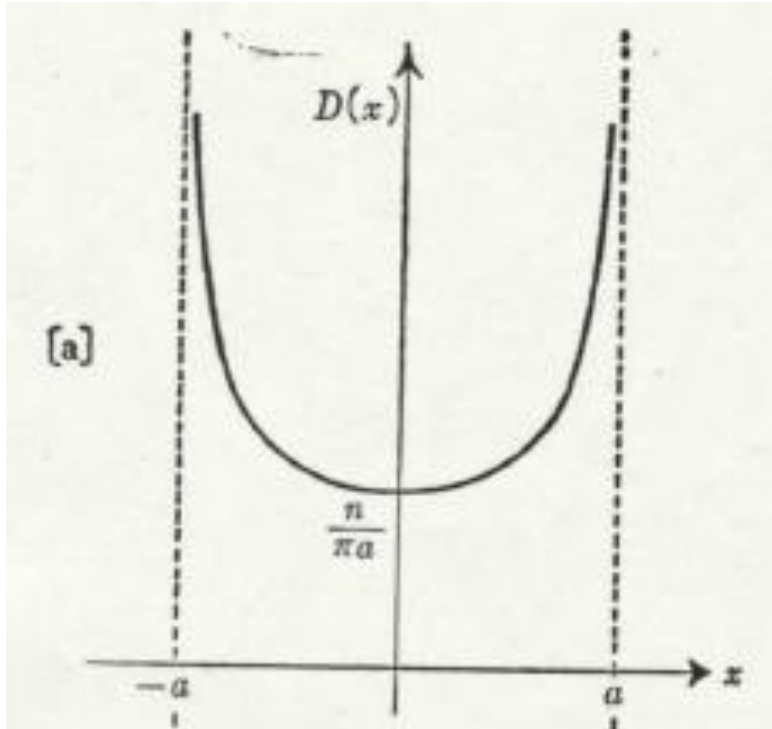
$$\tau(\xi) + \tau_a(\xi) = \tau_f$$

$$\tau_f - \tau_a(\xi) = A \int \frac{D(x)}{\xi - x} dx \quad \int_{-a}^{+a} D(x) \cdot dx = n$$

Hall-Petch relation 4

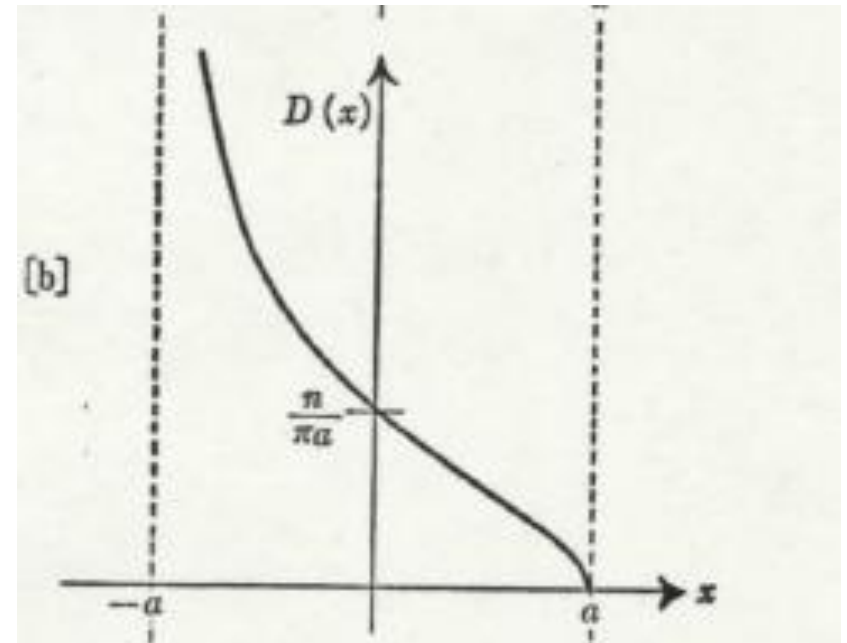


$$\tau_a(\xi) = \tau_f = 0$$



$$D(x) = \frac{n}{\pi} \cdot \frac{1}{(a^2 - x^2)^{1/2}}$$

$$\tau_a(\xi) = \text{constant}$$



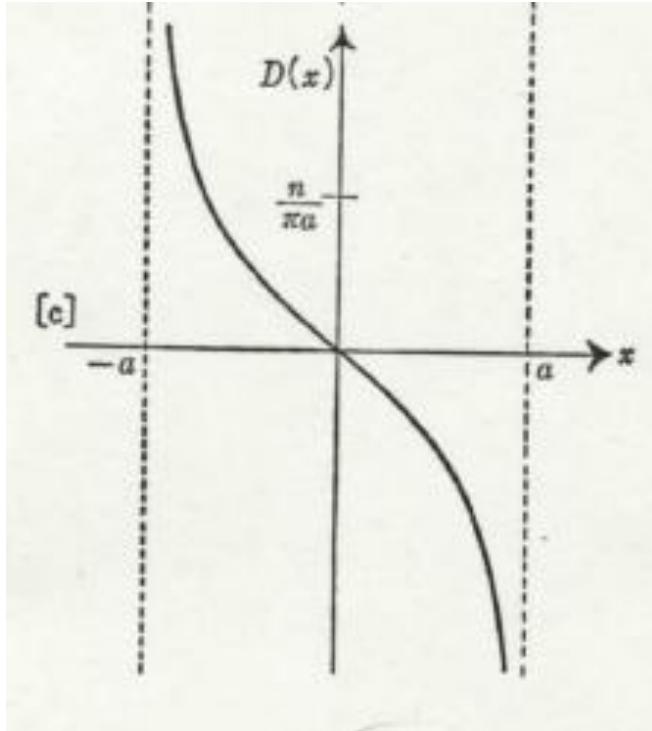
$$D(x) = \frac{n}{\pi} \cdot \left(\frac{a-x}{a+x} \right)^{1/2}$$

Hall-Petch relation 5



$$\int_{-a}^{+a} D(x) \cdot dx = 0$$

$$f(\delta) = A \int_{-a}^{+a} \frac{D(x)}{(a+\delta)-x} dx + \tau_a$$



$$f(\delta) = -\frac{\tau_a - \tau_f}{\pi} \int_0^\pi \frac{\cos \theta}{\left(1 + \frac{\delta}{a}\right) - \cos \theta} d\theta + \tau_a$$

$$= (\tau_a - \tau_f) \left[-1 + \frac{\delta + a}{\sqrt{2\delta a + \delta^2}} \right] + \tau_a$$

$$= (\tau_a - \tau_f) \frac{1}{\sqrt{2}} \sqrt{\frac{a}{\delta}} + \tau_f \quad \delta \ll a$$

$$D(x) = -\frac{(\tau_a - \tau_f)}{\pi A} \cdot \frac{x}{(a^2 - x^2)^{1/2}}$$

Hall-Petch relation 6

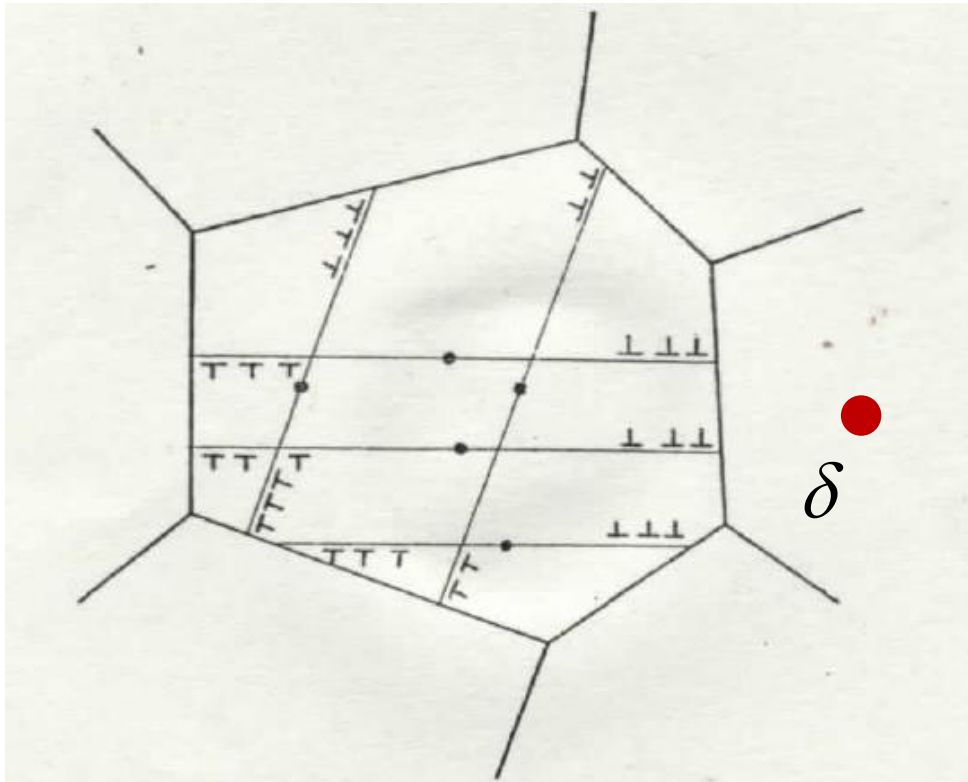


図 10・30 結晶粒界にできた転位の集積.
黒丸はフランク-リード源

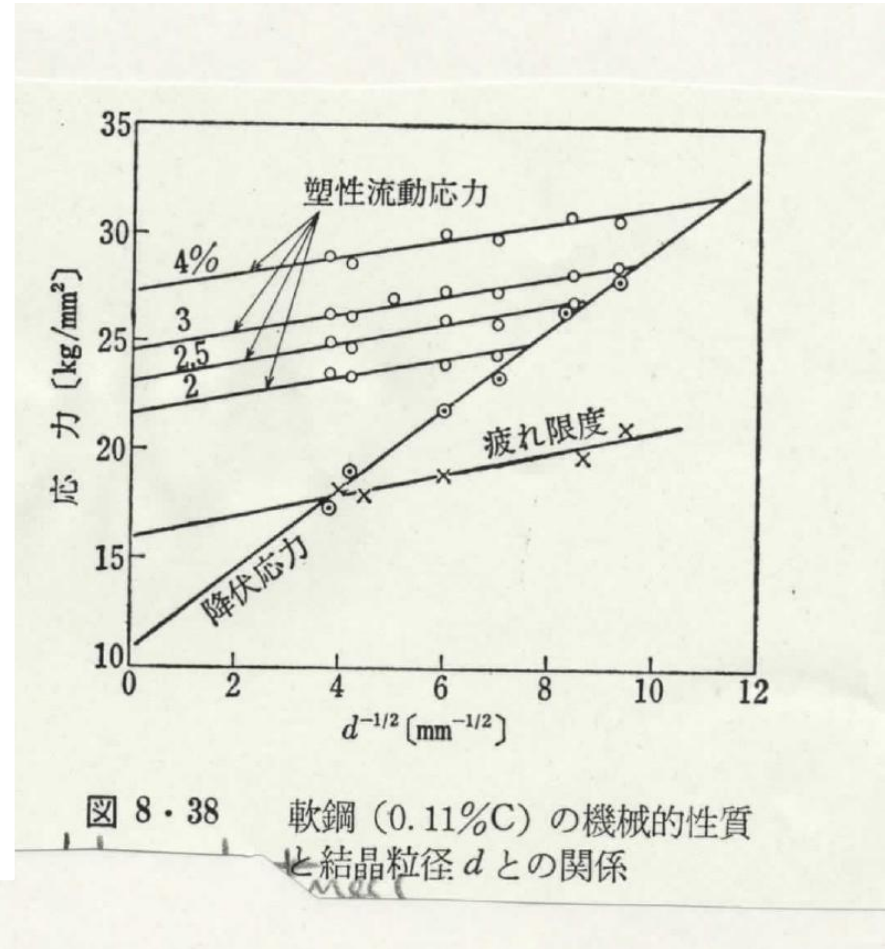


図 8・38 軟鋼 (0.11% C) の機械的性質
と結晶粒径 d との関係

$$\tau_a = \tau_f + (\tau_c - \tau_f) \sqrt{\delta} \cdot d^{-1/2}$$

A sunset scene with silhouetted trees and mountains. The sky transitions from a deep blue at the top to a bright orange and yellow near the horizon. The sun is partially obscured by clouds, creating a glowing effect. In the foreground, the dark silhouettes of several tall, slender trees stand on the left side. In the background, a range of mountains is visible against the horizon.

Thank you !

Division of Materials Science and Engineering, Graduate School of Engineering,